

# NIAC Phase 1 Final Report: *Venus Landsailer Zephyr*



**Requestor:** Dr. Geoffrey Landis

**COMPASS Lead:** Steve Oleson

**Concept Design Integration Lead:** Dave Grantier

## COMPASS Team Members

*Les Balkanyi  
Mike Bur  
Laura Burke  
Kristen Bury  
Anthony Colozza  
John Dankanich*

*Jon Drexler  
Ian Dux  
James Fincannon  
James Fittje  
John Gyekenyese  
Geoffrey Landis  
Mike Martini*

*Tom Packard  
Dave Smith  
Anita Tenteris  
Joe Warner  
Glenn L. Williams  
Jeff Woytach*

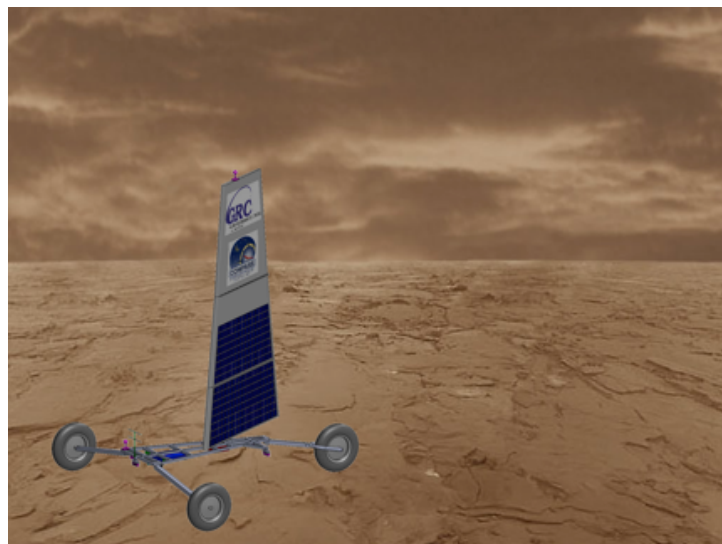






## TABLE OF CONTENTS

1.0	EXECUTIVE SUMMARY .....	1
2.0	STUDY BACKGROUND AND ASSUMPTIONS .....	3
2.1	Introduction .....	3
2.1.1	Background.....	3
2.1.2	Technology Background and Concept .....	3
2.1.3	Previous Studies .....	4
2.1.4	Wind on Venus .....	5
2.2	Assumptions and Approach.....	5
2.2.1	Report Perspective and Disclaimer .....	5
2.2.2	Report Assumptions .....	6
2.3	Study Summary Requirements .....	7
2.3.1	Figures of Merit.....	7
2.4	Growth, Contingency, and Margin Policy.....	7
2.4.1	Terms and Definitions .....	7
2.4.2	Mass Growth .....	9
2.4.3	Power Growth.....	10
3.0	BASELINE DESIGN .....	11
3.1	Concept Drawing and Description .....	11
3.2	Landsailer in Stowed Configuration.....	13
3.3	Concept of Operations (CONOPS).....	15
3.3.1	Interplanetary Cruise and Venus Entry .....	15
3.3.2	Zephyr Entry, Descent, and Landing and Post-Landing CONOPS.....	15
3.3.3	Zephyr Post-Landing CONOPS .....	17
3.3.4	Venus Environmental Details.....	18
3.4	System-Level Summary .....	19
3.5	Orbiter and Aeroshell .....	20
3.5.1	Orbiter.....	20
3.5.2	Aeroshell.....	21
3.6	Top-Level Design Details.....	21
3.6.1	Master Equipment List (MEL) .....	21
3.6.2	Spacecraft Total Mass Summary.....	21
3.6.3	Power Equipment List (PEL) .....	23
4.0	SUBSYSTEM BREAKDOWN.....	23
4.1	Science Package .....	23
4.1.1	Science Overview .....	23
4.1.2	Science Requirements .....	24
4.1.3	Instruments .....	24
4.1.4	Science Design and MEL .....	28
4.2	Launch, Trans-Venus Trajectory, Orbital Insertion, and Landing .....	28
4.2.1	Launch .....	28
4.2.2	Earth to Venus Trajectory .....	29
4.2.3	Orbit Insertion $\Delta V$ Details.....	30
4.2.4	Landing.....	30
4.3	Zephyr Landsailer Rover System Mobility .....	32
4.3.1	Zephyr Landsailer Rover System Mobility Requirements.....	32
4.3.2	Zephyr Landsailer Rover System Mobility Assumptions .....	32
4.3.3	Zephyr Landsailer Rover System Mobility Design and MEL.....	32
4.3.4	Zephyr Landsailer Mobility System Trades .....	37

4.3.5	Zephyr Landsailer Mobility System Analysis.....	41
4.3.6	Zephyr Landsailer Mobility Risk Inputs .....	41
4.3.7	Zephyr Landsailer Mobility Recommendation .....	42
4.4	Structures and Mechanisms .....	42
4.4.1	Structures and Mechanisms Requirements.....	42
4.4.2	Structures and Mechanisms Assumptions.....	42
4.4.3	Structures and Mechanisms Design and MEL .....	43
4.4.4	Structures and Mechanisms Trades .....	45
4.4.5	Structures and Mechanisms Analytical Methods .....	45
4.4.6	Structures and Mechanisms Risk Inputs.....	46
4.4.7	Structures and Mechanisms Recommendation.....	46
4.5	Communications.....	46
4.5.1	Orbiter Mission Analysis.....	46
4.5.2	Communications Requirements.....	48
4.5.3	Communications Assumptions.....	48
4.5.4	Communications Design and MEL .....	48
4.6	Command and Data Handling (C&DH) .....	49
4.6.1	C&DH Requirements .....	50
4.6.2	C&DH Assumptions.....	50
4.6.3	C&DH Design and MEL .....	51
4.7	Guidance, Navigation and Control (GN&C).....	54
4.7.1	GN&C Requirements .....	54
4.7.2	GN&C Assumptions.....	54
4.7.3	GN&C Design and MEL .....	54
4.7.4	GN&C Trades.....	55
4.7.5	GN&C Risk Inputs .....	55
4.7.6	GN&C Recommendation .....	55
4.8	Electrical Power System.....	55
4.8.1	Power Requirements.....	55
4.8.2	Power Assumptions.....	56
4.8.3	Power Design and MEL .....	56
4.8.4	Power Trades .....	57
4.9	Thermal Control .....	58
4.9.1	Cruise Deck Thermal Control .....	58
4.9.2	Aeroshell and Descent Thermal Control .....	61
4.9.3	Landsailer Thermal Control .....	64
4.9.4	Thermal MEL .....	64
4.9.5	Thermal Recommendation .....	65
5.0	COST AND RISK .....	65
5.1	Cost.....	65
5.1.1	Draft Lifecycle Cost ROM.....	66
5.1.2	Integration, Assembly and Checkout (IACO).....	66
5.1.3	System Test Operations (STO).....	66
5.1.4	Ground Support Equipment (GSE) .....	67
5.1.5	Systems Engineering and Integration (SE&I).....	67
5.1.6	Program Management (PM).....	67
5.1.7	Launch and Orbital Operations Support (LOOS).....	67
6.0	ARCHITECTURAL DETAILS AND MARGIN .....	68
7.0	BIBLIOGRAPHY.....	68
8.0	—ACRONYMS AND ABBREVIATIONS .....	72
	Appendix: “A Landsailing Rover For Venus Mobility” .....	74

## LIST OF FIGURES

Figure 1.1—“Zephyr” Venus Landsailer. ....	1
Figure 2.1—Landsailing vehicles on Earth: a Kansas “Windwagon” from the 1860s. ....	4
Figure 2.2—Conceptual design for a large Venus rover incorporating a radioisotope power system for the “HERRO-Venus” design study (from Landis <i>et al.</i> 2012). ....	5
Figure 2.3—Graphical illustration of the definition of basic, predicted, total and allowable mass. ....	7
Figure 3.1—Perspective views of the Zephyr Venus Rover as deployed on the surface. ....	11
Figure 3.2—Dimensioned view of rover chassis viewed from below, showing wheelbase. ....	12
Figure 3.3—Landsailer subsystem components. ....	13
Figure 3.4—Venus Landsailer stowed within the aeroshell. ....	14
Figure 3.5—Isometric views of the Venus Landsailer stowed within the aeroshell. ....	14
Figure 3.6—Landsailer in its stowed configuration. ....	15
Figure 3.7—Notional entry, descent and landing profile. ....	16
Figure 3.8—Various stages of deployment for the Venus Landsailer. ....	16
Figure 3.9—Zephyr transverse options. ....	17
Figure 3.10—Properties of the Venus Atmosphere. ....	19
Figure 3.11—Venus atmosphere structure. ....	19
Figure 3.12—Venus Landsailer block diagram. ....	20
Figure 4.1—SiC scanning camera, 128 pixel, 1.9 W dissipation. ....	26
Figure 4.2—Conceptual design of a sphere anemometer (From Hölling <i>et al.</i> 2007). ....	28
Figure 4.3—Falcon 9 launch profile, trans-Venus insertion (TVI) and cruise phases. ....	29
Figure 4.4—Notional trans-Venus trajectory. ....	30
Figure 4.5—Nextel filament properties. ....	31
Figure 4.6—Lunar rover wheel. ....	33
Figure 4.7—Honeybee High Temperature Electric Motor and GE Test Article. ....	34
Figure 4.8—Moog Type 7 Gimbal. ....	34
Figure 4.9—Sail dimensions. ....	35
Figure 4.10—Drag Polar for Landsailer Wing, showing the x and y components of the force on the sail with respect to the wind direction. ....	36
Figure 4.11—Sail force versus surface wind velocity. ....	38
Figure 4.12—Incline angle versus wind velocity. ....	39
Figure 4.13—NACA 0015 lift coefficient ( $C_L$ ) versus angle of attack. ....	41
Figure 4.14—NACA 0015 drag coefficient ( $C_d$ ) versus angle of attack. ....	41
Figure 4.15—Illustration of the Landsailer stowed in the aeroshell (transparent for illustration purposes) on the left and deployed on the right. ....	43
Figure 4.16—A view of the Landsailer bus underside with mounted hardware. ....	44
Figure 4.17—Targets in view of Lander and Orbiter. ....	48
Figure 4.18—Communication components. ....	49
Figure 4.19—SiC logic gate basics. ....	51
Figure 4.20—SiC microcontroller core, multichip topography, 3 W. ....	52
Figure 4.21—The 10 bit analog to digital converter, ~650 mW dissipation. ....	52
Figure 4.22—SiC motor drive circuit, 600 mW dissipation. ....	53
Figure 4.23—Motor control system schematic. ....	53
Figure 4.24—Avionics enclosure. ....	53
Figure 4.25—Power Output of solar array as function of mission time. ....	56
Figure 4.26—battery state of charge during the mission. ....	57
Figure 4.27—DuPont Kapton Strip Heater. ....	59
Figure 4.28—Example of MLI Blanket design and application. ....	60
Figure 4.29—Example of a cold plate with integrated heat pipes. ....	61

Figure 4.30—Radiator with integral heat pipes (ACT, Inc.) ..... 62

Figure 4.31—Illustration of heated Aeroshell during descent ..... 62

Figure 4.32—Orion Heat Shield structural makeup ..... 62

Figure 4.33—Stardust Aeroshell Geometry ..... 63

Figure 4.34—Descent velocity and time as a function of altitude ..... 63

Figure 4.35—Venus Landsailer electronics component locations ..... 64

## LIST OF TABLES

Table 1.1—Mission and Spacecraft Summary for the Venus Landsailer ..... 2

Table 2.1—Assumptions and Study Requirements ..... 6

Table 2.2—Definition of Masses Tracked in the Master Equipment List ..... 9

Table 2.3—MGA and Depletion Schedule (AIAA S-120-2006) ..... 10

Table 3.1—Zephyr Landsailer Orbiter Master Equipment List ..... 20

Table 3.2—Zephyr Landsailer Aeroshell Master Equipment List ..... 21

Table 3.3—Venus Landsailer MEL WBS Format—Baseline Case ..... 21

Table 3.4—Baseline Case 1 System Summary ..... 22

Table 3.5—Venus Landsailer PEL ..... 23

Table 4.1—Science Case 1 Master Equipment List ..... 28

Table 4.2—Propulsion System Master Equipment List ..... 36

Table 4.3—Survey of Rover Wheel Concepts ..... 38

Table 4.4—Venus Landsailer Structures Master Equipment List ..... 44

Table 4.5—Communications Master Equipment List ..... 49

Table 4.6—C&DH Master Equipment List ..... 54

Table 4.7—GN&C Case 1 Master Equipment List ..... 54

Table 4.8—Venus Lander Power Requirements ..... 55

Table 4.9—Electrical Power System Master Equipment List ..... 57

Table 4.10—Transit Environment Constants ..... 58

Table 4.11—Specifications for MLI ..... 59

Table 4.12—Cruise Deck Radiator Sizing ..... 60

Table 4.13—Heatshield Material Layer Properties ..... 62

Table 4.14—Thermal Master Equipment List ..... 64

Table 5.1—Preliminary Cost ROM (Represents Estimated Prime Contractor Cost Plus Fee) ..... 66

Table 6.1—Venus Landsailer Summary Mass Calculations ..... 68

Table 6.2—Architecture Details—example Launch system performance ..... 68



## STUDY PARTICIPANTS

<i>Study Name Design Session</i>			
Subsystem	Name	Center	Email
Design Customer POC/PI	Geoffrey A. Landis	GRC	<a href="mailto:Geoffrey.Landis@nasa.gov">Geoffrey.Landis@nasa.gov</a>
Design Customer	NASA Innovative Advanced Concepts office	HQ	
COMPASS Team			
COMPASS Team Lead	Steve Oleson	GRC	<a href="mailto:Steven.R.Oleson@nasa.gov">Steven.R.Oleson@nasa.gov</a>
System Integration, MEL, and Final Report Documentation	Melissa McGuire	GRC	<a href="mailto:Melissa.L.Mcguire@nasa.gov">Melissa.L.Mcguire@nasa.gov</a>
System Integration, MEL, and Final Report Documentation	Dave Grantier	GRC	<a href="mailto:David.T.Grantier@nasa.gov">David.T.Grantier@nasa.gov</a>
System Integration, MEL, and Final Report Documentation	Jen Jordan	GRC	<a href="mailto:jennifer.l.jordan@nasa.gov">jennifer.l.jordan@nasa.gov</a>
Technical Editing	Leslie Balkanyi	GRC	<a href="mailto:Leslie.R.Balkanyi@nasa.gov">Leslie.R.Balkanyi@nasa.gov</a>
Science and Payload	Geoffrey Landis	GRC	<a href="mailto:Geoffrey.Landis@nasa.gov">Geoffrey.Landis@nasa.gov</a>
Mission Design	Ian Dux	GRC	<a href="mailto:Ian.J.Dux@nasa.gov">Ian.J.Dux@nasa.gov</a>
Mission Design	Laura Burke	GRC	<a href="mailto:laura.m.burke@nasa.gov">laura.m.burke@nasa.gov</a>
Mission Design	Rob Falck	GRC	<a href="mailto:rfalck@nasa.gov">rfalck@nasa.gov</a>
Mission Design	Dave Smith	GRC	<a href="mailto:david.a.smith-1@nasa.gov">david.a.smith-1@nasa.gov</a>
ACS, GN&C, Mission Design	Mike Martini	GRC	<a href="mailto:Michael.C.Martini@nasa.gov">Michael.C.Martini@nasa.gov</a>
PEL, CONOPS	Carlos Rodriguez	GRC	<a href="mailto:carlos.d.rodriguez@nasa.gov">carlos.d.rodriguez@nasa.gov</a>
Propulsion	Jim Fittje	GRC	<a href="mailto:james.e.fittje@nasa.gov">james.e.fittje@nasa.gov</a>
Structures and Mechanisms	John Gyekenyesi	GRC	<a href="mailto:John.Z.Gyekenyesi@nasa.gov">John.Z.Gyekenyesi@nasa.gov</a>
Thermal	Tony Colozza	GRC	<a href="mailto:Anthony.J.Colozza@nasa.gov">Anthony.J.Colozza@nasa.gov</a>
Power	James Fincannon	GRC	<a href="mailto:james.fincannon@nasa.gov">james.fincannon@nasa.gov</a>
Power	Kristen Bury	GRC	<a href="mailto:kristen.m.bury@nasa.gov">kristen.m.bury@nasa.gov</a>
Configuration	Tom Packard	GRC	<a href="mailto:Thomas.W.Packard@nasa.gov">Thomas.W.Packard@nasa.gov</a>
Communications	Joe Warner	GRC	<a href="mailto:Joseph.D.Warner@nasa.gov">Joseph.D.Warner@nasa.gov</a>
C&DH / Software	Glenn Williams	GRC	<a href="mailto:Glenn.L.Williams@nasa.gov">Glenn.L.Williams@nasa.gov</a>
Cost	Jon Drexler	GRC	<a href="mailto:Jonathan.A.Drexler@nasa.gov">Jonathan.A.Drexler@nasa.gov</a>
Risk	Anita Tenteris	GRC	<a href="mailto:Anita.D.Tenteris@nasa.gov">Anita.D.Tenteris@nasa.gov</a>





## 1.0 EXECUTIVE SUMMARY

Imagine sailing across the hot plains of Venus! A design for a craft to do just this was completed by the COncurrent Multidisciplinary Preliminary Assessment of Space Systems (COMPASS) Team for the NASA Innovative Advanced Concepts (NIAC) project. The robotic craft could explore over 30 km of surface of Venus, driven by the power of the wind.

The Zephyr Venus Landsailer is a science mission concept for exploring the surface of Venus with a mobility and science capability roughly comparable to the Mars Exploration Rovers (MER) mission, but using the winds of the thick atmosphere of Venus for propulsion. It would explore the plains of Venus in the year 2025, near the Venera 10 landing site, where wind velocities in the range of 80 to 120 cm/s were measured by earlier Soviet landing missions. These winds are harnessed by a large wing/sail which would also carry the solar cells to generate power. At around 250 kg, Zephyr would carry an 8 m tall airfoil sail (12 m<sup>2</sup> area), 25 kg of science equipment (mineralogy, grinder, and weather instruments) and return 2 Gb of science over a 30 day mission. Due to the extreme temperatures (450 °C) and pressures (90 bar) on Venus, Zephyr would have only basic control systems (based on high temperature silicon carbide (SiC) electronics) and actuators. Control would come from an orbiter which is in turn controlled from Earth. Due to the time delay from the Earth a robust control system would need to exist on the orbiter to keep Zephyr on course. Data return and control would be made using a 250 MHz link with the orbiter with a maximum data rate of 2 kbps. At the minimal wind speed required for mobility of 35 cm/s, the vehicle move at a slow but steady 4 cm/s by positioning the airfoil and use of one wheel that is steered for pointing control. Navigation commands from the orbiter will be based upon navigation cameras, simple accelerometers and stability sensors; Zephyr's stability is robust, using a wide wheel base along with controls to 'feather' or 'luff' the airfoil and apply brakes to stop the vehicle in the case of unexpected conditions. This would be the science gathering configuration. The vehicle itself would need to be made from titanium (Ti) as the structural material, with a corrosion-barrier overcoating due to extreme temperatures on the surface.

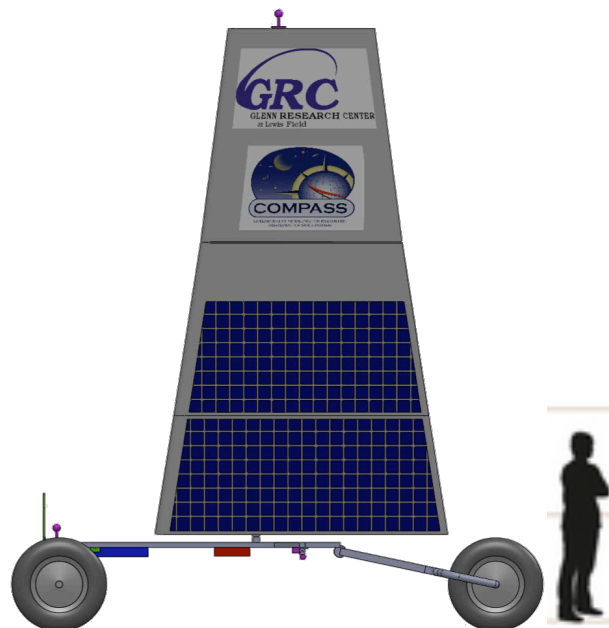


Figure 1.1—"Zephyr" Venus Landsailer.

The conceptual study learned many lessons during the design process.

- Using a sail can provide lift—not just drag—which allows for sailing not just downwind but upwind to a certain degree.

- The wind speed is key—need at least 35 cm/s wind or larger sail area and/or lightened craft to enable use of less wind
- Larger wheels reduce rolling friction
- Zephyr designed to have mobility over 10 cm debris
- Pressure vessels and cooling electronics would be too heavy to allow sailing
- Components (especially actuators and electronics) must be capable of operating in Venus environment (~450 °C, 90 bar, hostile atmosphere) SiC (or equivalent high-temperature semiconductor) electronics key to operations
- controlling of vehicle in real-time from a ‘Smart’ Orbiter
- The large sail area and low power requirements allow for solar power
- Solar cells (0.33% effective efficiency at Venus conditions) and sodium-sulfur (NaS) batteries exist for Venus high temps

For a phase two of Zephyr several activities should be pursued and tested on small scale but at proper Venus conditions:

- Refine design, develop simulations, and test models in similar density environment (e.g., liquid ether)
- Layout control scheme with Orbiter
- Develop Orbiter concept and layout
- Refine communications/control approach with Orbiter
- Refine high temp electronics concept
- Trade study of wind powered orbiter versus conventional motorized rover versus Radioisotope powered approaches
- Test materials in the Glenn Extreme Environments Rig (GEER) simulating the Venus environment

Table 1.1 summarizes the top-level details of each subsystem that was incorporated into the design.

Table 1.1—Mission and Spacecraft Summary for the Venus Landsailer

Main Subsystems	Basic Mass (kg)	Growth (kg)	Predicted Mass (kg)	Aggregate Growth (%)
<b>Venus Landsailer System</b>	<b>1581.0</b>	<b>295.7</b>	<b>1877</b>	
<b>Landsailer Rover</b>	<b>220.1</b>	<b>44.9</b>	<b>265</b>	20%
Science Instruments	17.9	7.0	25	39%
Attitude Determination and Control	2.3	0.7	3	30%
Command & Data Handling	15.3	6.3	22	41%
Communications and Tracking	4.0	1.3	5	33%
Electrical Power Subsystem	32.1	4.4	37	14%
Thermal Control (Non-Propellant)	1.0	0.2	1	18%
Propulsion (Sail System)	84.2	13.6	98	16%
Propellant (Chemical) (not Used)	0.0		0	
Propulsion (EP Hardware) (Not Used)	0.0	0.0	0	-
Propellant (EP) (Not Used)	0.0		0	
Structures and Mechanisms	63.2	11.4	75	18%
Element 1 consumables (if used)	1		1	
Estimated Spacecraft Dry Mass (no prop, consum)	220	45	264	20%
Estimated Spacecraft Wet Mass	220	45	265	
<b>System Level Growth Calculations Landsailer Rover</b>				<b>Total Growth</b>
Dry Mass Desired System Level Growth	202	61	263	30%
Additional Growth (carried at system level)		16		8%
Total Wet Mass with Growth	220	61	281	



## **2.0 STUDY BACKGROUND AND ASSUMPTIONS**

### **2.1 Introduction**

This report documents a study by the COMPASS Team at NASA Glenn to do a conceptual design study of a new concept to explore the surface of Venus, a Venus rover powered only by the wind. (The initial justification for the project is outlined in a paper “A Landsailing Rover for Venus Mobility,” is attached as an appendix.) The design study was supported by the NASA Innovative Advanced Concepts (“NIAC”) office at NASA headquarters.

Dubbed “Zephyr,” the Landsailer was designed to provide a month of science on Venus.

#### **2.1.1 Background**

The surface of Venus has the most hostile environment of any planetary surface in the solar system. The average temperature of 450 °C is hotter than an oven, and the corrosive atmosphere, at a pressure of 90 bars, is difficult to withstand. Although humans have sent rovers to Mars with operating lifetimes of 8 years and counting, the Venus surface has currently been explored only by short-lived Soviet and American probes, none of which were mobile, and the longest-lived of which operated for only 2 hr on the surface before succumbing to the harsh Venus environment. Nevertheless, it is a scientifically fascinating planet, and one that, due to its similarity and differences from Earth, for which a mobile exploration rover would produce great public interest. It has been shown by missions to Mars that mobility on the surface is of great value to science exploration, and for a future mission to Venus, it is desired to be able to land a mission with a longer lifetime, and capable of mobility.

While mobility using motors capable of high temperature operations exist, the power to drive on the surface is limited by power available. Solar power is limited by the thick cloud cover, through which only ~1% of the solar illumination penetrates, and the high temperatures, which decrease the efficiency of photovoltaic cells.

The Soviet probes, however, noted the existence of slow winds on the surface—such winds could be used for propelling a craft across the surface. While ‘tumbleweed’ type vehicles have been envisioned the Venus Landsailer design seeks to actively steer the science vehicle to avoid just getting stuck in a valley and ending the science mission. Major challenges in power production, high temperature electronics, controls, and communications must be addressed to develop a functioning Venus Landsailer.

Exploring the surface of Venus with a rover would be a “stretch” goal, which will push the limits of technology in high-temperature electronics, robotics, and robust systems. Yet it would be an exciting goal, since Venus is an unknown planet, a planet with significant scientific mysteries, and a planet larger than Mars with equally interesting (although less well known) geology and geophysics. A mission to the surface of Venus would expand our knowledge of the surfaces of terrestrial planets.

#### **2.1.2 Technology Background and Concept**

In work to develop sensors to work inside of jet engines, NASA Glenn Research Center (GRC) has developed electronics that will continue to function even at the Venus temperature of 450 °C. GRC Technology for a high-temperature switched-reluctance electric motor which operates at up to 500 °C has been transferred to Honeybee Robotics, where it is now being commercialized. These electronic components represent a breakthrough in technological capability for high temperatures. We have also tested solar cells up to Venus surface temperatures. Although the power density produced is low (because of the high cloud levels and thick atmosphere), we now know that it is possible to produce electrical power on the surface. So the fundamental elements of a rover for Venus are not beyond the bounds of physics: we could survive the furnace of Venus—if we can come up with an innovative concept for a rover that can move on extremely low power levels.

The atmospheric pressure at the surface is more than 50 times greater than that of Earth. Even though the winds at the surface of Venus are low (under 1 m/s), at Venus pressure even low wind speeds develop significant force. We have thus proposed a new concept for a planetary rover: a sail-propelled rover to explore the surface of Venus. Such a rover could open a new frontier: converting the surface of a new planet into a location that can be explored by robotic exploration.

A landsail operates on the same principle as a sailboat with wheels. The basic idea of landsailing is not new: landsailing vehicles on Earth, dating back to the “windwagons” of the 19th century to sail across the American plains (see Figure 2.1). Modern landsailing vehicles are much more sophisticated; with good design they can move at speeds of up to ten times the speed of the wind. And yet the basic concept is extremely simple; using the lift force on a sail. While the detailed aerodynamic design of the sail for Venus will be somewhat different, due to the slow wind speeds but high density atmosphere, the basic design principles are well known. Most notably, a landsail can be done with only two moving parts; the sail, and the steering.

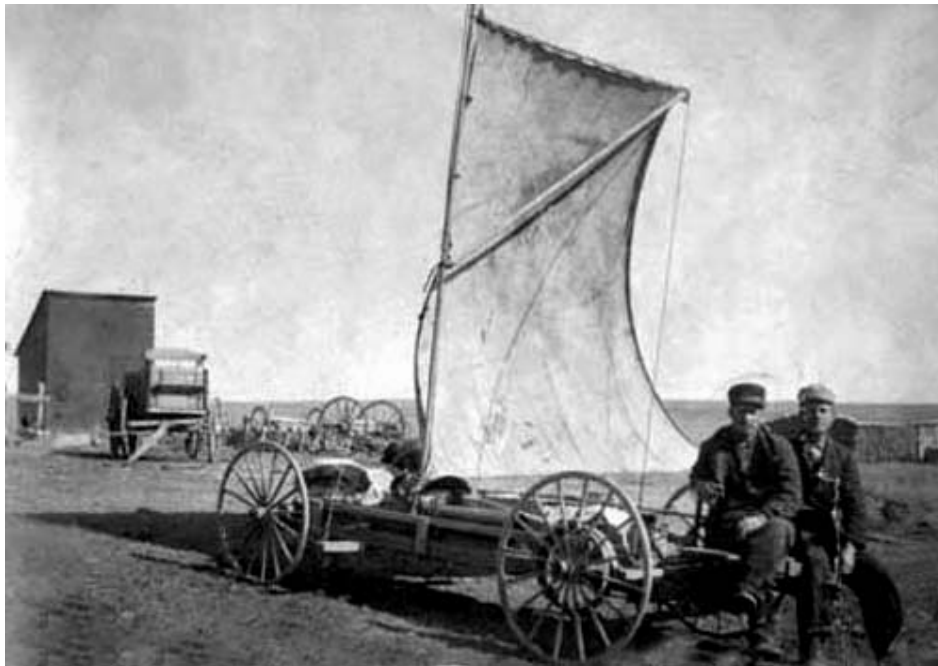


Figure 2.1—Landsailing vehicles on Earth: a Kansas “Windwagon” from the 1860s.

### 2.1.3 Previous Studies

In 2003, Geoffrey Landis led the NASA Revolutionary Aerospace Systems Concepts (RASC) study “Robotic Exploration of Venus,” which looked at the technologies needed for a future (2048) NEP mission to Venus incorporating rovers, aircraft, and orbiters. This mission baselined use of a future radioisotope power system that would be used to both refrigerate the inside of a rover against the Venus environment, and also provide power [Landis 2004].

In 2010, the GRC Innovative Partnerships Program (IPP) studied a combination of human and robotic mission to Venus, HERRO-Venus, in which a crew vehicle in Venus orbit operates a rover on the surface via teleoperation, allowing virtual presence on the surface. This study, also done by the GRC COMPASS team, an interdisciplinary spacecraft design and optimization team that has the capability of doing end to end mission design and analysis. For this mission, the COMPASS team did a conceptual design of a highly-capable rover design with the ability to operate for extended periods in the Venus environment [Landis *et al.* 2012]. While the rover vehicle designed (shown in Figure 2.2) was highly capable, the design was for a total rover mass of 1059 kg (including anticipated mass growth allowance), intended for a 2039 launch date. Like the earlier RASC study, the design study assumed the availability of

Radioisotope Stirling power and cooling, which is currently being developed, and required 16 plutonium (Pu) GPHS bricks to provide the thermal input, an amount that exceeds the amount of plutonium currently available for planetary science missions.

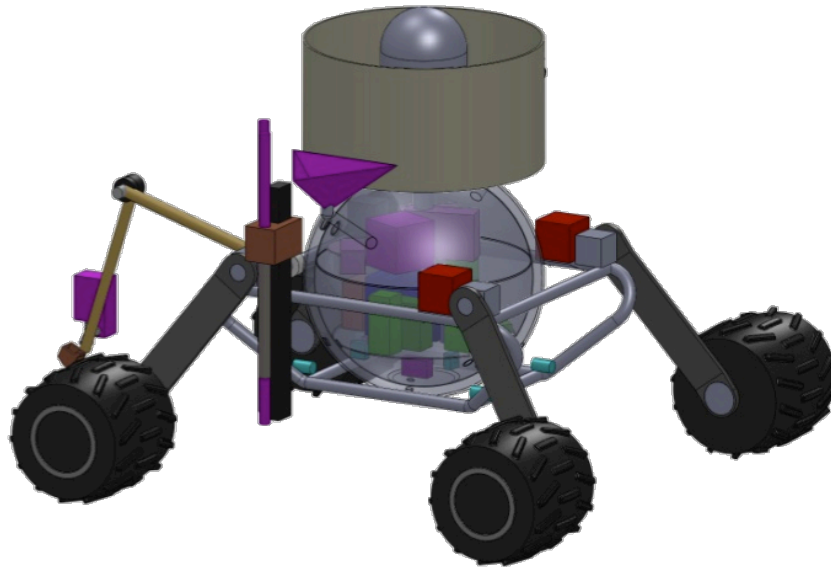


Figure 2.2—Conceptual design for a large Venus rover incorporating a radioisotope power system for the “HERRO-Venus” design study (from Landis *et al.* 2012).

#### 2.1.4 Wind on Venus

Venus is a planet with exceptional high-altitude winds, but the wind speed decreases with altitude. Nevertheless, the wind speeds at the surface are not zero, and the high density of the atmosphere means that, although the speeds are low, a significant amount of force is produced.

The first wind measurements on the Venus surface were done with the Soviet Venera 9 and Venera 10 landers [Keldysh 1977, Basilevsky and Head 2003], showing surface wind speeds in the range of 0.4 to 1.3 m/s. No anemometers were flown on later Venera landers, but a wind speed was determined on two later Venera landers from acoustic measurements made by a microphone [Ksanfomaliti *et al.* 1983]. The four Venera landers that measured surface wind speeds found average wind speed of 0.4 to 0.7 m/sec (Venera 9), 0.8 to 1.3 m/sec (Venera 10), 0.3 to 0.6 m/sec (Venera 13), and 0.3 to 0.6 m/sec (Venera 14) [Garvin, Head, Zuber and Helfenstein 1984, Marov 1978]. This is a remarkably consistent surface wind of 0.6 m/sec plus or minus 0.3, (with the Venera 10 value slightly less than two standard deviations high). Wind streaks associated with craters and other landforms also indicate nonzero winds at the surface.

The speed at the surface has also been extrapolated from Doppler wind measurements of the radio signals from atmospheric descent probes, most notably the Veneras, and to a lesser extent from the Pioneer Venus Probes. The variability over a Venus day, as well as changes in direction, if any, is not known

From the Venus atmospheric density at the surface,  $64.8 \text{ kg/m}^3$  (compared to  $1.225 \text{ kg/m}^3$  at Earth’s surface), the momentum density in the wind can be estimated, and using this, the force that can be produced on a sail can be estimated.

## 2.2 Assumptions and Approach

### 2.2.1 Report Perspective and Disclaimer

This report is meant to capture the study performed by the COMPASS Team, recognizing that the level of effort and detail found in this report will reflect the limited depth of analysis that was possible to achieve

during a concept design session. All of the data generated during the design study is captured within this report in order to retain it as a reference for future work.

### 2.2.2 Report Assumptions

The assumptions and requirements about the Venus Landsailer, including those that were known prior to starting the COMPASS design study session, are shown in Table 2.1. This table gathers the assumptions and requirements and calls out trades that were considered during the course of the design study, and off-the-shelf (OTS) materials that were used wherever possible.

Due to limited time and funding, the design of Zephyr focused only on the Landsailer itself and packaging in an aeroshell. Design of the controlling orbiter was not done in this study. The design was assumed to be based on existing communications satellites of similar capability, and is not considered to be a large challenge, except in the design of a smart control system for the rover.

Table 2.1—Assumptions and Study Requirements

Item	Requirements / Assumptions	Trades
<b>Top-Level</b>	1 month Venus Landsailer for scientific exploration of Venus, 1 km transit Figures of merit (FOMs): Surface duration, Science collected, Science data returned, Cost	Science approach, duration, fuel
<b>System</b>	Identify new technologies, technology readiness level (TRL) 6 cutoff 2018, 2025 launch year, single fault tolerant. Earth directed, orbiter controlled, operations for 30 days on Venus surface, 1 km traverse Mass Growth per to AIAA S-120-2006 (add growth to make system level 30%)	
<b>Mission, Ops, GN&amp;C</b>	Direct to Venus, $C_3 = 7 \text{ km}^2/\text{s}^2$ , $-10^\circ$ entry angle, genesis aeroshell, parachute to remove aeroshell and backshell, fixed drag-flap to slow landing speed, navcams, accelerometers, tilt sensors data sent to orbiter for logic	
<b>Launch Vehicle</b>	Atlas 401 class Launch Loads: Axial SS $\pm 4.5g$ , Lateral $\pm 1g$	
<b>Science</b>	Comparable to Mars Exploration Rovers Requirement for ambient temperature operation	Placement of instruments, number of images
<b>Propulsion</b>	Landsailer: $12 \text{ m}^2$ unfoldable sail, lift for 'sailing' $<50^\circ$ to wind direction, Winds estimated from Venera 10 at least 0.4 m/s up to 1.3 m/s, sail feathered when not in use, sail pointed to keep speeds $\sim 4 \text{ cm/s}$ , 1 m diameter wheels to reduce rolling friction/avoid debris Orbiter: Solid rocket for insertion, monoprop for control	Solid Wing Sail versus fabric versus combined, linear versus rotating ambient motors
<b>Power</b>	$\sim 100 \text{ W}$ from $12 \text{ m}^2$ of solar cells (0.33% eff at $460^\circ\text{C}$ , $8.7 \text{ W/m}^2$ ) mounted on sail, 1 day of battery storage, NaS batteries, 70% depth of discharge (DOD)	Batteries only versus Solar Cells versus wind turbine
<b>Avionics/ Communications</b>	Control from orbiter for all operations using simple instruments, cameras, switches, motors – only 'fixed' logic on Landsailer (simpler than Apollo Guidance Computer), 2 kbps data rates for landed science, <i>no</i> onboard storage (science/housekeeping sent to orbiter as collected), 10 W (RF) ultra high frequency (UHF) to orbiter. Yagi antenna integral to sail	Bluetooth controllers to eliminate feedthroughs
<b>Thermal &amp; Environment</b>	External Venus temperatures 90 bar/ $460^\circ\text{C}$ max, all components designed for ambient Venus. 3.6 m Aeroshell base on $-10^\circ$ entry angle and Genesis	Aeroshell size
<b>Mechanisms</b>	Deployable Legs with 3 wheels, deployable, pointable X-band antenna, Aeroshell and cruise deck separations	Number, size of wheels, deployment
<b>Structures</b>	$\sim 5g$ launch, $40g$ entry and $5g$ landing loads, all metallic, all components rated for Venus ambient	What pressure for cold box? Trade 1 bar versus 90 bar spacecraft (S/C)
<b>Cost</b>	New Frontiers Assumptions, costing in FY-2015 dollars	Discovery and New Frontiers assumptions
<b>Risk</b>	Major Risks: high temp mechanisms/gimbals, landing	Level of fault tolerance on major systems

## 2.3 Study Summary Requirements

### 2.3.1 Figures of Merit

Figures of merit help guide the subsystem designers into what is most important for the vehicle being designed (say cost cap versus science return.) In the case of the Venus Landsailer mobility and science return were deemed most important while keeping the total launch mass low.

## 2.4 Growth, Contingency, and Margin Policy

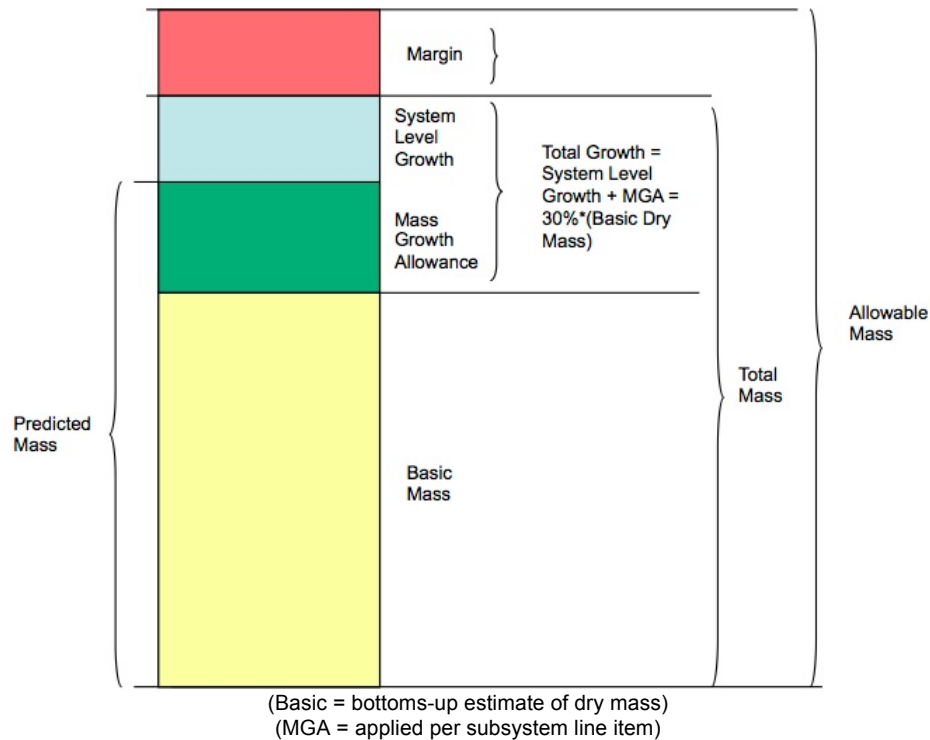


Figure 2.3—Graphical illustration of the definition of basic, predicted, total and allowable mass.

### 2.4.1 Terms and Definitions

**Mass**

*The measure of the quantity of matter in a body.*

**Basic Mass (aka CBE Mass)**

*Mass data based on the most recent baseline design. This is the bottoms-up estimate of component mass, as determined by the subsystem leads.*

*Note 1: This design assessment includes the estimated, calculated, or measured (actual) mass, and includes an estimate for undefined design details like cables, multi-layer insulation, and adhesives.*

*Note 2: The mass growth allowances (MGA) and uncertainties are not included in the basic mass.*

*Note 3: COMPASS has referred to this as current best estimate (CBE) in past mission designs.*

*Note 4: During the course of the design study, the COMPASS Team carries the propellant as line items in the propulsion system in the Master Equipment List (MEL). Therefore, propellant is carried in the basic mass listing, but MGA is **not** applied to the propellant. Margins on propellant are handled differently than they are on dry masses.*

	<b>CBE Mass</b>	<i>See Basic Mass.</i>
<b>Dry Mass</b>		<i>The dry mass is the total mass of the system or S/C when no propellant is added.</i>
<b>Wet Mass</b>		<i>The wet mass is the total mass of the system, including the dry mass and all of the propellant (used, predicted boil-off, residuals, reserves, etc.). It should be noted that in human S/C designs the wet masses would include more than propellant. In these cases, instead of propellant, the design uses Consumables and will include the liquids necessary for human life support.</i>
<b>Inert Mass</b>		<i>In simplest terms, the inert mass is what the trajectory analyst plugs into the rocket equation in order to size the amount of propellant necessary to perform the mission delta-Velocities (<math>\Delta V</math>s). Inert mass is the sum of the dry mass, along with any non-used, and therefore trapped, wet materials, such as residuals. When the propellant being modeled has a time variation along the trajectory, such as is the case with a boil-off rate, the inert mass can be a variable function with respect to time.</i>
<b>Basic Dry Mass</b>		<i>This is basic mass (aka CBE mass) minus the propellant or wet portion of the mass. Mass data is based on the most recent baseline design. This is the bottoms-up estimate of component mass, as determined by the subsystem leads. This does not include the wet mass (e.g., propellant, pressurant, cryo-fluids boil-off, etc.).</i>
<b>CBE Dry Mass</b>		<i>See Basic Dry Mass.</i>
<b>Mass Growth Allowance (MGA)</b>		<i>MGA is defined as the predicted change to the basic mass of an item based on an assessment of its design maturity, fabrication status, and any in-scope design changes that may still occur.</i>
<b>Predicted Mass</b>		<i>This is the basic mass plus the mass growth allowance for to each line item, as defined by the subsystem engineers.</i>  <i>Note: When creating the MEL, the COMPASS Team uses Predicted Mass as a column header, and includes the propellant mass as a line item of this section. Again, propellant is carried in the basic mass listing, but MGA is not applied to the propellant. Margins on propellant are handled differently than they are handled on dry masses. Therefore, the predicted mass as listed in the MEL is a wet mass, with no growth applied on the propellant line items.</i>
<b>Predicted Dry Mass</b>		<i>This is the predicted mass minus the propellant or wet portion of the mass. The predicted mass is the basic dry mass plus the mass growth allowance as the subsystem engineers apply it to each line item. This does not include the wet mass (e.g., propellant, pressurant, cryo-fluids boil-off, etc.).</i>
<b>Mass Margin (aka Margin)</b>		<i>This is the difference between the allowable mass for the space system and its total mass. COMPASS does not set a Mass Margin, it is arrived at by subtracting the Total mass of the design from the design requirement established at the start of the design study such as Allowable Mass. The goal is to have Margin greater than or equal to zero in order to arrive at a feasible design case. A negative mass margin would indicate that the design has not yet been closed and cannot be considered feasible. More work would need to be completed.</i>





**System-Level Growth**

*The extra allowance carried at the system level needed to reach the 30% aggregate MGA applied growth requirement.*

*For the COMPASS design process, an additional growth is carried and applied at the system level in order to maintain a total growth on the dry mass of 30%. This is an internally agreed upon requirement.*

*Note 1: For the COMPASS process, the total growth percentage on the basic dry mass (i.e., not wet) is:*

$$\text{Total Growth} = \text{System Level Growth} + \text{MGA} * \text{Basic Dry Mass}$$

$$\text{Total Growth} = 30\% * \text{Basic Dry Mass}$$

$$\text{Total Mass} = 30\% * \text{Basic Dry Mass} + \text{basic dry mass} + \text{propellants.}$$

*Note 2: For the COMPASS process, the system level growth is the difference between the goal of 30% and the aggregate of the MGA applied to the Basic Dry Mass.*

$$\text{MGA Aggregate \%} = (\text{Total MGA mass} / \text{Total Basic Dry Mass}) * 100$$

*Where Total MGA Mass = Sum of (MGA% \* Basic Mass) of the individual components*

$$\text{System Level Growth} = 30\% * \text{Basic Dry Mass} - \text{MGA} * \text{Basic Dry Mass} = (30\% - \text{MGA aggregate \%}) * \text{Basic Dry Mass}$$

*Note 3: Since CBE is the same as Basic mass for the COMPASS process, the total percentage on the CBE dry mass is:*

$$\text{Dry Mass total growth} + \text{dry basic mass} = 30\% * \text{CBE dry mass} + \text{CBE dry mass.}$$

*Therefore, dry mass growth is carried as a percentage of dry mass rather than as a requirement for launch vehicle performance, etc. These studies are Pre-Phase A and considered conceptual, so 30% is standard COMPASS operating procedure, unless the customer has other requirements for this total growth on the system.*

**Total Mass**

*The summation of basic mass, applied MGA, and the system-level growth.*

**Allowable Mass**

*The limits against which margins are calculated.*

*Note: Derived from or given as a requirement early in the design, the allowable mass is intended to remain constant for its duration.*

Table 2.2 expands definitions for the MEL column titles to provide information on the way masses are tracked through the MEL used in the COMPASS design sessions. These definitions are consistent with those above in Figure 2. and in the terms and definitions. This table is an alternate way to present the same information to provide more clarity.

Table 2.2—Definition of Masses Tracked in the Master Equipment List

CBE mass	MGA growth	Predicted mass	Predicted dry mass
Mass data based on the most recent baseline design (includes propellant)	Predicted change to the basic mass of an item phrased as a percentage of CBE dry mass	The CBE mass plus the MGA	The CBE mass plus the MGA — propellant
CBE dry + propellant	MGA% * CBE dry = growth	CBE dry + propellant + growth	CBE dry + growth

**2.4.2 Mass Growth**

The COMPASS Team normally uses the AIAA S-120-2006, “Standard Mass Properties Control for Space Systems,” as the guideline for its mass growth calculations. Table 2.3 shows the percent mass growth of a piece of equipment according to a matrix that is specified down the left-hand column by level of design maturity and across the top by subsystem being assessed.

The COMPASS Team’s standard approach is to accommodate for a total growth of 30% or less on the dry mass of the entire system. The percent growth factors shown above are applied to each subsystem before an additional growth is carried at the system level, in order to ensure an overall growth of 30%. Note that for designs requiring propellant, growth in the propellant mass is either carried in the propellant calculation itself or in the  $\Delta V$  used to calculate the propellant required to fly a mission.

In Table 2.3, a timeline shows how the various mass margins are reduced and consolidated over the mission’s life span. The system-integration engineer carries a system-level MGA, called “margin”, in order to reach a total system MGA of 30%. This is shown as the mass growth for the allowable mass on the authority to precede line in mission time. After setting the margin of 30% in the preliminary design, the rest of the steps shown below are outside the scope of the COMPASS Team.

Table 2.3—MGA and Depletion Schedule (AIAA S-120-2006)

Major category	Maturity code	Design maturity (basis for mass determination)	MGA (%)												
			Electrical/electronic components			Structure	Brackets, clips, hardware	Battery	Solar array	Thermal control	Mechanisms	Propulsion	Wire harness	Instrumentation	ECLSS, crew systems
			0 to 5 kg	5 to 15 kg	>15 kg										
E	1	<b>Estimated</b> (1) An approximation based on rough sketches, parametric analysis, or undefined requirements; (2) A guess based on experience; (3) A value with unknown basis or pedigree	30	25	20	25	30	25	30	25	25	25	55	55	23
	2	<b>Layout</b> (1) A calculation or approximation based on conceptual designs (equivalent to layout drawings); (2) Major modifications to existing hardware	25	20	15	15	20	15	20	20	15	15	30	30	15
C	3	<b>Prerelease designs</b> (1) Calculations based on a new design after initial sizing but prior to final structural or thermal analysis; (2) Minor modification of existing hardware	20	15	10	10	15	10	10	15	10	10	25	25	10
	4	<b>Released designs</b> (1) Calculations based on a design after final signoff and release for procurement or production; (2) Very minor modification of existing hardware; (3) Catalog value	10	5	5	5	6	5	5	5	5	5	10	10	6
A	5	<b>Existing hardware</b> (1) Actual mass from another program, assuming that hardware will satisfy the requirements of the current program with no changes; (2) Values based on measured masses of qualification hardware	3	3	3	3	3	3	3	2	3	3	5	5	4
	6	<b>Actual mass</b> Measured hardware	No mass growth allowance—Use appropriate measurement uncertainty values												
	7	<b>Customer furnished equipment or specification value</b>	Typically a “not-to-exceed” value is provided; however, contractor has the option to include MGA if justified												

### 2.4.3 Power Growth

The COMPASS Team typically uses a 30% growth on the bottoms-up power requirements of the bus subsystems when modeling the amount of required power. The electric propulsion subsystem applies a 5% growth to the power requirements needed for the electric thrusters. No additional margin is carried on top of this power growth. The power system assumptions for this study will be show in in Table 3.5 in Section 3.6.3 on the Power Equipment List (PEL).

## 3.0 BASELINE DESIGN

### 3.1 Concept Drawing and Description

Figure 3.1 shows perspective views of the Zephyr vehicle, as deployed on the surface. The sail provides propulsive force, as well as serving as a substrate for mounting of a solar array. Note the relatively large size of the sail to gain enough force to propel the Landsailer as well as carry the solar arrays. The wheels are also large to reduce the force to climb over rocks. The wheelbase is wide for stability, as shown in Figure 3.2.

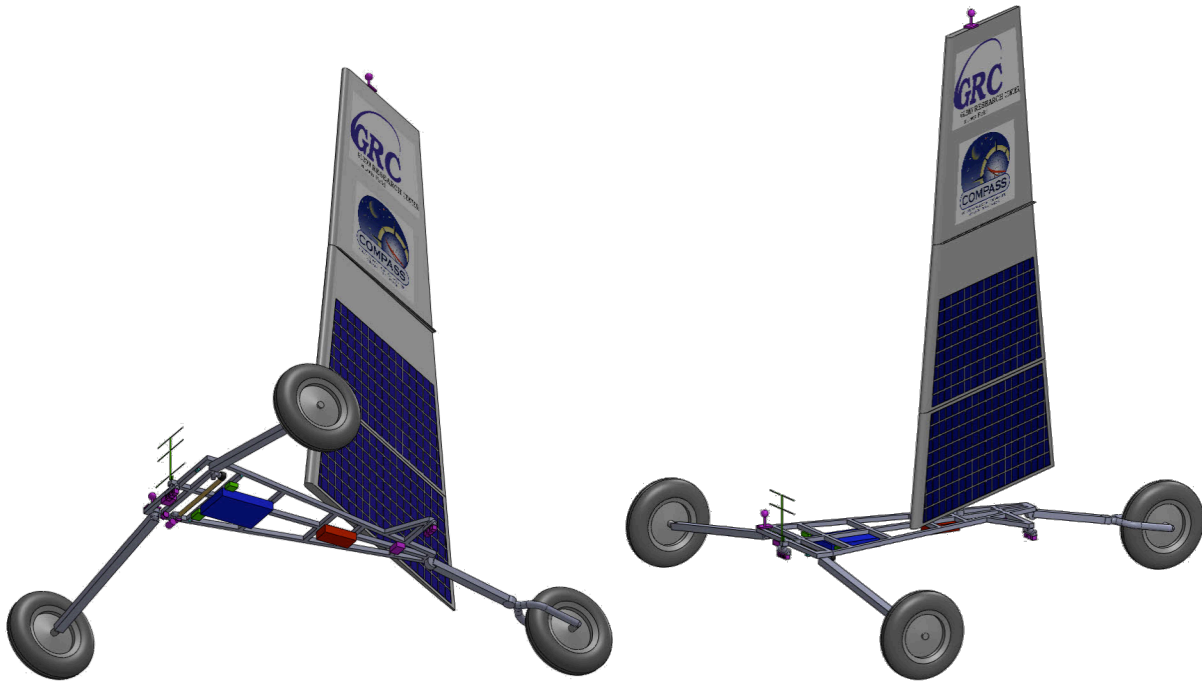


Figure 3.1—Perspective views of the Zephyr Venus Rover as deployed on the surface.

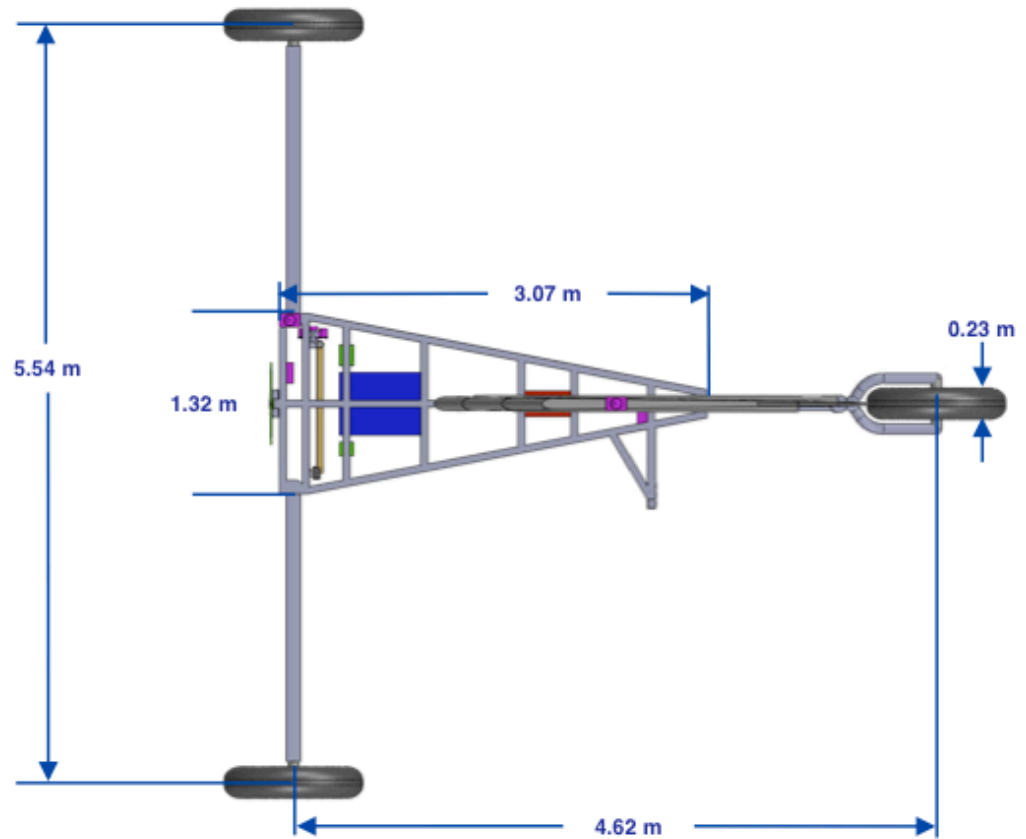


Figure 3.2—Dimensioned view of rover chassis viewed from below, showing wheelbase.

In comparison to the sail, the instrumentation and control for the rover is comparatively small. The components of the Landsailer are shown by subsystem in **Error! Reference source not found.**Figure 3.3.

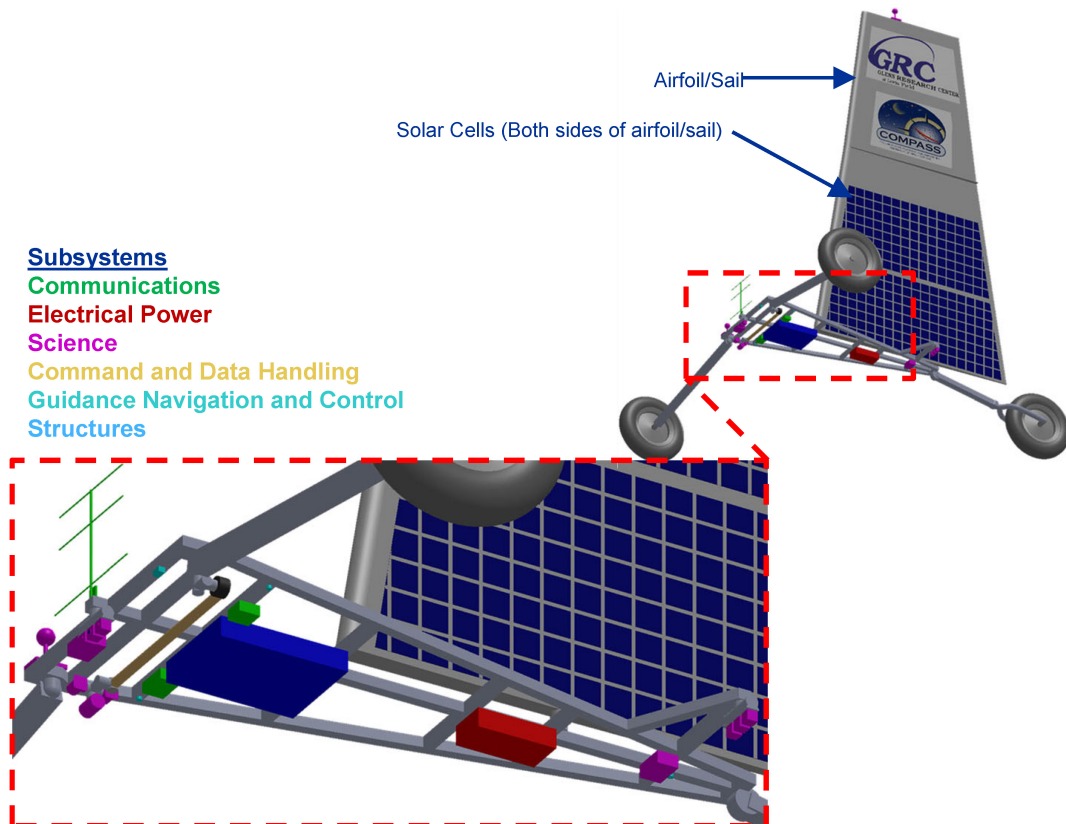


Figure 3.3—Landsailer subsystem components.

### 3.2 Landsailer in Stowed Configuration

The Venus rover must be designed to stow within the aeroshell for entry into the Venus atmosphere, and be designed for the components that require deployment to be deployed throughout the various phases of descent and landing.

An aeroshell based on the Genesis mission design was selected for this design and was scaled up to a maximum external diameter of 3.6-m with a maximum internal diameter of 3.39-m. This was done to create the necessary volume for the required sail area and tire diameter to feasibly be stowed within the aeroshell. Figure 3.4 shows the overall basic dimensions of the aeroshell used during the study as well as two other elevation views of the Venus Landsailer stowed within the aeroshell. Two isometric views of the stowed Venus Landsailer within the aeroshell can be seen in Figure 3.4.

Those components that require deployment prior to and after landing on the Venusian surface include the three sections of the rigid airfoil that comprises the sail, the wheels and their associated booms, the Yagi antenna, and a robotic arm containing some of the science instrumentation. Once the backshell is jettisoned during descent, the wheels and Yagi antenna will deploy while the sail will deploy after the Venus Landsailer has safely landed. The robotic arm will be deployed once the Landsailer arrives at a suitable location for science. Figure 3.5 shows a top and bottom view of the Landsailer in its stowed configuration.

The Yagi antenna is attached to the front of the Landsailer chassis frame and is angled inward to allow it to fit within the aeroshell. Once the backshell is jettisoned upon descent, the Yagi antenna will spring to an upright position.

The single rear wheel is located out on a boom that is angled underneath the chassis frame when stowed, placing the wheel below the middle of the chassis. A spring lock mechanism deploys the boom containing

the rear wheel once the backshell is jettisoned. Both front wheels are also located on booms that are stowed back along the sides of the chassis. In order to fit within the aeroshell, each of the front wheels is stowed so that the wheels are parallel with their respective booms. Once the backshell is jettisoned, each off the booms will deploy utilizing a single axis mechanism that will swing the booms outwards to their deployed location. Each wheel is then rotated by a mechanism, located where the boom interfaces to the wheel, to its fully deployed and operational orientation. The robotic arm is composed of one member (no elbow) and is stowed underneath the front of the chassis frame. Finally, the airfoil is split into three sections attached to one another by hinges that run across the entire chord length. When stowed, the airfoil is folded down so that the sections are stacked on top of one another on top of the chassis frame. Once landed on the surface, the hinges will deploy the entire airfoil upright to its fully deployed position. The various stages of deployment can be seen in Figure 3.6.

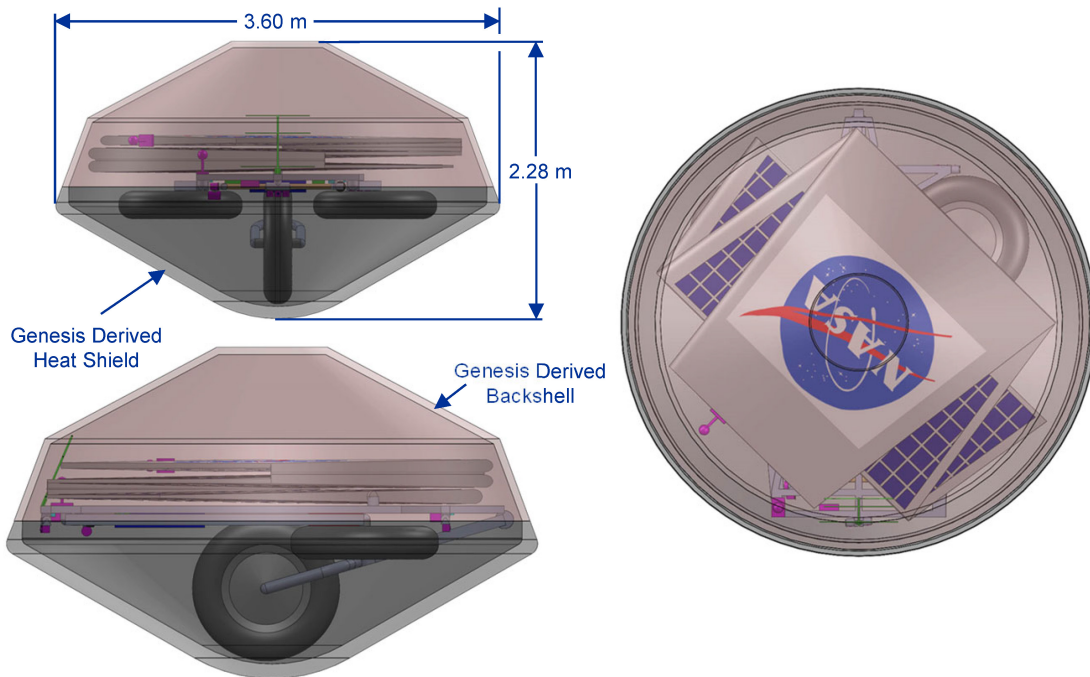


Figure 3.4—Venus Landsailer stowed within the aeroshell.

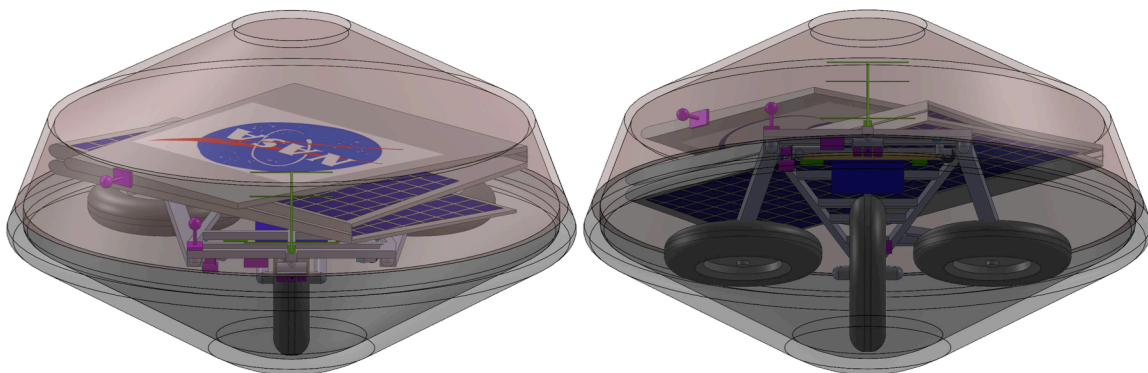


Figure 3.5—Isometric views of the Venus Landsailer stowed within the aeroshell.

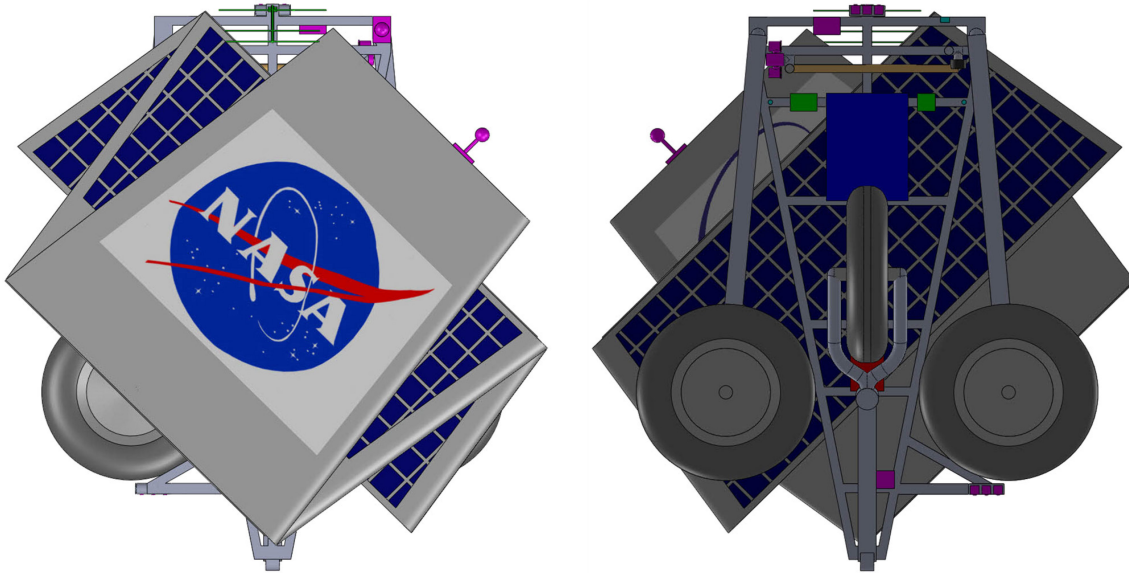


Figure 3.6—Landsailer in its stowed configuration.

### 3.3 Concept of Operations (CONOPS)

#### 3.3.1 Interplanetary Cruise and Venus Entry

During the cruise to Venus, Zephyr will remain in a dormant state most of the time. Occasionally, it will be activated for a health check, then deactivated. This in-flight checkout would last between 3 and 4 hr and would follow as closely as possible the preprogrammed descent scenario.

Zephyr is installed on the Orbiter by a support structure with guide rails. Spring loaded pyrotechnic devices maintain Zephyr in place on the ring. An umbilical links Zephyr to the Orbiter and provides all electrical connections—power, radio frequency (RF) link, and temperature monitoring—between Zephyr and the Orbiter when they are attached during the cruise.

Prior to the Probe separation from the Orbiter, a final health-check will be performed. Upon firing at Zephyr separation, the umbilical will be disconnected and Zephyr will separate from the Orbiter with a small relative velocity of  $\sim 0.3$  m/s and a spin of  $\sim 7$  RPM.

Once Zephyr is released from the Orbiter it will then enter a coast phase **Error! Reference source not found.** Zephyr will coast to Venus atmospheric entry with no possibility of changing the attitude parameters acquired at separation. At the end of the coast period, the Probe will be switched *on* via on-board sensing of the g-load experienced during atmospheric entry.

After Zephyr separation, the Orbiter will initiate a maneuver to avoid Venus impact, placing itself on a trajectory for Venus Orbit Insertion (VOI). On reaching VOI, the Orbiter will propulsively brake into a highly eccentric orbit around the planet. This orbit will have a 24 hr period, permitting communication with the Zephyr for 12 to 18 hr during each orbit.

#### 3.3.2 Zephyr Entry, Descent, and Landing and Post-Landing CONOPS

The entry, descent, and landing (EDL) sequence is shown in schematic in Figure 3.7. This is similar to the EDL sequence used on Mars rovers, except that the thicker atmosphere allows a parachute landing directly on the wheels (as discussed in the detailed design section).

Figure 3.8 shows the stages of deployment of the vehicle following the jettisoning of the backshell: in its original folded state; with its wheels unfolded during parachute descent, with the sail deployed after landing, and finally in its science-operations, with the science arm deployed on the surface.

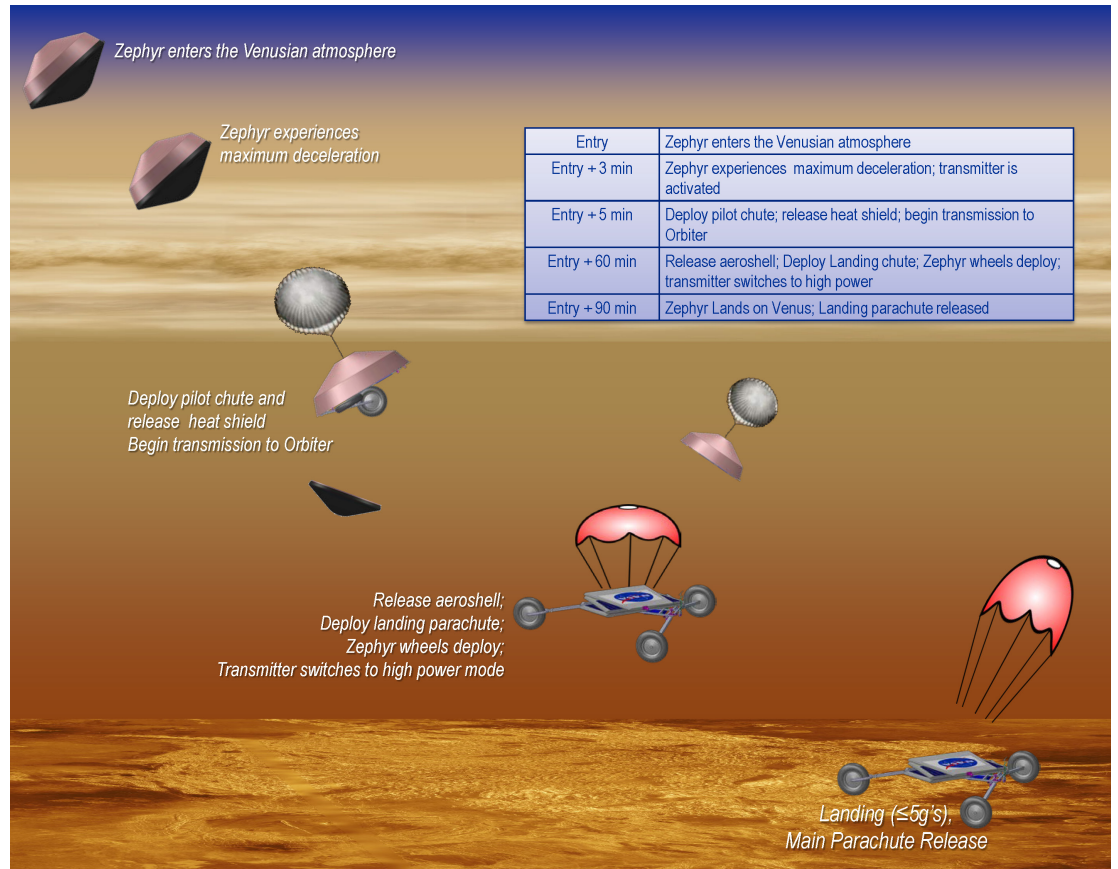


Figure 3.7—Notional entry, descent and landing profile.

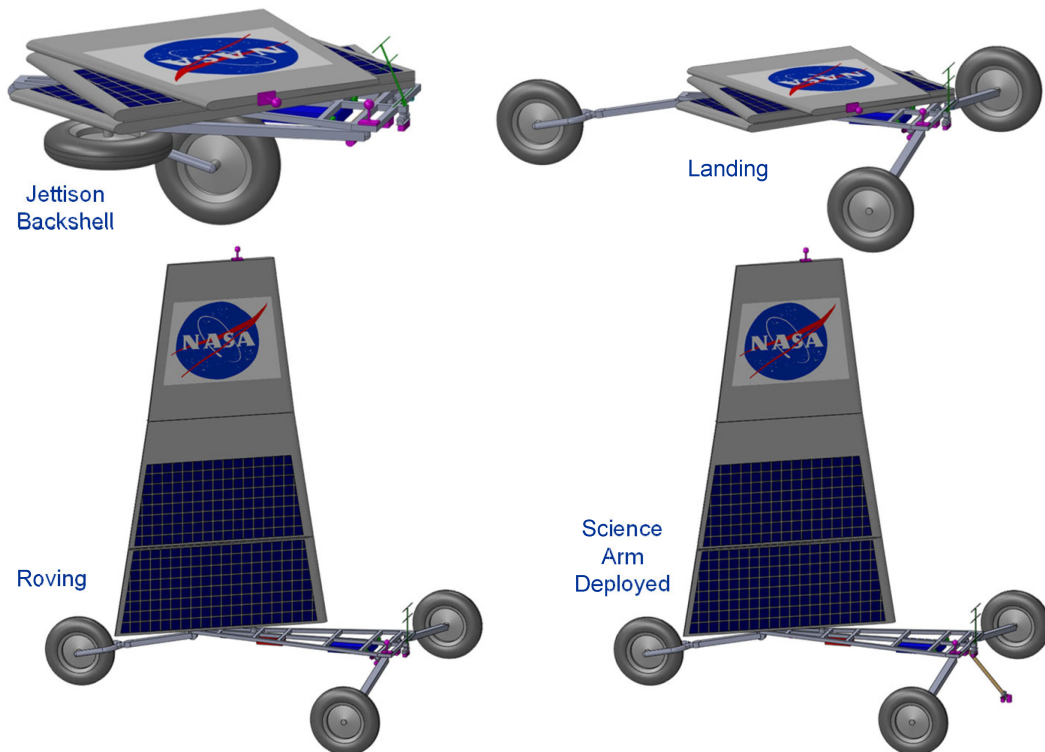


Figure 3.8—Various stages of deployment for the Venus Landsailer.



### 3.3.3 Zephyr Post-Landing CONOPS

Following the landing, commissioning of the rover and initial locomotion follows:

- Orbiter acquires Zephyr and commands deployment of sail/antennas/cameras/weather station, as needed
- Commissioning—panorama image returned to Earth via Orbiter
- Ground Team inspects local panorama and wind conditions (Traverse – 60 min)
- Ground Team selects initial traverse plan based on pre-planning and Zephyr data

Once the rover is operational, daily operation follows the flow chart shown in Figure 3.9. The operations phase will be divided into three segments:

- When the satellite is above the horizon (assumed 16 hr per 24-hr orbit), we will do 8 hr of traverse and 8 hr of science.
- When the satellite is not high above the horizon, we will do 8 hr of charging.

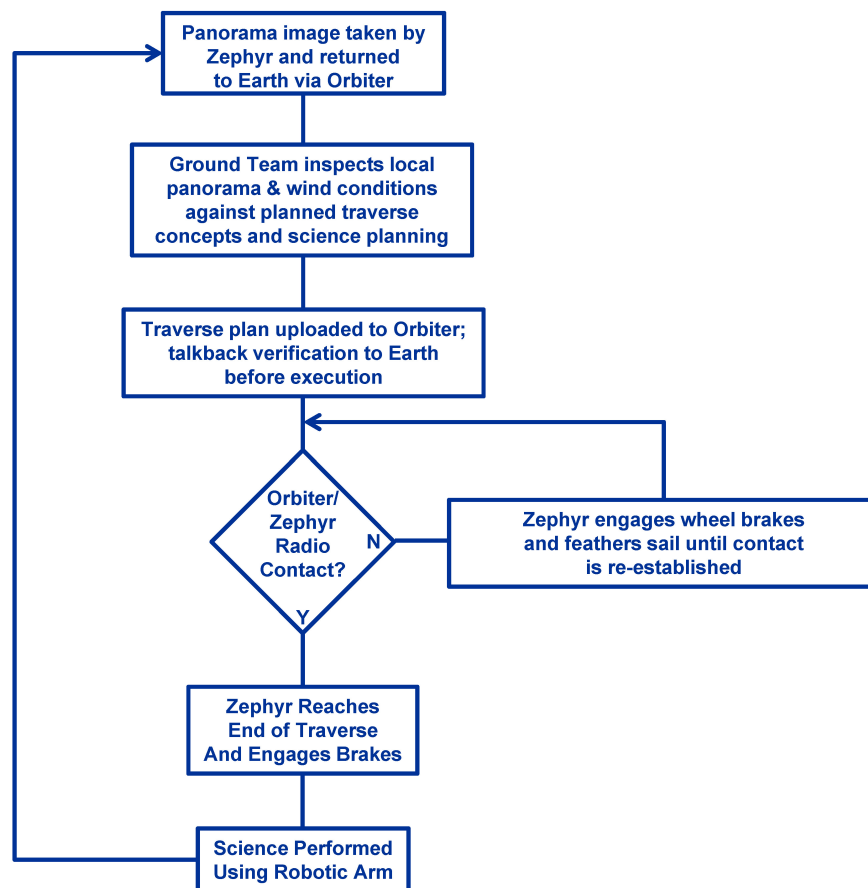


Figure 3.9—Zephyr transverse options.

Each traverse will include 1 hr of sailing, and 7 hr of analyzing the position and planning the next drive. The operations consist of:

- Ground Team inspects local panorama and wind conditions (Traverse – 60 min)
- Ground Team selects traverse plan based on preplanning and Zephyr data
  - Traverse plan uploaded to Orbiter; talkback verification to Earth before execution

- Zephyr traverse commanded/controlled by Orbiter
  - Traverse occurs only during Orbiter contact
  - No carrier received from Orbiter, Zephyr engages wheel brakes and feathers sail
- Heading (limit head to  $\pm 45^\circ$  w.r.t. to wind)
- Distance (up to 30 m)
- Set steering and sail positions ( $\pm 180^\circ$  sail direction)
- Release brakes
- Count wheel rotations
- Engage brake
  - Option to use a science arm as anchor
- Science return through Orbiter during Traverse; Orbiter also records data.
- Contingency options
  - Sense if tipping (tilt sensor)—release sail and turn into wind
  - Sense if stuck on obstacle (wheel sensor)—release sail
- Sailing (<1 hr/day)
- One day traverse (~30 m/day)
  - Total traverse comprised of multiple legs

### 3.3.4 Venus Environmental Details

The harsh environment of Venus provides a number of challenges in the operation of equipment and materials. The atmosphere is composed of mainly Carbon Dioxide, but does contain corrosive components, such as droplets of sulfuric acid in the cloud layers above the planet. The planet has a very thick atmosphere, completely covered with clouds. The temperature and pressure near the surface is 455 °C at 90 Bar. Figure 2.7 shows the properties of the Venus atmosphere. Figure 2.8 shows the various layers of the Venus atmosphere.

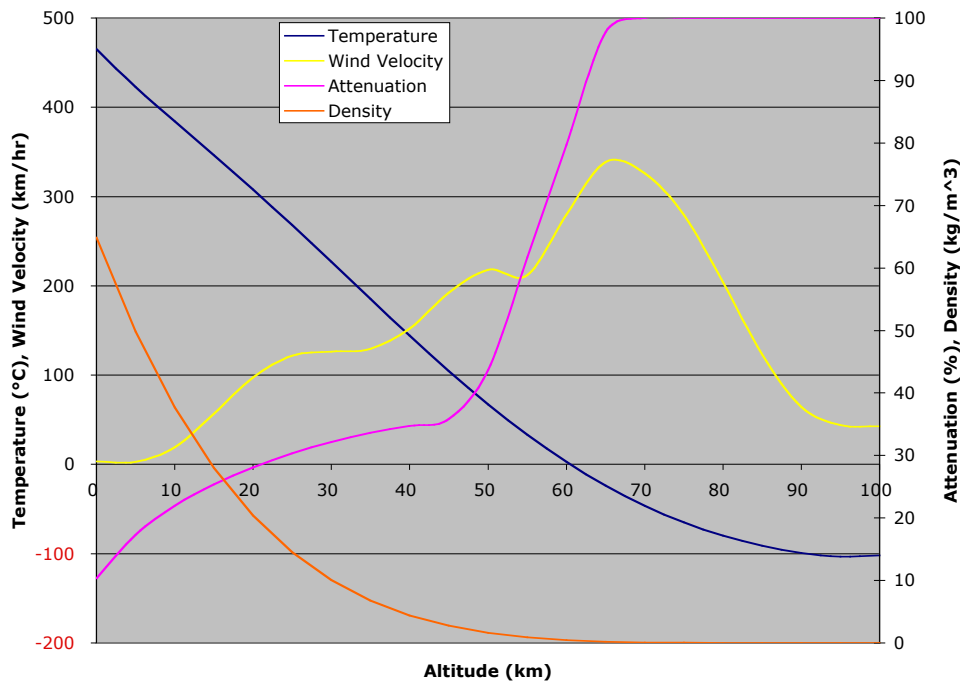


Figure 3.10—Properties of the Venus Atmosphere

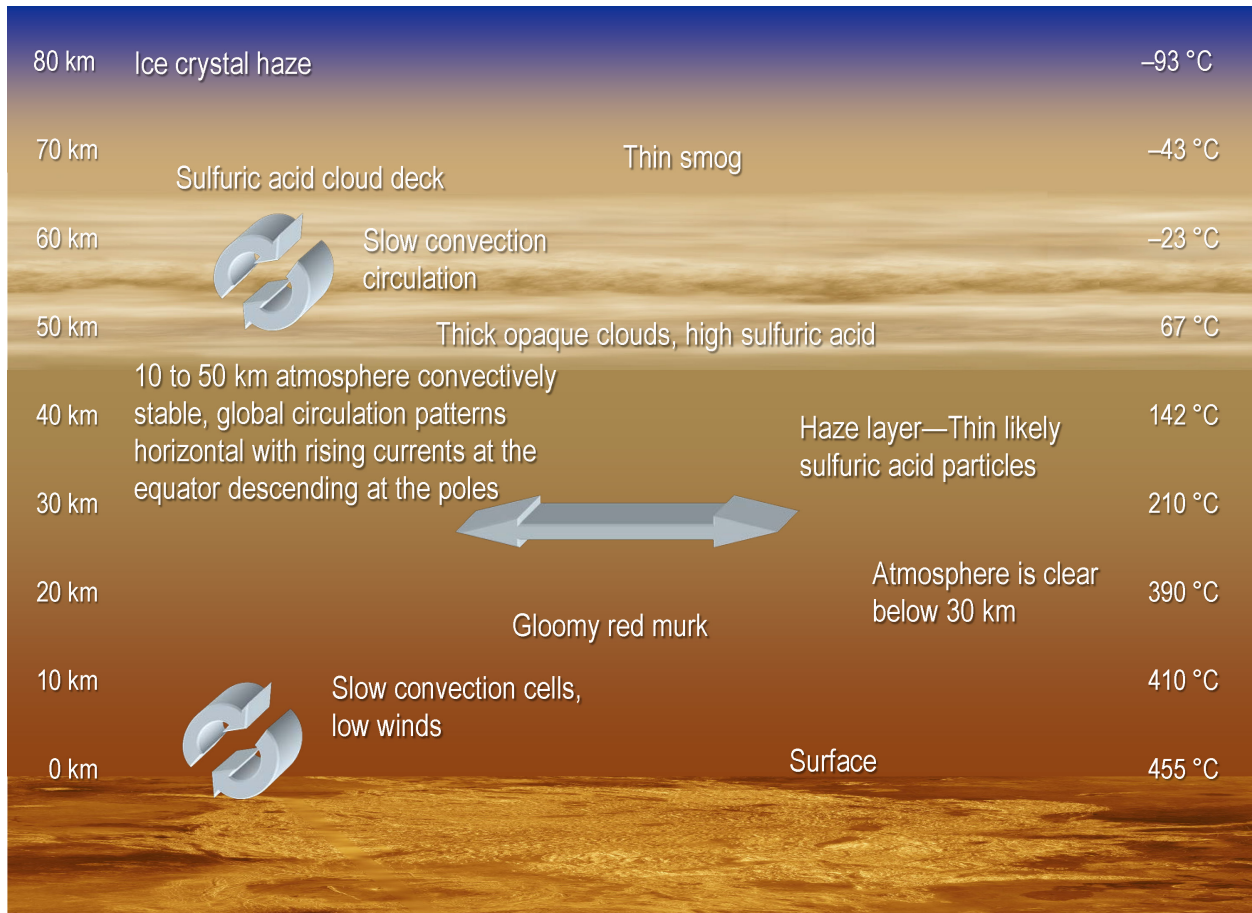


Figure 3.11—Venus atmosphere structure

### 3.4 System-Level Summary

The system block diagram that captures the components of the Venus Landsailer design is shown in Figure 3.12. The three main modules are shown: the Landsailer, the Aeroshell, and the Orbiter. As mentioned previously the focus of the design was on the Venus Landsailer and the other two modules were scaled.

The Landsailer includes a sail, wheels and motors for mobility. Other motors are used for deployment of the vehicle components. Solar arrays and batteries are connected to the other systems by the power management and distribution (PMAD). Steering is controlled by the orbiter through a communications link that also controls all of the other systems. Four science instruments are carried by Zephyr: a PanCam sensor, weather station (anemometer, pressure and temperature), X-rad diffraction sensor, and a grinder motor.

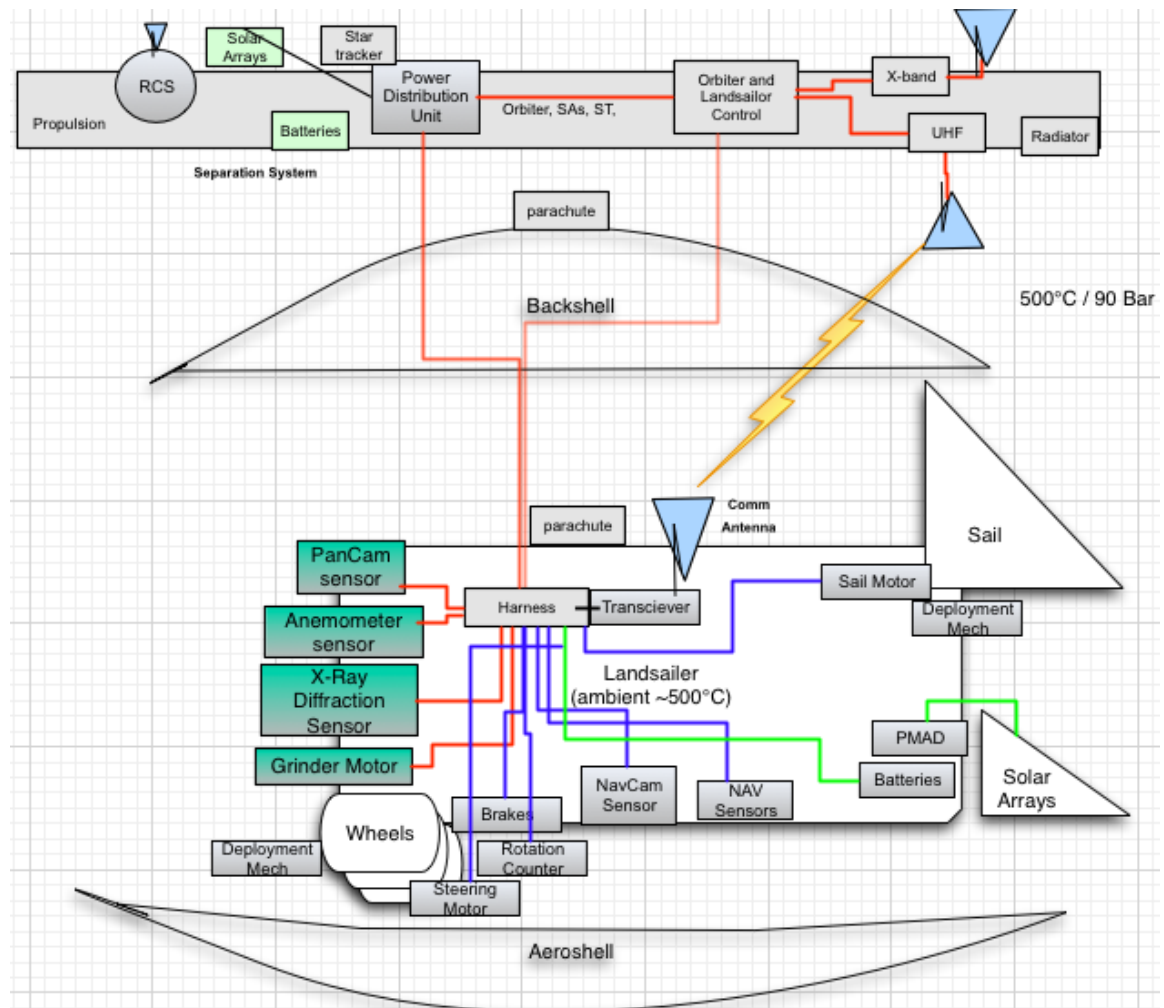


Figure 3.12—Venus Landsailer block diagram.

### 3.5 Orbiter and Aeroshell

#### 3.5.1 Orbiter

The configuration design of the Zephyr study focused primarily on the Landsailer in its deployed state as it would be in while functioning on the surface of Venus, and in its stowed state within the aeroshell. Computer aided design (CAD) models of the cruise stage/orbiter were not created during this study, nor were the issues associated with integration of the cruise stage with the launch vehicle studied.

Since the Landsailer was the focus of the design study, the orbiter and aeroshell were scaled based on similar past designs.

Table 3.1—Zephyr Landsailer Orbiter Master Equipment List

WBS Number	Description	QTY	Unit Mass (kg)	Basic Mass (kg)	Growth (%)	Growth (kg)	Total Mass (kg)
06	Case #1 Venus Landsailer CD-2013-86			1581.03	18.7%	295.74	1876.77
	Venus Landsailer System						
06.3	Orbiter			1058.49	15.9%	167.88	1226.37
06.3.1	Cruise Deck			956.00	15.4%	147.60	1103.60
06.3.1.a	Cruise Deck (ALIVE)			956.00	15.4%	147.60	1103.60
06.3.6	Thermal Control (Non-Propellant)			37.49	18.0%	6.75	44.24
06.3.6.a	Active Thermal Control			2.25	18.0%	0.41	2.66
06.3.6.b	Passive Thermal Control			18.02	18.0%	3.24	21.26
06.3.6.c	Semi-Passive Thermal Control (cruise deck and internal)			17.22	18.0%	3.10	20.32

### 3.5.2 Aeroshell

Table 3.2—Zephyr Landsailer Aeroshell Master Equipment List

WBS Number	Description	QTY	Unit Mass (kg)	Basic Mass (kg)	Growth (%)	Growth (kg)	Total Mass (kg)
06	Venus Landsailer System			1581.03	18.7%	295.74	1876.77
06.2	Aeroshell			302.46	27.4%	83.00	385.46
06.2.1	Aeroshell			238.00	30.0%	71.40	309.40
06.2.1.a	Aeroshell (ALIVE)			238.00	30.0%	71.40	309.40
06.2.1.a.a	Aeroshell	1	238.00	238.00	30.0%	71.40	309.40
06.2.6	Thermal Control			64.46	18.0%	11.60	76.06
06.2.6.a	Aeroshield			64.46	18.0%	11.60	76.06
06.2.6.a.a	Ablative Shield	1	64.46	64.46	18.0%	11.60	76.06

### 3.6 Top-Level Design Details

#### 3.6.1 Master Equipment List (MEL)

The Zephyr is required to fit inside of the aeroshell physical volume and to fit inside a total mass allocation set by the launch vehicle and the entry requirements. Table 3.3 shows the MEL listing of the Rover, the aeroshell and the orbiter as the elements of Zephyr.

Table 3.3—Venus Landsailer MEL WBS Format—Baseline Case

WBS Number	Description	Basic Mass (kg)	Growth (%)	Growth (kg)	Total Mass (kg)
06	Venus Landsailer System	1581.03	18.7%	295.74	1876.77
06.1	Landsailer Rover	220.08	20.4%	44.86	264.94
06.1.1	Science Instruments	17.90	39.3%	7.03	24.93
06.1.2	Attitude Determination and Control	2.29	30.0%	0.69	2.98
06.1.3	Command & Data Handling	16.30	41.4%	6.75	23.05
06.1.4	Communications and Tracking	4.00	32.5%	1.30	5.30
06.1.5	Electrical Power Subsystem	32.13	13.8%	4.44	36.57
06.1.6	Thermal Control (Non-Propellant)	1.02	18.0%	0.18	1.20
06.1.7	Propulsion (Sail System)	84.23	16.1%	13.58	97.82
06.1.11	Structures and Mechanisms	63.21	18.0%	11.38	74.59
06.2	Aeroshell	302.46	27.4%	83.00	385.46
06.2.1	Aeroshell	238.00	30.0%	71.40	309.40
06.2.6	Thermal Control	64.46	18.0%	11.60	76.06
06.3	Orbiter	1058.49	15.9%	167.88	1226.37
06.3.1	Cruise Deck	956.00	15.4%	147.60	1103.60
06.3.4	Communications and Tracking	65.00	20.8%	13.53	78.53
06.3.6	Thermal Control (Non-Propellant)	37.49	18.0%	6.75	44.24

#### 3.6.2 Spacecraft Total Mass Summary

The MEL shown in Table 3.4 captures the bottoms-up estimation of CBE and growth percentage of the Zephyr that the subsystem designers calculated for each line subsystem. Section 3.6.2 provides additional detail about the basic and total masses of the different subsystems and of the entire platform after mass growth percentage is applied. In order to meet the total required mass growth of 30%, an allocation is necessary for growth on basic dry mass at the system level, in addition to the growth calculated on each individual subsystem. This additional system-level mass is counted as part of the inert mass to be flown along the required trajectory. Therefore, the additional system-level growth mass impacts the total propellant required for the mission design.

The Zephyr system-level summary for the baseline case, which includes the additional system-level growth, is shown in Table 3.4. With 30% growth on the basic dry mass, the total mass with the 30% growth is 286 kg. The inert mass and dry mass of the Zephyr also shown. After summarizing the bottoms-up masses from Table 3.4, an additional system level growth was applied and shown in Table 3.4. In order to reach the 30% total MGA on basic dry mass required for this study, an additional system-level margin growth mass of 21 kg was carried. This amount is an additional 20% MGA of the basic dry mass. Therefore, the total growth mass of 66 kg (45 + 21) is 30% growth on basic dry mass. With 30% growth

on the basic dry mass, the total mass is 286 kg. Note that there is rounding in this calculation. The inert mass and dry mass of the Zephyr are also shown.

Table 3.4—Baseline Case 1 System Summary

GLIDE details: VenusLandsailer:Venuslandsailer_1					
Spacecraft Master Equipment List Rack-up (Mass) -Case #1 Venus Landsailer CD-2013-86					
WBS	Main Subsystems	Basic Mass (kg)	Growth (kg)	Predicted Mass (kg)	Aggregate Growth (%)
06	Venus Landsailer System	1581.0	295.7	1877	
06.1	Landsailer Rover	220.1	44.9	265	20%
06.1.1	Science Instruments	17.9	7.0	25	39%
06.1.2	Attitude Determination and Control	2.3	0.7	3	30%
06.1.3	Command & Data Handling	15.3	6.3	22	41%
06.1.4	Communications and Tracking	4.0	1.3	5	33%
06.1.5	Electrical Power Subsystem	32.1	4.4	37	14%
06.1.6	Thermal Control (Non-Propellant)	1.0	0.2	1	18%
06.1.7	Propulsion (Sail System)	84.2	13.6	98	16%
06.1.8	Propellant (Chemical) (not Used)	0.0		0	TBD
06.1.9	Propulsion (EP Hardware) (Not Used)	0.0	0.0	0	TBD
06.1.10	Propellant (EP) (Not Used)	0.0		0	TBD
06.1.11	Structures and Mechanisms	63.2	11.4	75	18%
	Element 1 consumables (if used)	1		1	
	Estimated Spacecraft Dry Mass (no propellant or consumables)	220	45	264	20%
	Estimated Spacecraft Wet Mass	220	45	265	
<b>System Level Growth Calculations Landsailer Rover</b>					<b>Total Growth</b>
	Dry Mass Desired System Level Growth	220	66	263	30%
	Additional Growth (carried at system level)		21		10%
	Total Wet Mass with Growth	220	66	286	
06.2	Aeroshell	302.5	83.0	385	27%
06.2.1	Aeroshell	238.0	71.4	309	30%
06.2.2	Attitude Determination and Control	0.0	0.0	0	TBD
06.2.3	Command & Data Handling	0.0	0.0	0	TBD
06.2.4	Communications and Tracking	0.0	0.0	0	TBD
06.2.5	Electrical Power Subsystem	0.0	0.0	0	TBD
06.2.6	Thermal Control	64.5	11.6	76	18%
06.2.7	Propulsion (Chemical Hardware)	0.0	0.0	0	TBD
06.2.8	Propellant (Chemical)	0.0		0	TBD
06.2.9	Propulsion (EP Hardware)	0.0	0.0	0	TBD
06.2.10	Propellant (EP)	0.0		0	TBD
06.2.11	Structures and Mechanisms	0.0	0.0	0	TBD
	Element 2 consumables (if used)	0.0		0	
	Estimated Spacecraft Dry Mass	302	83	385	27%
	Estimated Spacecraft Wet Mass	302	83	385	
<b>System Level Growth Calculations Aeroshell</b>					<b>Total Growth</b>
	Dry Mass Desired System Level Growth	302	91	393	30%
	Additional Growth (carried at system level)		8		3%
	Total Wet Mass with Growth	302	91	393	
06.3	Orbiter	1058.5	167.9	1226.4	16%
06.3.1	Cruise Deck	956.0	147.6	1103.6	15%
06.3.2	Attitude Determination and Control	0.0	0.0	0.0	TBD
06.3.3	Command & Data Handling	0.0	0.0	0.0	TBD
06.3.4	Communications and Tracking	65.0	13.5	78.5	21%
06.3.5	Electrical Power Subsystem	0.0	0.0	0.0	TBD
06.3.6	Thermal Control (Non-Propellant)	37.5	6.7	44.2	18%
06.3.7	Propulsion (Chemical Hardware)	0.0	0.0	0.0	TBD
06.3.8	Propellant (Chemical)	0.0		0.0	TBD
06.3.9	Propulsion (Aux Hardware)	0.0	0.0	0.0	TBD
06.3.10	Propellant (Aux)	0.0		0.0	TBD
06.3.11	Structures and Mechanisms	0.0	0.0	0.0	TBD
	Element 3 consumables (if used)	0.0		0.0	
	Estimated Spacecraft Dry Mass	1058	168	1226	16%
	Estimated Spacecraft Wet Mass	1058	168	1226	
<b>System Level Growth Calculations Orbiter</b>					<b>Total Growth</b>
	Dry Mass Desired System Level Growth	1058	318	1376	30%
	Additional Growth (carried at system level)		150		14%
	Total Wet Mass with Growth	1058	318	1376	



### 3.6.3 Power Equipment List (PEL)

To model the power systems in this Zephyr design study, eight modes of operation were defined. These modes were defined based on the mission profile and they identify which items and subsystems of the Zephyr are operating, and which items are dormant and require no power, at any time throughout the mission.

Table 3.5 shows the assumptions about the power requirements in all the modes of operation. The power requirements from the bottoms-up analysis on the Zephyr listed in Table 3.5 are used by the power system designers (described in Section 4.8) to size the power system components. Zephyr is assumed unpowered until descent. After landing and deployment of the vehicle the Landsailer will be controlled by the orbiter to perform one of four modes during communications, during the periods when the orbiter is not in view the Landsailer is ‘parked’, the sail feathered, and the battery charging. Three different power modes include science, traverse, and traverse planning while the orbiter is communicating. Since the vehicle is windpowered, no power draw for the motors is needed—only small motors to steer the wheel or sail. Power for the aeroshell and orbiter are not included here.

Table 3.5—Venus Landsailer PEL

WBS	Description	Power Mode 1	Power Mode 2	Power Mode 3	Power Mode 4	Power Mode 5	Power Mode 6	Power Mode 7	Power Mode 8
Number	Case #1 Venus Landsailer CD-2013-86	(W)	(W)	(W)	(W)	(W)	(W)	(W)	(W)
	Power Mode Name	Pre-Launch	Launch	Cruise	Descent/ Deploy	Science	Traverse	Charge	Communicating Traverse Planning
	Power Mode duration	TBD min	TBD min	TBD min	TBD min	8 hr	1 hr	8 hr	7 hr
06	Venus Landsailer System								
06.1	<b>Landsailer Rover</b>	<b>0</b>			<b>20.50</b>	<b>73.80</b>	<b>51.30</b>	<b>19.00</b>	<b>37.00</b>
06.1.1	Science Instruments	0.0	0.0	0.0	0	22.5	0	0	0
06.1.2	Attitude Determination and Control	0.0	0.0	0.0	1.5	7.5	7.5	0	0
06.1.3	Command & Data Handling	0.0	0.0	0.0	19.0	19.0	19.0	19.0	19.0
06.1.4	Communications and Tracking	0.0	0.0	0.0	0	18.0	18.0	0	18.0
06.1.5	Electrical Power Subsystem	0.0	0.0	0.0	0	0	0	0	0
06.1.6	Thermal Control (Non-Propellant)	0.0	0.0	0.0	0.0	6.8	6.8	0.0	0.0
06.1.7	Propulsion (Sail System)	0.0	0.0	0.0	5.0	0.0	10.0	0.0	0.0
06.1.8	Propellant (Chemical) (not Used)	0.0	0.0	0.0	0.0	0.0	0.0	0.0	0.0
06.1.9	Propulsion (EP Hardware) (Not Used)	0.0	0.0	0.0	0.0	0.0	0.0	0.0	0.0
06.1.10	Propellant (EP) (Not Used)	0.0	0.0	0.0	0.0	0.0	0.0	0.0	0.0
06.1.11	Structures and Mechanisms	0.0	0.0	0.0	0.0	0.0	0.0	0.0	0.0
06.2	<b>Total</b>	<b>0.0</b>	<b>0.0</b>	<b>0.0</b>	<b>20.5</b>	<b>70.0</b>	<b>80.0</b>	<b>10.0</b>	<b>70.0</b>
	<b>Aeroshell</b>								
	<b>Total</b>	<b>0.0</b>	<b>0.0</b>	<b>0.0</b>	<b>0.0</b>	<b>0.0</b>	<b>0.0</b>	<b>0.0</b>	<b>0.0</b>
	<b>Orbiter</b>								
	<b>Total</b>	<b>0.0</b>	<b>0.0</b>	<b>0.0</b>	<b>0.0</b>	<b>0.0</b>	<b>0.0</b>	<b>0.0</b>	<b>0.0</b>
	<b>Power, system total</b>	<b>0.0</b>	<b>0.0</b>	<b>0.0</b>	<b>20.5</b>	<b>73.8</b>	<b>51.3</b>	<b>19.0</b>	<b>37.0</b>
	<b>30% growth</b>	<b>0.0</b>	<b>0.0</b>	<b>0.0</b>	<b>6.8</b>	<b>24.6</b>	<b>17.1</b>	<b>6.3</b>	<b>12.3</b>
	<b>Total</b>	<b>0.0</b>	<b>0.0</b>	<b>0.0</b>	<b>27.3</b>	<b>98.4</b>	<b>68.4</b>	<b>25.3</b>	<b>49.3</b>

## 4.0 SUBSYSTEM BREAKDOWN

### 4.1 Science Package

#### 4.1.1 Science Overview

The rover is designed for a surface science mission, and hence the choice of science instruments is critical to the ability to achieve the mission objectives. Primary science objectives are geology (including geomorphology and mineralogy), and atmospheric science.

The rover will have three groups of science instruments:

## *Imaging*

Cameras are used as a planning tool, used for path planning, and also to provide a public engagement. However, cameras are also a tool for geology and geomorphology. Images proven to be a powerful science tool on MER mission

## *Weather*

The atmospheric science package, or Venus weather station, comprises the following instruments. temperature sensors are assumed.

- Anemometer (wind speed and direction)
- Temperature sensor
- Pressure sensor

## *In-situ mineralogy*

In-situ mineralogy instruments examine the composition and mineralogy of rocks. These instruments need an instrument deployment device (“robotic arm”) to place the instruments onto rocks to determine composition and mineralogy.

- Robotic arm instruments
  - Robotic arm (2 degrees of freedom)
  - Rock Abrasion Grinder
  - Alpha Particle X-ray Spectrometer (APXS) or Energy-Dispersive Analysis by X-rays (EDAX) (composition)
  - X-ray diffraction (mineralogy)

In addition to the surface science instruments, the vehicle may also have science packages that operate during descent, and may deploy stationary science instruments (e.g., a seismometer) that are not carried on the rover. These instruments were not analyzed in this study.

### **4.1.2 Science Requirements**

Since the objective of the present study is a conceptual design study of the mission, and not an instrument development project, the requirement here is to produce a candidate set of instruments that can accomplish the requirements, in order to be able to ensure that the design will accommodate instrument placement, mass and power requirements, data handling, and CONOPS. The instrument set here is thus to be considered a set representative of the type of science to be acquired, and not a final design. The requirements are that the instruments must be capable of achieving the science goals, and must be capable of operating for the required mission duration.

The most difficult requirement for science is that all instruments must be capable of operating in the Venus ambient environment, without cooling.

### **4.1.3 Instruments**

#### **4.1.3.1 Camera**

Object is to build a camera that will operate without cooling at Venus temperature, 450 °C, and under Venus illumination conditions and spectrum. It would be desirable to spec the camera to a maximum operating temperature 500 °C, to give it some margin, allow for some internal heat, and to give it flexibility to operate on lower (and hence hotter) regions of the surface. The difficult part of this is the focal plane and associated electronics; we do not need to concentrate our efforts on the optical train (lenses, mirrors, scan platform, etc.) which is primarily known technology.



The basic concept is to use a mechanically scanned camera, to avoid sophisticated electronics that are not yet designed for high temperature. The design is to use a linear photodiode array as the light-sensing element, and in order to build up a picture, use a scanning mirror to sweep the image across the sensor.

A proposal was that for the near term, the photodiode array might start as a 1×8 array, large enough to demonstrate the principle and make relatively crude pictures, with the thought that if this can be demonstrated, it would show the principle and in the future a larger array could be made. This is similar to, but slightly more advanced than, the Viking Lander camera, which used a mechanical scan using a photodiode. It is also similar to the Venera-9 camera, which also used mechanical scanning on a photodiode.

The current design does not require a preamp for the individual sensor elements. The eight sensors feed into a switcher element, which consists of eight transistors; the transistor for the photodiode currently being measured is “on” and the other ones “off,” and the design successively switches to each photodiode and measure it in turn until it has queried all of them. The switcher feeds the photodiode output into an op-amp. The electronic design team suggested several amplifier configurations, the simplest of which was simply to a resistor to make a voltage-follower. This need not be linear, and could be just a single-transistor amplifier: there is not a problem if it’s not very linear, as long as it’s consistent: since the data can always be linearized at the receiving end).

The amplifier feeds an A-D converter, which produces the digital output. This is to be sent to the high-temperature radio, so that the whole system has no cooled parts. Feeding this circuitry, we would also need to have an oscillator driving the switcher. The difficult part of this, of course, is that it all has to be done with high-temperature electronics, in this case, SiC. A prototype circuit for the camera is shown in Figure 4.1.

The next question is what photodiodes to use. The SiC electronics used for the primary electronics are comparatively poor as photodiode material, and also operate at somewhat shorter wavelengths (near ultraviolet) than desired, given that the surface spectrum is blue deficient due to Rayleigh scattering in the thick atmosphere. The candidate material for the photodiodes is gallium-indium phosphide ( $\text{GaInP}_2$ ): this material is well-understood because of its use in solar cells, it has a wide enough bandgap that it will work at Venus temperature, and it can be grown with commercial processes on gallium arsenide (GaAs) wafers (or Germanium (Ge) wafers). It responds to light in the band of about 360 to 660 nm. This is still a slightly longer in wavelength response than desired for optimal use on Venus, but it is in a wavelength range in which surface illumination exists on Venus. Quaternary compounds can be made to adjust the bandgap and put the photo response elsewhere, at the cost of increasing dark current and hence noise in the camera, but these will not be analyzed here.)

Using  $\text{GaInP}_2$  has the disadvantage that the photodiode array would be a different chip than the rest of the circuitry (so it can’t be a one-chip camera), but since the high temperature electronics technology is not yet available for a single chip camera, this is expected.

### ***Camera Electronics***

- 128 pixel photodiode, panned mirror
- Integral mirror actuator drive
- Continuous operation with start bit
- Two 128 pin Quad Flat Packages (QFPs), one 32 pin QFP
- 1.9 W power consumption

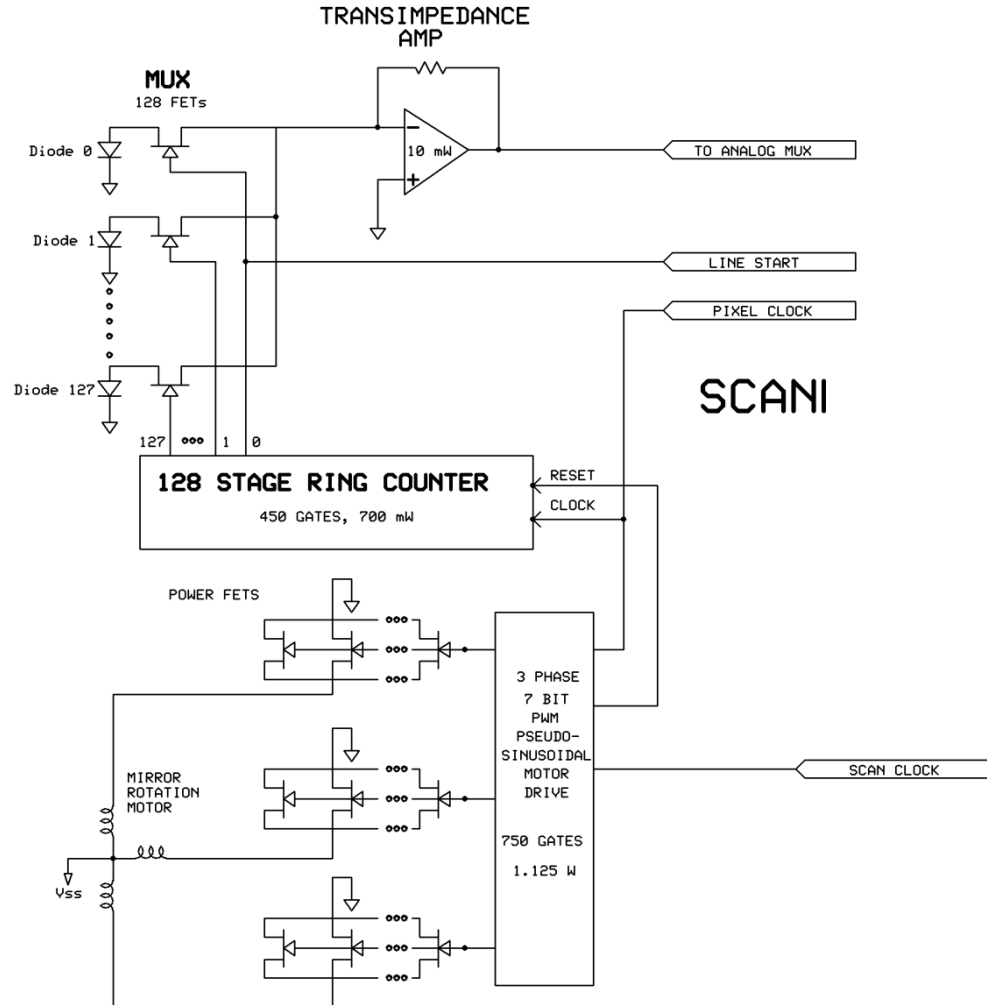


Figure 4.1—SiC scanning camera, 128 pixel, 1.9 W dissipation.

#### 4.1.3.2 Robotic Arm and Rock Abrasion Tool

Motors for mechanical parts have been designed for Venus. (Motor technology for Venus is discussed in the “Mobility” section, and motor controls in the Section 4.4.3 C&DH Design.) The instrument placement arm (“robotic arm”) design is based on the Mars Phoenix robotic arm, but simplified to a two-joint arm, to minimize complexity.

Drills have previously been flown to Venus on the Soviet Venera and Vega missions, and Honeybee Robotics has developed and tested drill and Rock Abrasion Tool (RAT) designed for Venus operation.

#### 4.1.3.3 Mineralogy

Mineralogy is to be accomplished by a chemical analysis tool to analyze composition and an X-ray diffraction tool to investigate crystal structure. Tools based on the principle of EDAX are capable tools for chemical composition. Soviet missions to Venus used X-ray fluorescence as a compositional tool. On the Mars Pathfinder and MER missions, APXS was proven to be a highly capable tool for chemical analysis of rocks. This tool uses an Americium source to irradiate rocks, and then an energy-dispersive solid-state detector to analyze the X-ray fluorescence, which is characteristic of the rock composition. The emission from the radioisotope source is independent of operating temperature, however, the APXS system used for Sojourner and for the two MER rovers used a silicon X-ray detector designed for operation at low temperatures, in order to minimize dark current noise in the system. However, x-ray

detectors have been made from SiC instead of silicon; the same noise floor can be achieved at a higher temperature.

A tool which is capable of analyzing not merely the composition but also the crystalline structure of minerals would be a x-ray diffraction. This requires a collimated, monochromatic x-ray source. For terrestrial use, this is typically an electron tube, however, it is also possible to use an isotope source for x-ray diffraction, although the source intensity is typically lower. Fe-55 has been used as a source for past missions, while the isotopes Am-241 and Rh-101 have also been proposed [Stenzel *et al.* 2009]. The detector for this will be an array of SiC x-ray detectors.

#### 4.1.3.4 Weather

The weather measurement will consist of measurements of wind (speed and direction), temperature, and pressure. The weather measurement is duplicated with one instrument mounted on the rover deck, and one at the top of the mast, in order to measure the wind velocity at different heights above the surface. Likewise, multiple temperature sensors are placed at different heights.

Temperature and pressure sensors are straightforward, using MEMS technology with SiC electronics for A/D, and are based on similar sensors used for jet engine diagnostics [Okojie *et al.* 2001; Lei and Will 1998].

Although there are many mechanical anemometers in use for wind speed measurements on the Earth, typical anemometers use moving parts such as vanes or rotating cups. Most designs also only measure wind speed, and a separate sensor is required for wind direction.

An exception is the “hot wire” anemometer, with no moving parts. Here a current heats a wire exposed to the air. Since moving air removes heat from the wire, the current needed to maintain temperature is related to the wind speed. A hot-wire anemometer design was used on Mars in the Mars Pathfinder mission, and several difficulties with the design were discovered. Among these was the fact that the response depended in a nonlinear way on both ambient pressure and temperature, and hence the Mars Pathfinder anemometer results were difficult to interpret. (In fact, calibrated wind speed was only calculated well after the mission ended.) Another difficulty is that, as a thermal device, power consumption is high. This would be a poor design to use on Venus.

The proposed instrument here is a simplified variation of the “Sphere anemometer” design demonstrated by Hölling *et al.* (2007), as shown in Figure 4.2. It avoids these difficulties and is constructed to be mechanically rugged, electrically simple, and able to operate with a low-power consumption. The technical approach to the Venus anemometer is straightforward. The wind is incident on a spherical drag body. In the point of departure design, this is a 7-cm diameter (2 ¾-in.) sphere. The sphere is emplaced on the top of a vertical shaft, which is affixed to a baseplate, which (in the operational version) would be attached to the spacecraft. The wind will produce a drag force on the drag body; this force will put a bending force on the shaft. Two pairs of strain gauges will be used to measure the force in orthogonal directions, and thus the vector velocity of the wind can be determined.

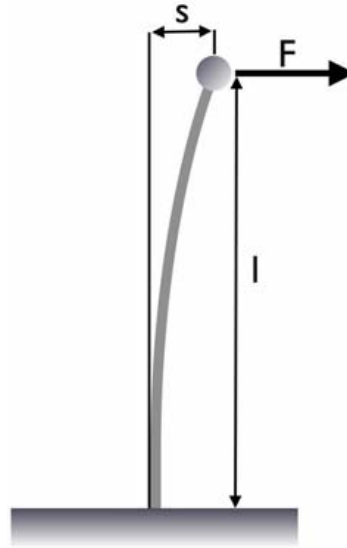


Figure 4.2—Conceptual design of a sphere anemometer (From Hölling et al. 2007)

#### 4.1.4 Science Design and MEL

The full science payload is summarized in the MEL for the Venus Landsailer in Table 4.1.

Table 4.1—Science Case 1 Master Equipment List

WBS	Description	QTY	Unit Mass	Basic Mass	Growth	Growth	Total Mass
Number	Case #1 Venus Landsailer CD-2013-86		(kg)	(kg)	(%)	(kg)	(kg)
06	Venus Landsailer System			1581.03	18.7%	295.74	1876.77
06.1	Landsailer Rover			220.08	20.4%	44.86	264.94
06.1.1	Science Instruments			17.90	39.3%	7.03	24.93
06.1.1.a	Venus Landsailer Science Instruments			17.90	39.3%	7.03	24.93
06.1.1.a.a	X Ray Diffraction	1	5.00	5.00	50.0%	2.50	7.50
06.1.1.a.b	EDAX	1	0.5	0.50	50.0%	0.25	0.75
06.1.1.a.c	Grinder	1	1.0	1.00	50.0%	0.50	1.50
06.1.1.a.d	Panoramic Camera (with motor)	2	1.0	2.00	50.0%	1.00	3.00
06.1.1.a.e	Weather Station	1	0.5	0.50	50.0%	0.25	0.75
06.1.1.a.f	Robotic Arm	1	6.0	6.00	18.0%	1.08	7.08
06.1.1.a.g	Electronics Box	3	0.3	0.90	50.0%	0.45	1.35
06.1.1.a.h	NavCams	4	0.5	2.00	50.0%	1.00	3.00

## 4.2 Launch, Trans-Venus Trajectory, Orbital Insertion, and Landing

### 4.2.1 Launch

Notional launch vehicle chosen was the Falcon-9, based on cost, availability, and ability to launch the required mass at the required value of  $C_3$ . Figure 4.3 shows the launch sequence from launch to the trans-Venus insertion.

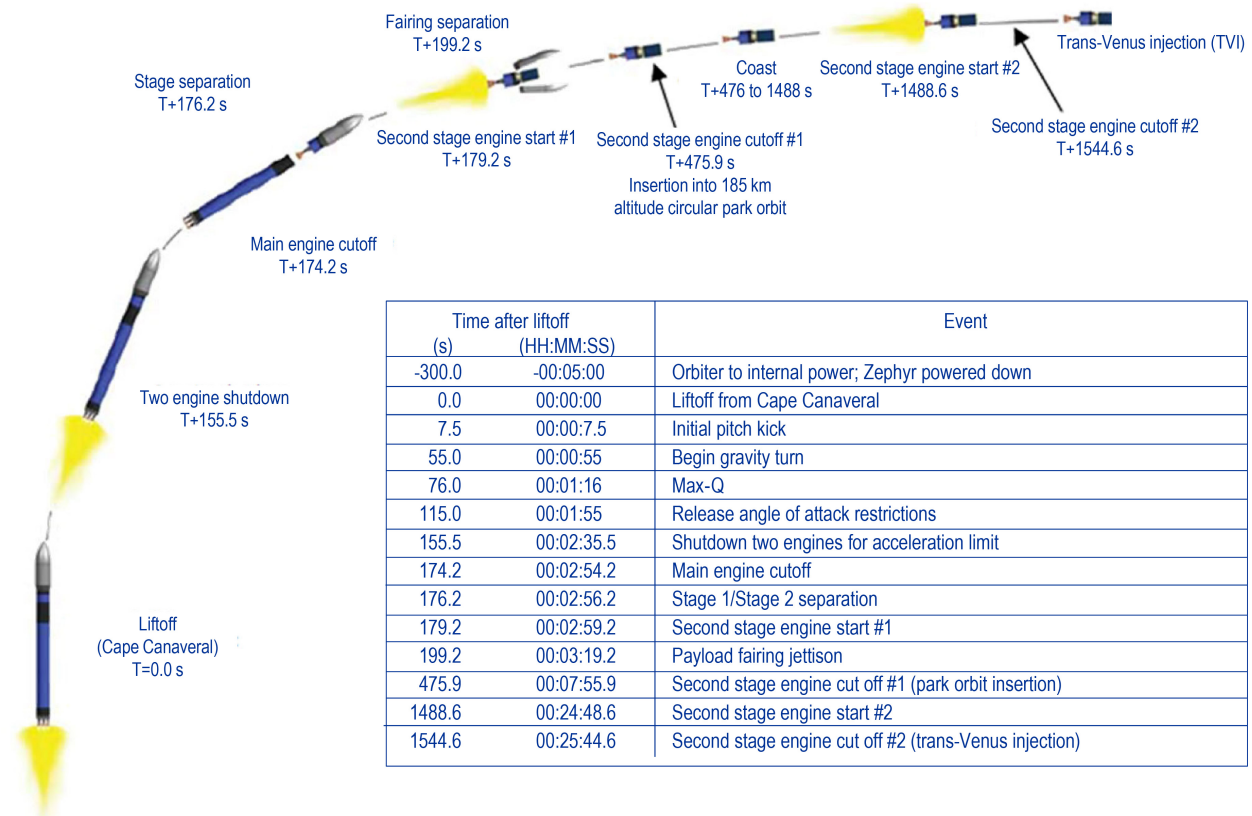


Figure 4.3—Falcon 9 launch profile, trans-Venus insertion (TVI) and cruise phases.

Following launch the Zephyr/Orbiter will execute course correction maneuvers to correct trajectory errors incurred during TVI. The composite Orbiter/Zephyr will be on a trajectory that intersects the orbit of Venus.

#### 4.2.2 Earth to Venus Trajectory

The primary focus of the study was on the design of the Landsailer itself, however a small amount of mission analysis was performed to determine the launch date from Earth, arrival date at Venus and a rough estimate of the amount of  $\Delta V$  required to insert the orbiter into an appropriate orbit to be in communication with the Landsailer. The reference trajectory for the Landsailer launches from Earth on December 25, 2024, and arrives at Venus on May 9, 2025, for an interplanetary transfer time of 135 days and arrival  $V_{inf}$  of 3.79 km/s. A  $\Delta V$  of 1.1 km/s is required by the orbiter to insert into a 24-hr period, 400-by 66,410-km orbit with apoapsis above the Landsailer.

The interplanetary trajectory was generated using the Mission Analysis Low-Thrust Optimization (MALTO) program. Figure 4.4 shows a notional Earth to Venus transfer.

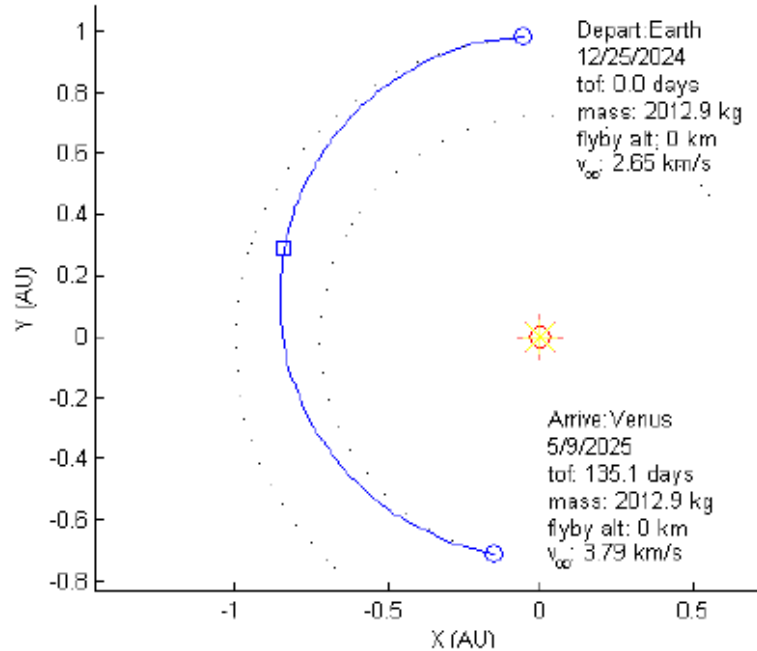


Figure 4.4—Notional trans-Venus trajectory.

### 4.2.3 Orbit Insertion $\Delta V$ Details

For communication between the orbiter and the Landsailer, the orbiter is placed in a 24-hr period, equatorial orbit with an altitude of periapsis of 400 km and an altitude of apoapsis of 66,410 km. (The 24 hr period of the orbit is chosen for the convenience of the science team, allowing the ground personnel to operate on a standard Earth schedule). Also, it was assumed that the orbiter would be placed in such an orbit to use the slow, retrograde rotation rate of Venus to have the apoapsis of the orbiter occur above the longitude of the lander approximately half way through the mission, thus maximizing the contact time between the lander and orbiter during the mission.

The  $\Delta V$  required to insert the orbiter into orbit was calculated using orbital mechanics equations. An altitude of 400 km was assumed for periapsis to avoid the effects of atmospheric drag perturbing the orbiter throughout the mission. The arrival  $V_{inf}$  at Venus for the reference trajectory is 3.79 km/s, leading to a semi-major axis of 22,616 km by solving the equation for specific orbital energy for semi-major axis with the radius of the S/C assumed to be at infinity.

$$\epsilon = v^2/2 - \mu/r = -\mu/(2a)$$

Solving the same equation for velocity while using the 22,616 km for the semi-major axis and a 400 km altitude (6452 km radius) leads to a velocity at periapsis of 10.7 km/s for the hyperbolic orbit. A 24-hr period orbit around Venus requires a semimajor axis of 39,457 km, and again assuming an altitude of periapsis of 400 km, this leads to a velocity at periapsis of 9.6 km/s for the 24-hr period orbit. The difference between the 10.7 km/s for the hyperbolic orbit and the 9.6 km/s for the 24-hr period orbit is the amount of  $\Delta V$  required at periapsis to insert into the 24-hr period orbit from the hyperbolic orbit, and this is 1.1 km/s.

### 4.2.4 Landing

Entry of Zephyr is accomplished using the aeroshell, followed by a high-altitude parachute, which is jettisoned after slowing the vehicle to subsonic velocity, and a low-altitude parachute for the final landing.

The landing system is required to safely deploy the rover on the surface of Venus after separation with the heat shield. This requires a high temperature parachute system capable of slowing the lander’s descent to an acceptable terminal velocity at the surface for landing.

Venus parachute designs have been analyzed by Kelley, Sinclair, and Sengupta (2012). Due to the severe surface environment on Venus, it assumed that the final parachute is fabricated from a high temperature fabric such as Nextel™. As shown in Figure 4.5, the fiber retains strength at temperatures considerably higher than Venus temperatures. An alternative technique is to baseline a parachute from glass fiber. The terminal descent speed provided by the parachute system is assumed to be 3.0 m/s (9.84 ft/s).

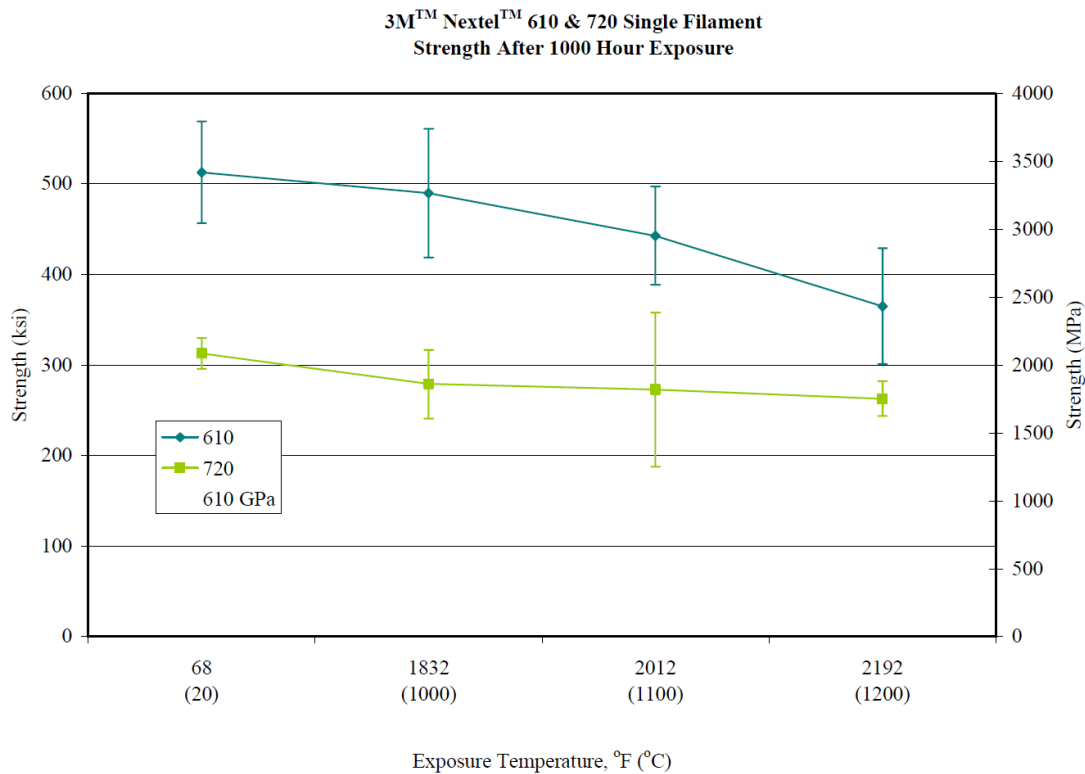


Figure 4.5—Nextel filament properties.

The parachute has a diameter of 4.0 m (13.1 ft) and is designed to provide a terminal descent velocity of 3.0 m/s (9.84 ft/s) at the Venusian surface. It is a standard high drag design with a drag coefficient of 0.8. To survive in the Venus atmosphere during descent, the parachute and lines are made from Nextel™ fiber. Although this fiber can maintain its strength at the expected environmental temperatures, as shown in the figure **Error! Reference source not found.**, it is unclear at this time if it can survive the chemical attack expected from the various acid components in the atmosphere. Once on the surface, the parachute will be released, and the vehicle will touchdown on its deployed wheels. Landing on wheels is a technology that has been demonstrated with the Mars Science Laboratory “Curiosity,” and at the anticipated descent velocity of 3 m/s it should be relatively straightforward.

The parachute system was designed by determining the parachute size required to meet the Venus surface landing requirements, finding an equivalent commercial off the shelf (COTS) Earth-based parachute system, and then substituting Nextel fabric for the nylon typically used for the canopy and lines. Additional mass was then added for a harness, connectors, and margin. Parachute release mechanisms are discussed under structures and mechanisms.

### 4.3 Zephyr Landsailer Rover System Mobility

A vertically mounted wing serving as a rigid sail converts the local dynamic pressure from surface winds into a propulsive force. This propulsive force has to overcome both the friction produced by the wheels on the surface and the horizontal component of the rover's weight when climbing a hill. The wheels need to be large enough to overcome small surface obstacles while still maintaining low rolling friction in order to minimize the sail surface area required to provide adequate mobility. Steering of both the sail and the central wheel assembly is achieved by gimbals capable of operating in Venus environment, while a combination of brakes and sail feathering provide vehicle stability during science operations.

#### 4.3.1 Zephyr Landsailer Rover System Mobility Requirements

The surface of Venus is a harsh environment for any mobility system. The average surface temperature is 455 °C (851 °F), surface pressure is 92 atmospheres (1,350 psia), and atmospheric density at the surface is 65 kg/m<sup>3</sup> (4.06 lbm/ft<sup>3</sup>), which is approximately 65 times the density of the Earth's atmosphere at sea level. From the limited surface data collected during the Russian Venera landing missions, the surface wind velocity is very small, on the order of 0.5 m/s (1.6 ft/s) with variations of ± 0.3 m/s (0.98 ft/s).

The mobility system utilizes surface winds for propulsion on the surface. Wheels that are large enough to overcome the expected terrain roughness, withstand the environmental conditions, provide adequate steering and braking, and have a low rolling coefficient are required for surface mobility. The very low average surface wind velocity means that even though the atmospheric density is much greater than Earth's, the available surface dynamic pressure is quite low relative to Earth. Therefore, a relatively large sail area is required to produce enough force to move the vehicle. The sail is also required to be steerable to account for changes in wind direction and to vary its angle of attack. In an effort to save mass, the mobility system is also required to be zero fault tolerant.

#### 4.3.2 Zephyr Landsailer Rover System Mobility Assumptions

In order to survive for any extended amount of time on the surface, it assumed that the sail, wheels, gimbal motors, actuators, and sail structure are fabricated from materials compatible with the Venus surface environment. The sail is assumed to be a rigid design in order to avoid the issues of deploying and managing a flexible high temperature fabric based system. For the purposes of propulsion, surface wind velocities of at least 0.4 m/s (1.31 ft/s) and up to 1.3 m/s (4.26 ft/s) are assumed. Based on pictures from Venera, the largest expected surface irregularities are ~10.0 cm (3.94 in) in height.

#### 4.3.3 Zephyr Landsailer Rover System Mobility Design and MEL

The Zephyr mobility system design consists of a rigid steerable sail for propulsion, and three lunar roving vehicle (LRV) derived wheels for surface mobility which can provide both braking and steering on the surface. The wheels are 1.0 m (3.28 ft) in diameter and 22.9 cm (9.0 in.) wide.

For mobility on the Venusian surface, various wheel designs were evaluated, and wheels based on the LRV wheel design were selected based on their height, low rolling friction, mass, obstacle performance, and potential environmental compatibility (assuming suitable material substitutions). The LRV wheel design is shown in Figure 4.6 **Error! Reference source not found.** and consists of all metal construction with a solid main hub, a rigid cage like inner rim, and a wire mesh surface with Ti cleats. The outer mesh surface is constructed of zinc plated wire and was designed to elastically deform and change contour to help maintain good contact with the surface. This outer mesh surface can only deform until it reaches the inner rim, thus limiting its allowable elastic deformation range. It was, however, designed for a nominal deflection of 4.45 cm (1.75 in.). For use on the Venusian surface, some of the LRV wheel materials need to be replaced with suitable ones, such as 6Al4V Ti alloy. The original LRV wheel was also designed to operate on a sandy surface, while the photos from Venera show a smooth yet rocky surface akin to slate. This suggests that the wheel design may require the addition of friction enhancing cleats to increase surface traction.





Figure 4.6—Lunar rover wheel.

#### 4.3.3.1 Motors

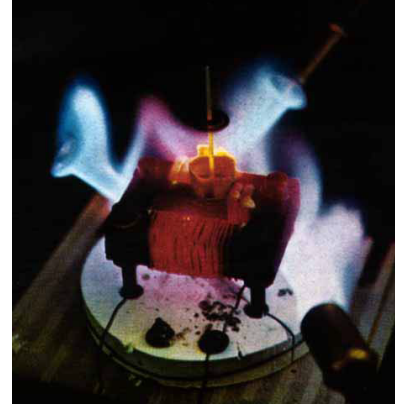
Although a primary propulsion does not require a motor, motors are needed to adjust the sail position, and for steering.

In order to provide steering to both the middle (aft) wheel and the sail, high temperature motors compatible with the Venusian surface environment are necessary. Unfortunately, there are currently no COTS gimbals or actuators available that meet the required environmental compatibility. Honeybee Robotics, however, does produce a motor designed to survive at temperatures above 460 °C (860 °F) in Earth atmosphere, and has been noncontinuously operated for over 20 hr in Venus surface like conditions. Although designed as a high speed drill motor, it may be applicable for use in a gimbal or actuator assembly with the addition of a properly designed harmonic drive transmission.

If a new motor is required, the primary components needed to fabricate a high temperature electrical motor have been developed in the past, and would be applicable to the development of a new actuator/gimbal system for use on Venus. For example, in the early 1970s General Electric (GE) built and tested a simple electrical motor which utilized multiple high temperature material technologies. The motor windings were made from nickel oxide clad silver-palladium wire 0.762 mm (0.030 in) diameter, and the poles were made from laminated 6% silicon iron. This test motor exhibited sustained operation at 575 °C (1067 °F) and operated at temperatures as high as 725 °C (1337 °F), which was the Curie temperature of silicon iron laminate core. Both the Honeybee and GE test motor (being tested while heated by three ox/gas torches) are shown in Figure 4.7 **Error! Reference source not found.**



Honeybee Robotics Motor



GE High Temperature Motor Component Test

Figure 4.7—Honeybee High Temperature Electric Motor and GE Test Article.

Although these two motors might not be suitable for use as they currently are, they prove that a fully functional motor capable of operating at (or beyond) measured Venus surface temperatures can be built with the appropriate material substitutions. Given the current understanding of electrical motor design, and the demonstrated high temperature operation of these two motors, developing a gimbal or actuator for use on Venus is clearly an engineering development issue, and not one requiring a large investment in high temperature materials research.

In order to provide steering of both the central wheel and sail, a gimbal based on a Moog Type 7 gimbal shown in Figure 4.8 **Error! Reference source not found.** is used. This gimbal has a 200:1 harmonic drive giving it up to 294 N-m (2,600 lbf-in) holding torque. Although this gimbal is a space rated COTS unit, it is assumed for this study that an equivalent unit can be built with materials and technology compatible with the Venusian surface environment, such as those mentioned above.

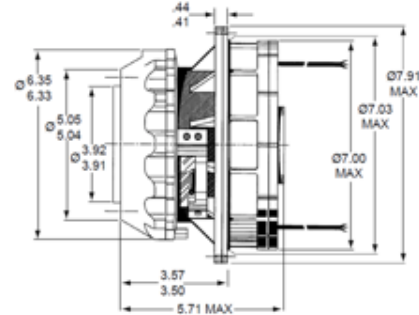
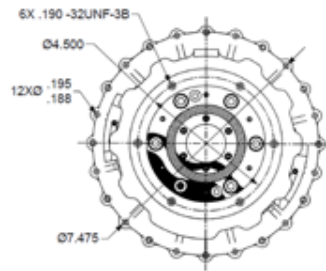
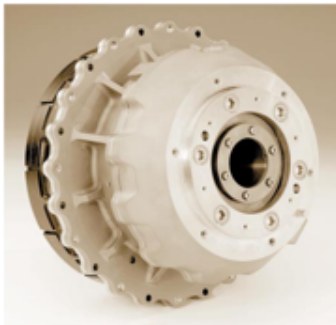


Figure 4.8—Moog Type 7 Gimbal.

#### 4.3.3.2 Sail

The single rigid sail used for surface propulsion is folded into three sections for storage in the aeroshell, and is deployed just prior to landing. For the purposes of this study, a symmetrical thin airfoil design was chosen, along with a trapezoidal planform that tapers from the root of the wing (at its base) to its tip. The wing is mounted perpendicular to the base and can rotate via its gimbal about its mean aerodynamic center to produce a lift (thrust) vector at any orientation to the wheels of the rover, depending on the orientation of the local wind. The wing can also be “nulled”, or set parallel to the local wind, to bring the rover to a halt, to sit in place, or avoid tipping over the rover. Construction of the wing is standard spar, rib, and skin, using materials appropriate for the corrosive high temperature environment.

The diameter of the aeroshell sets the root chord length of the wing to be 3.10 m (10.17 ft). From the required force diagram and the lift equation described below, a total wing area of 12 m<sup>2</sup> (129.1 ft<sup>2</sup>) is required. The resulting height of the wing is 5.44 m (17.84 ft), and is shown in a side profile of the wing

and rover in Figure 4.9 **Error! Reference source not found.** The sail has a constant aerodynamic cross section (no aerodynamic twist) corresponding to a NACA 0015 airfoil. The drag polar for this design was determined by using low angle of attack results from a NASA software package and high angle of attack test data from Sandia National Laboratory. The resultant drag polar is shown in Figure 4.10 **Error! Reference source not found.**

The rather large size of the sail relative to the rover chassis raised the concern of the vehicle toppling over during a gust of wind. Initial calculations show that assuming the rover is sitting on level ground, a wind gust hits the sail at just the right angle as to produce the maximum amount of force it could from the sail, and that the sail was at the correct angle so that all the force vector was exactly perpendicular to the rollover axis formed by one out board wheel and the center wheel, it would take a wind gust of 2.39 m/s (7.84 ft/s) to initiate a roll-over of the vehicle. The gust would need to be sustained, however, to actually cause the vehicle to topple over. The time it would take for this to occur is long enough for the sensors to recognize the situation and the control system can slack the sail, allowing it to rotate to a zero-lift position, before actual tilting occurs.

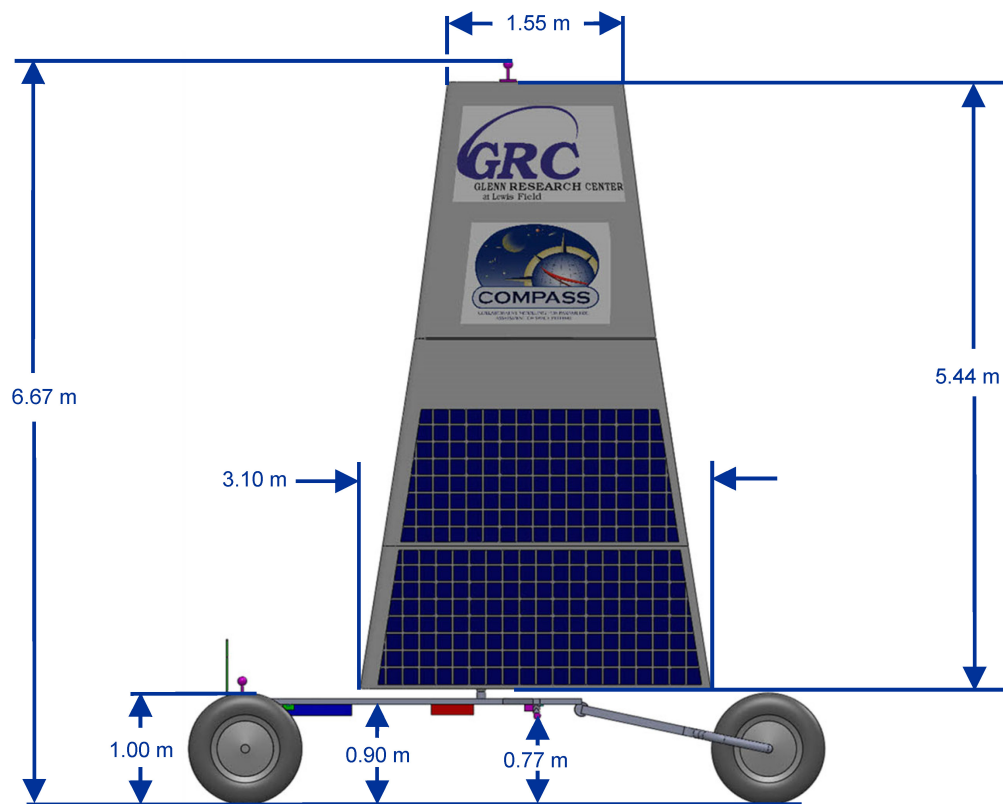


Figure 4.9—Sail dimensions.

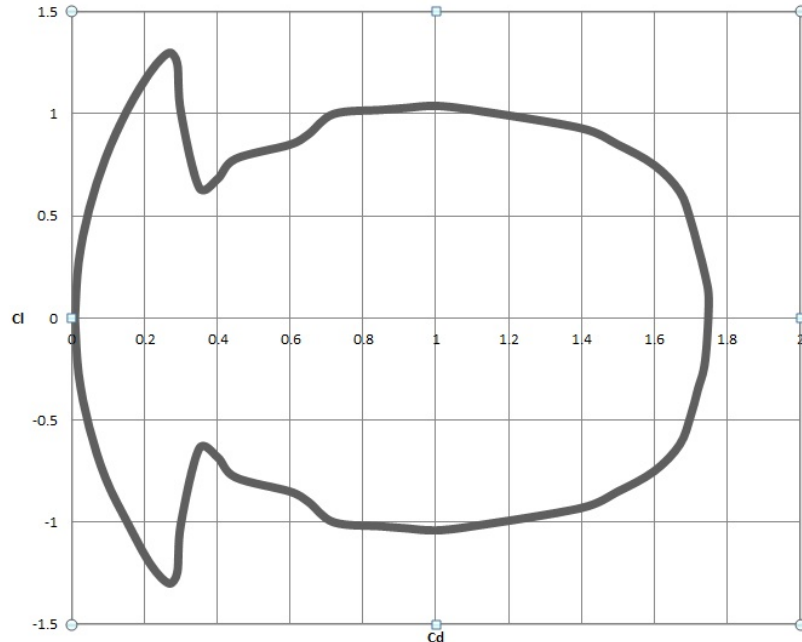


Figure 4.10—Drag Polar for Landsailer Wing, showing the x and y components of the force on the sail with respect to the wind direction.

Another analysis performed during this study was to determine the performance of the wheel design over objects of various heights. This analysis assumed a solid wheel trying to roll over a rectangular object with one third of the rovers’ weight acting on the wheel in question. The results showed that a 20.0 cm (7.87 in) high obstacle could be overcome with this design given the maximum expected wind velocity of 1.30 m/s (4.26 ft/s). This does assume, however, that the force generated by the sail is exactly in line with the desired forward motion of the vehicle in overcoming the obstacle. This analysis does give some insight, but is simplistic in that the real wheels will deform somewhat around the object, thus changing their geometry slightly, and that the object can be almost any random shape, although the vertical step assumed in the analysis should represent a worst case scenario.

### 4.3.3.3 MEL

A listing of the various components in the Landsailer mobility system and their corresponding masses is shown in Table 4.2 **Error! Reference source not found.**

Table 4.2—Propulsion System Master Equipment List

WBS Number	Description	QTY	Unit Mass (kg)	Basic Mass (kg)	Growth (%)	Growth (kg)	Total Mass (kg)
06	Venus Landsailer System			1582.03	18.7%	296.24	1878.27
06.1	Landsailer Rover			221.08	20.5%	45.36	266.44
06.1.7	Propulsion (Sail System)			84.23	16.1%	13.58	97.82
06.1.7.a	Sail System			52.93	18.0%	9.53	62.46
06.1.7.a.a	Sail			48.93	18.0%	8.81	57.74
06.1.7.a.a.a	Steering Mechanism	1	7.70	7.70	18.0%	1.39	9.09
06.1.7.a.a.b	Sail Structure	1	29.94	29.94	18.0%	5.39	35.33
06.1.7.a.a.c	Deployment Mechanism, Sail	3	3.77	11.30	18.0%	2.03	13.33
06.1.7.a.b	Parachute System			4.00	18.0%	0.72	4.72
06.1.7.a.b.a	Parachute	1	4.00	4.00	18.0%	0.72	4.72
06.1.7.b	Wheel System			31.30	13.0%	4.06	35.36
06.1.7.b.a	Wheels			31.30	13.0%	4.06	35.36
06.1.7.b.a.a	Wheels	3	6.60	19.80	12.0%	2.38	22.18
06.1.7.b.a.b	Brake	2	2.50	5.00	18.0%	0.90	5.90
06.1.7.b.a.c	Steering Mechanism	1	6.50	6.50	12.0%	0.78	7.28
06.1.7.b.a.d	Deployment Mechanism, Wheels	0	0.00	0.00	0.0%	0.00	0.00

#### 4.3.4 Zephyr Landsailer Mobility System Trades

During a preliminary study, several different wing designs were considered. There was an initial discussion concerning the use of a controllable sail or wing versus a “tumbleweed” design that would be freely blown across the surface. The tumbleweed saves the weight of the wheels, but because of the low surface wind velocity this idea was rejected. There was an additional discussion about the use of a fabric sail as opposed to a movable wing. The sail has less weight than the wing, but is harder to control and trim. Since the rover will be controlled remotely by the orbiter, a simpler control system worked in favor of the wing. The wing also provides a more stable surface on which to mount the solar cells used to power instruments on the rover.

Having selected a wing design, the question of airfoil design was then addressed. A cambered (curved) surface would produce more aerodynamic lift than a flat or symmetric design, but the control logic becomes more complicated since there is a definite suction surface and pressure surface on a cambered wing which must be properly oriented relative to the wind to generate the higher lift. A symmetric airfoil, however, is much easier to control at the sacrifice of a small amount of lift. Another idea that was discussed was the use of a movable rear flap on the wing to produce additional aerodynamic force. Once again, the added complexity in the control system and the added weight of the structure was cause for rejection, since additional lift could be achieved by simply rotating the entire wing structure relative to the base.

With the removal of the tumbleweed type rover designs, various wheel designs were evaluated as possible candidates. Since the rover is propulsively unpowered, a tracked system was removed from the trade space because it was deemed too complicated and required excessive amounts of delivered sail force to overcome the internal friction of the system. Due to the nature of the surface environment, any polymer based or inflatable system was ruled out as well. This left various metallic wheel designs, many of which were evaluated during the Apollo program for use on the LRV. A summary of these designs is shown in Table 4.3 **Error! Reference source not found.** Using both the qualitative and quantitative data available for these designs, the Apollo rover wheel design was selected primarily for its low weight, low rolling coefficient, and obstacle performance. Although this design was originally for the soft sandy lunar surface, appropriate material substitutions would allow it to survive the Venusian surface environment. It is currently unclear, however, how this design will perform on the non-sandy Venus surface. The addition of traction enhancing cleats may be needed for this design, and although beyond the scope of this study, this is seen as an easy modification to the Ti cleats which cover 50% of the tread surface.

With a propulsion concept selected, a trade was conducted to determine size of the sail given the geometric constraints of the aeroshell, the anticipated winds on the Venusian surface, and the force required to move the rover across both level terrain and an incline. For this design, it was desirable to keep the wind velocity required for sailing along level terrain near 0.3 m/s (0.98 ft/s). This allows for some margin from the 0.4 m/s (1.32 ft/s) anticipated wind velocity to account for unknowns in terrain roughness and vehicle rolling friction. Using a 1.0 m (3.28 ft) wheel diameter, a vehicle rolling friction coefficient of 0.01 (assumes nominal bearings and lunar rover derived wheels on a hard surface), and a sail force coefficient of 1.26, a parametric set of curves were calculated for various values of sail surface area. These curves are plotted in Figure 4.11 **Error! Reference source not found.**, and show that a sail area of 12 m<sup>2</sup> (129.1 ft<sup>2</sup>) can propel the rover at steady state on level terrain with a wind velocity of 0.32 m/s (1.05 ft/s).

With the sail surface area determined, another trade was conducted to determine both how the current design would perform on a smooth incline, and how rover mass would affect incline performance as a function of surface wind velocity. The resulting curves are plotted in Figure 4.12 **Error! Reference source not found.**, and show that as the mass of the rover increases, so does the required wind velocity to overcome a given slope angle. The current design requires a sustained wind velocity of approximately 1.2 m/s (3.9 ft/s) to just overcome both gravity and rolling friction on a 15° slope.

Table 4.3—Survey of Rover Wheel Concepts

Wheel type:			Rigid rim	Pneumatic	Wire mesh	Spiral spring	Hoop spring	Elliptical	Cone	Hubless
Example reference:			Gromov 2003	Goodyear 1969	GM 1970a	Markov 1963	Bendix 1965	Markov 1963	Grumman 1970	Lockheed 1972
Criteria	Method	Weighting factor								
			Mechanical reliability	J	0.15	<b>6.0</b>	4.5	5.0	4.7	4.7
Soft ground performance	C/E	0.14	3.8	7.3	7.3	<b>8.7</b>	<b>8.7</b>	8.2	8.3	<b>8.7</b>
Weight	C	0.14	6.6	3.3	<b>8.7</b>	2.5	4.5	1.0	5.8	0.5
Ride comfort	J	0.13	0.0	8.0	<b>9.0</b>	3.0	5.0	6.0	2.0	3.0
Obstacle performance	C	0.10	6.8	<b>7.4</b>	<b>7.4</b>	6.4	6.4	6.8	<b>7.4</b>	6.4
Stability	J	0.08	<b>8.0</b>	7.0	7.0	2.8	5.7	4.3	7.0	2.8
Wear resistance	J	0.08	3.0	1.5	5.3	<b>6.0</b>	<b>6.0</b>	<b>6.0</b>	5.3	<b>6.0</b>
Steerability	J/E	0.06	<b>7.3</b>	5.8	5.8	2.0	2.0	4.1	6.6	2.0
Environmental compatibility	J	0.06	<b>8.0</b>	0.0	6.0	7.0	7.0	6.0	6.0	3.0
Development risk and cost	J	0.06	<b>10</b>	1.3	8.0	8.0	8.0	4.0	5.3	2.7
Total		1.0	Eliminated	Eliminated	<b>7.1</b>	5.0	5.8	4.7	5.6	3.8

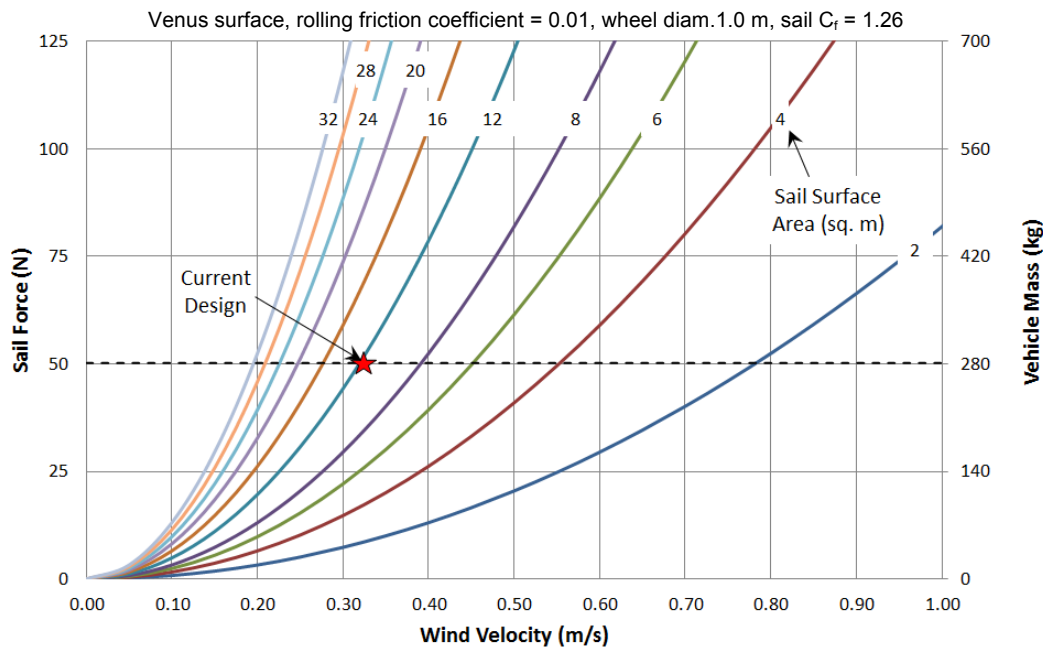


Figure 4.11—Sail force versus surface wind velocity.

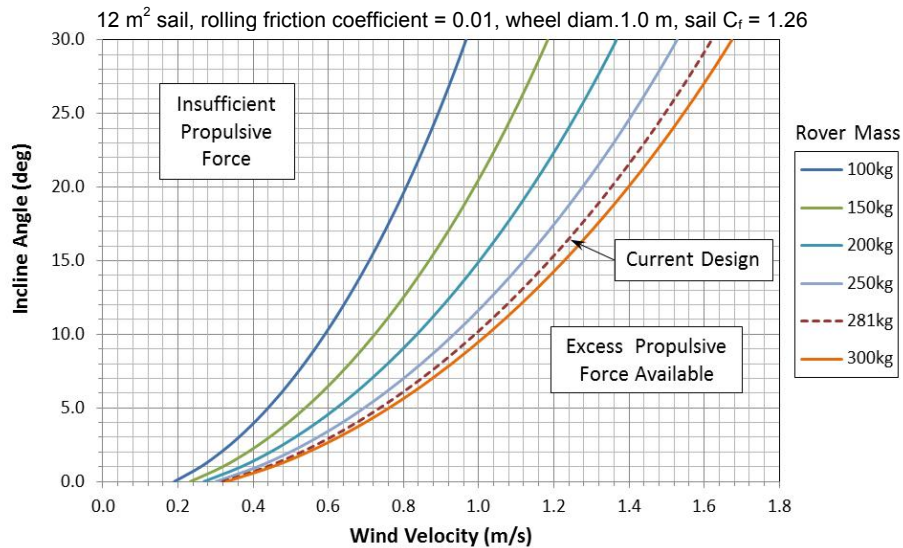


Figure 4.12—Incline angle versus wind velocity.

### 4.3.5 Zephyr Landsailer Mobility System Analysis

#### 4.3.5.1 Analytic Methods

The methods used to design the rover propulsion system involved using a mix of published values, empirical data, and analytical tools. Published values and empirical data were used wherever possible, with analytical tools being employed as necessary. Empirical data was used to aid in the mass and size estimation of similar or derivative systems when published values were not available. Numerous NASA reports and journal articles were used in this analysis, as well as current NASA software and custom analytical tools developed from basic physical relationships and conservation equations with empirical based inclusions for real life hardware requirements (mounting bosses, flanges, etc.).

#### 4.3.5.2 Wheels

The rovers' wheels were designed using both empirical and analytical data from the Apollo program. This data included not just alternative designs and testing results, but also masses, rolling friction, and performance characteristics. The bearings, brakes, steering mechanism, and sail gimbal are all designed in much the same fashion as the parachute system, where design starts with the equivalent COTS components, and then suitable materials are substituted and geometric changes are made as needed to meet design requirements. These changes, and the AIAA recommended margins, are reflected in the masses listed in the MEL.

#### 4.3.5.3 Sail

The sail operates just like a wing on Earth. As the wind passes the wing, the flow is perturbed which generates an aerodynamic force on the wing. For analysis purposes the aerodynamic force is resolved into two components, lift and drag. Lift is measured perpendicular to the flow; drag is in the direction of the flow. The amount of the lift force is described by the classic lift equation:

$$L = C_L q A$$

where  $L$  is the lift force,  $C_L$  is the lift coefficient,  $q$  is the dynamic pressure, and  $A$  is the projected wing surface area. The value of  $C_L$  depends on a number of factors including the shape of the wing, its orientation to the flow, and some parameters that relate the relative importance of compressibility of the atmosphere, and viscosity of the atmosphere. In normal wing design, a model of the wing would be built and wind tunnel tested to determine the value of  $C_L$ . For some simple designs, a theoretical value of  $C_L$  can be computed mathematically during preliminary design. There are also classical techniques to

compute  $C_L$  for a thin, symmetrical airfoil. The drag equation is similar to the lift equation, except for a different multiplier, the drag coefficient ( $C_d$ ). For a well-designed, aerodynamic wing, the lift is nearly 10 times greater than the drag.

In the lift equation,  $q$  is the dynamic pressure which is given by the classic equation:

$$q = (\frac{1}{2}) \rho V^2$$

where  $\rho$  is the atmospheric density and  $V$  is the relative velocity between the wing and the atmosphere. As mentioned previously, on the surface of Venus the atmospheric density is high but the average velocity is very low, so  $q$  is a small number. Therefore, to generating a larger aerodynamic force requires a large surface area  $A$ , as described in the lift equation.

Because this is only a preliminary design study, and the wing design is fairly straightforward, a NASA-developed interactive computer program (FoilSim) was used to initially determine lift and drag coefficients. The program performs a classic Kutta-Joukowsky analysis for lift of a thin, two-dimensional, airfoil under low speed and ideal flow conditions. The drag was determined by low speed wind tunnel testing of a series of Joukowsky foils at representative angles of attack. A flat plate and symmetric thin airfoils are included in the Joukowsky class (J-class) of airfoils. At the beginning of the design study, the software was modified to include a model of the atmospheric conditions on the surface of Venus and to include a weight calculation for a variety of high temperature materials. The program verified that lift coefficients would be on the order of 1.25 at moderate angle of attack ( $\sim 10^\circ$ ). The code was used to evaluate the use of wing camber (which was rejected) and the use of a single surface fabric sail (which was also rejected). A 15% thick airfoil was used for this design.

As the study progressed, it was determined that the wing would be subjected to much larger angles of attack than could be properly modeled by FoilSim. FoilSim is limited to  $\pm 20^\circ$  angle of attack because of an analytical stall model included in the program. Above  $10^\circ$  angle of attack, the flow on a thin airfoil will separate and produce a time dependent stall that decreases lift and increases drag. A literature search produced performance curves for an NACA 0015 airfoil that was tested from  $0^\circ$  to  $180^\circ$  angle of attack. The results, shown in Figure 4.13 **Error! Reference source not found.** and Figure 4.14 **Error! Reference source not found.**, are part of Sandia National Lab Report (SAND80-2114) in support of wind turbine research. Combining the FoilSim results at low angles of attack with the Sandia results for high angles of attack, a drag polar (drag versus lift curve) was produced for the Zephyr sail.

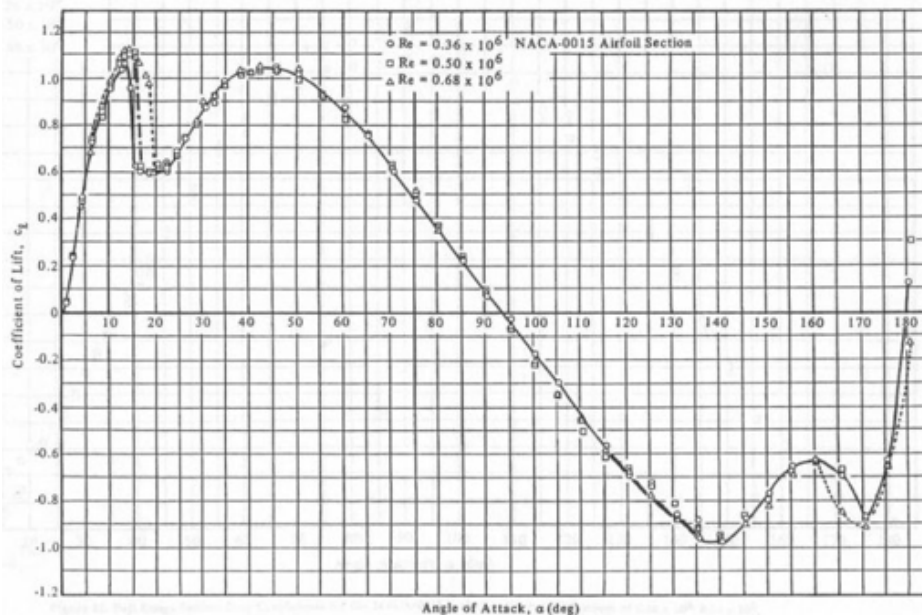




Figure 4.13—NACA 0015 lift coefficient ( $C_L$ ) versus angle of attack.

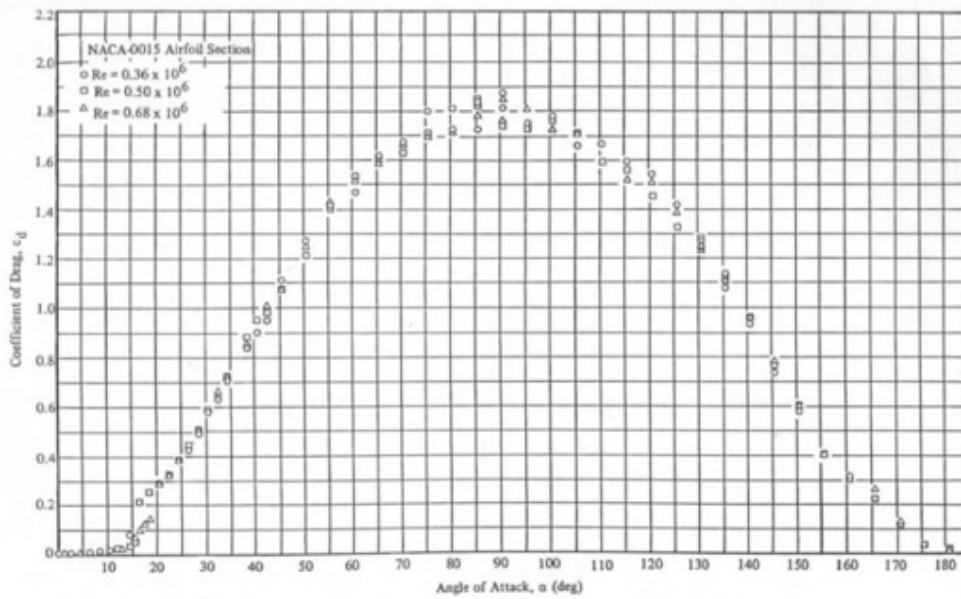


Figure 4.14—NACA 0015 drag coefficient ( $C_D$ ) versus angle of attack.

The final force coefficient can be calculated as the vector sum of the lift (perpendicular to the wind vector) and the drag (parallel to the wind vector) as a function of the sail angle. For the speeds analyzed, the rover's velocity can be neglected. These input are summed in figure 4.10, shown earlier, in which the magnitude of the force is equal to the length of the vector from the zero on the left side of the graph, and the direction of the vector indicates the direction of the force. As is clear, the force vector can never be in the direction of the wind (the negative x direction in the figure), and hence the rover cannot drive directly upwind. This is also characteristic of sailboats and landsailing vehicles on Earth, and driving in the windward direction, if desired, can be done by the well-known technique of tacking.

#### 4.3.6 Zephyr Landsailer Mobility Risk Inputs

Although the Venusian atmosphere is very dense, a parachute system is required to safely deploy the rover on the surface. This design utilizes a parachute made from a high temperature material not typically used in parachutes, thus there are possible development risks associated with using Nextel™ as a parachute material. Testing can minimize this risk, but testing parachute performance at the expected environmental conditions is well beyond the capacity of any current test facility. Therefore, extensive testing of the selected parachutes material under the appropriate environmental conditions along with a robust design is needed to minimize the potential risks.

Should the parachute fail to operate properly, the resulting rough landing could leave the rover partially damaged and immobilized. Even if the parachute performs flawlessly, landing on an odd rock formation or with excessive vertical velocity could damage the rover's wheels, resulting in a loss of, or reduced, mobility.

The wing is the sole propulsion device for the Zephyr on the surface of Venus. It must provide sufficient force to overcome the friction of the wheels. The amount of force that the wing will generate depends linearly on the dynamic pressure at the Venus surface, which, in turn, depends on the square of the wind velocity. Very limited data is available about the average surface wind velocity on Venus, but that data indicates that the velocity is quite low. The wing has been designed based on this low average velocity, and the resulting wing is quite large. If the surface wind velocity on Venus is actually larger than

indicated by the limited data, then the wing may be over-sized. This is not a bad condition, since the wing can be feathered into the wind direction to reduce the aerodynamic force it creates. If the surface wind velocity is smaller than indicated by the data, then the rover won't be able to move. More reliable surface data would be welcomed to help mitigate the risk of an incorrectly sized wing.

#### **4.3.7 Zephyr Landsailer Mobility Recommendation**

It is recommended that alternative wheel designs be evaluated for use with this Landsailer configuration. Although numerous wheel designs have been tested and evaluated over the years for many missions, the vast majority have been in support of missions to Mars and the Moon, which have loose sandy soil. Pictures obtained from the Russian probes, however, show Venus to have fairly flat rocky terrain, which is quite different. It is possible that an alternative or modified wheel geometry can provide better performance on the Venusian terrain than the slightly modified LRV wheel selected for this design. The lunar rover design had different design criteria for different terrain and a different environment, thus it is recommended that alternative wheel geometries specifically designed for the anticipated Venus surface environment be evaluated.

### **4.4 Structures and Mechanisms**

#### **4.4.1 Structures and Mechanisms Requirements**

The Venus Landsailer structures must contain the necessary hardware for instrumentation, avionics, communications, propulsion, and power. The structural components must be able to withstand applied loads from the launch vehicle and operational maneuvers and provide minimum deflections, sufficient stiffness, and vibration damping. The maximum anticipated vertical acceleration is 5 g. The goal of the design is to minimize weight of the components that comprise the structure of the Landsailer bus, and it must also fit within the physical confines of an aeroshell and the launch vehicle. The bus must survive the Venus atmospheric conditions including, 400 °C+ temperature, 93 bar pressure, sulfuric acid, and hydrogen sulfide.

The mechanisms are required to function for single events or continuously throughout the mission, depending on the types of mechanisms. The wheels and sail are deployed from their stowed configurations.

#### **4.4.2 Structures and Mechanisms Assumptions**

The main bus consists of tubular members forming a ladder frame, which is assumed to provide the optimum architecture for supporting the necessary operational hardware. The frame is easily adapted to the aeroshell and launch vehicle. The bus material is of the Ti-6Al-4V Ti alloy. Properties for the Ti alloy, Ti-6Al-4V, are from the Metallic Materials Properties Development and Standardization (MMPDS) (Federal Aviation Administration, 2006). **Error! Reference source not found.** Figure 4.15 illustrates the Landsailer and its bus. The bus is assumed to be of a welded construction along with the use of threaded fasteners for joining components.

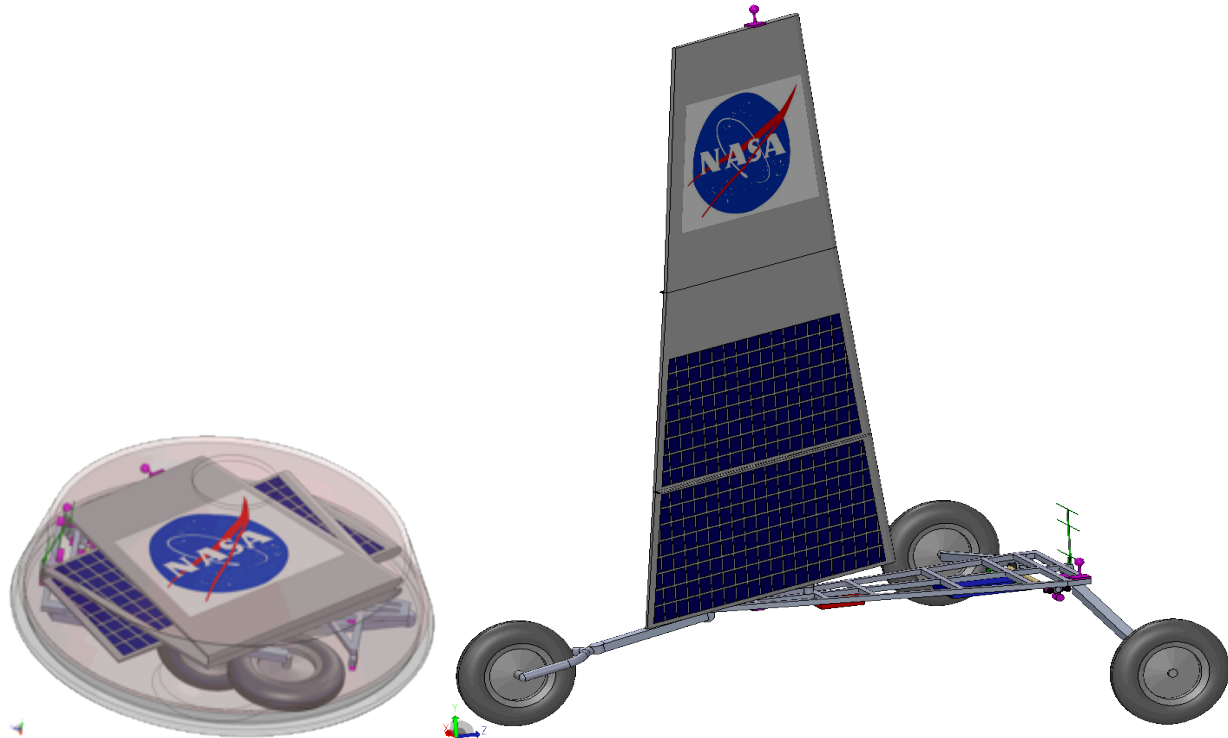


Figure 4.15—Illustration of the Landsailer stowed in the aeroshell (transparent for illustration purposes) on the left and deployed on the right.

The subsystem includes the wheels, suspension, and sail. The suspension consists of cantilevered beams which deflect vertically for a sprung suspension. The sail utilizes three segments. The segments are constructed similar to an aircraft wing using ribs and stringers under the skin. The sail mass is reported in the propulsion section of this report.

The analysis performed in this study assumed a maximum axial load 5 g from the landing with a Landsailer mass of approximately 175 kg.

The assumptions for mechanisms include separation from the launch vehicle utilizing the launch vehicle's system and separation from the aeroshell. Also, mechanisms are utilized to deploy the wheels and sail. The wheel beams are deployed and the wheels are positioned relative to the wheel beams. As with the sail the sail mechanisms' mass is reported with the propulsion section of this report.

#### 4.4.3 Structures and Mechanisms Design and MEL

The necessary system components are mounted on the ladder frame of the Landsailer. The hardware includes components for communications and tracking; control and data handling; guidance, navigation, and control; electrical power; and propulsion. The power SAs are mounted to the sail. An overall view of the Landsailer with mounted hardware is illustrated in Figure 4.16 **Error! Reference source not found.**

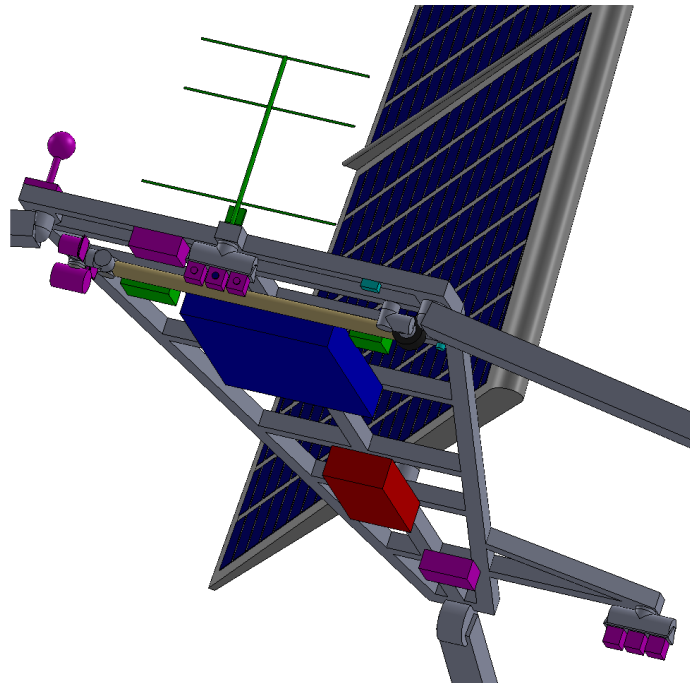


Figure 4.16—A view of the Landsailer bus underside with mounted hardware.

Table 4.4 **Error! Reference source not found.** shows the expanded MEL for the structures subsystem on the Venus Landsailer. This MEL breaks down the structures line elements to the lowest WBS.

Table 4.4—Venus Landsailer Structures Master Equipment List

WBS	Description	QTY	Unit Mass	Basic Mass	Growth	Growth	Total Mass
Number	Case #1 Venus Landsailer CD-2013-86		(kg)	(kg)	(%)	(kg)	(kg)
06	Venus Landsailer System			1581.03	18.7%	295.74	1876.77
06.1	Landsailer Rover			220.08	20.5%	44.86	264.94
06.1.11	Structures and Mechanisms			63.21	18.0%	11.38	74.59
06.1.11.a	Structures			57.19	18.0%	10.29	67.48
06.1.11.a.a	Chassis			57.19	18.0%	10.29	67.48
06.1.11.a.a.a	Chassis	1	24.86	24.86	18.0%	4.47	29.33
06.1.11.a.a.b	wheel beams total	1	32.33	32.33	18.0%	5.82	38.15
06.1.11.a.b	Sail Support Structure			0.00	0	0.00	0.00
06.1.11.b	Mechanisms			6.02	18.0%	1.08	7.11
06.1.11.b.f	Installations			6.02	18.00%	1.08	7.11
06.1.11.b.f.c	GN&C Installation	1	0.10	0.10	18.00%	0.02	0.12
06.1.11.b.f.d	Command and Data Handling Installation	1	0.65	0.65	18.00%	0.12	0.77
06.1.11.b.f.e	Communications and Tracking Installation	1	0.36	0.36	18.00%	0.06	0.42
06.1.11.b.f.f	Electrical Power Installation	1	1.38	1.38	18.00%	0.25	1.63
06.1.11.b.f.g	Thermal Control Installation	1	0.04	0.04	18.00%	0.01	0.05
06.1.11.b.f.i	Chemical Propulsion Installation	1	3.49	3.49	18.00%	0.63	4.11



#### 4.4.4 Structures and Mechanisms Trades

A Ti alloy was chosen due to the harsh environmental conditions on the surface of Venus. If needed, a corrosion barrier coating could be applied, based on corrosion barriers developed for jet engines. The possible use of a nickel alloy was discussed briefly but was not investigated further. No other trades were considered at this time.

#### 4.4.5 Structures and Mechanisms Analytical Methods

Preliminary structural analysis and modeling were performed using a spreadsheet. The maximum allowable acceleration is 5 g. The approach velocity of the Landsailer is estimated at 3.1 m/s as it approaches the Venusian surface. The resulting minimum distance needed to decelerate the Landsailer to zero velocity is approximately 9.5 cm. The suspension beams deflect vertically for the necessary displacement. As a worst case scenario any displacement by the wheel assemblies were ignored.

The mass of the Landsailer is assumed to be supported equally among the three points of the suspension system. The length of the suspension beams were derived from the limitations imposed by the aeroshell while the vehicle is in a stowed form and the need for stability when deployed. A rectangular tube cross section was chosen to allow for the compliance needed vertically while providing greater stiffness in the directions parallel to the ground plane.

Material properties for the Ti-6Al-4V Ti alloy at ~400 °C are a Young's modulus of 90 GPa and a yield strength of 480 MPa as per the MMPDS (Federal Aviation Administration, 2006). A safety factor of 1.25 is applied as per the NASA standard, NASA-STD-5001 (1996), for a prototype design. The resulting allowable stress is 384 MPa.

The rear suspension beams are each 2.1 m long and utilize rectangular tubing with 102 mm width and 76 mm height. The wall thickness was specified at 3.2 mm. Modeling the wheel beams as a cantilevered beam under bending conditions, the resulting maximum stress is 223 MPa which provides a positive margin of 0.72.

The front suspension uses a rectangular tubular member with a length of 0.96 m. As with the rear suspension beams the width is 102 mm and the height is 76 mm. The wall thickness is 4.3 mm. The highest stress at the maximum deflection is 231 MPa providing a positive margin of 0.66.

The sail consists of three segments as noted in the previous section. Each section uses 0.13 mm thick skin of Ti. The segments use a 100 mm diameter round tubular member with a 1.5 mm wall thickness for the leading edge and a triangular tubular member with a 0.8 mm wall thickness for the trailing edge. Formed C channels are used for the top and bottom of each section. The C channels are specified with flanges that are 25 mm wide and a thickness of 0.8 mm. Lastly, one rib, with I cross sections, is located midway for each sail segment. The ribs have an I cross section and use a flange of 25 mm wide and 0.8 mm thick. The width of the C channels and ribs conforms to the sail width at any point along the sail. The sail sections are joined with spring loaded hinges and a locking mechanism. A release pin is used to release the sail segments from a stowed position. The final mass is carried in the propulsion section.

An additional installation mass was added for each subsystem in the mechanisms section of the structures subsystem. These installations were modeled using 4% of the CBE dry mass for each of the subsystems. The 4% magnitude for an initial estimate compares well with values reported by Heineman (1994) for various systems. This is to account for attachments, bolts, screws and other mechanisms necessary to attach the subsystem elements to the bus structure and not book kept in the individual subsystems. An 18% growth margin was applied to the resulting installation mass. These margins are placed onto the subsystem elements prior to the additional margin that was added in order to reach the 30% MGA required on the dry mass elements.

Component masses for the structures and mechanisms are provided in Table 4.4. **Error! Reference source not found.** The structures are itemized with the bus or chassis and the suspension system with the beams. Installations for the various systems are itemized also.

#### **4.4.6 Structures and Mechanisms Risk Inputs**

Structural risks may include excessive g loads, impact from a foreign object, or harsh landing on Venus which may cause too much deformation, vibrations, or fracture of sections of the support structure. Consequences include lower performance from mounted hardware to loss of mission.

Excessive deformation of the structure can misalign components dependent on precise positioning, therefore, diminishing their performance. Other components may be damaged or severed from the rest of the system resulting in diminished performance or incapacitation of the system. Excessive vibrations may reduce instrumentation performance and/or potentially lead to long term structural failure due to fatigue. Overall, the mission may not be completed in an optimum manner or it can be terminated in the worst case.

In an effort to mitigate the structural risk the structure is to be designed to NASA standards to withstand expected g loads, a given impact, and to have sufficient stiffness and damping to minimize issues with vibrations. Trajectories are to be planned to minimize the probability of impact with foreign objects.

The likelihood for structural risks is low at 2. The cost would be ranked at 3, the mission schedule and performance would each be affected to high degree at 4. As a robotic mission there would be no risk to humans making the risk with safety a low ranking of 1.

Similar to the structural risks excessive g loads, impact from a foreign object, harsh landing, or environmental conditions may damage mechanisms. Consequences include lower performance from mounted hardware to loss of mission.

Failure of mechanisms may prevent optimum hardware operation or may inhibit mission completion. Failure of separation or deployment units can prevent planned mission completion.

Mitigation of the risks with mechanisms would include the mechanisms are to be designed to NASA standards to withstand expected environmental conditions. All precautions should be taken to prevent damage from installation, launch, and operating conditions. Additionally, material selection is to minimize issues with corrosion and creep.

The rankings with the risks for mechanisms is similar to the risk rankings for structures. The likelihood for risks with mechanisms is ranked a 2. The “effects on mission costs” is ranked at 3. The schedules and performance would be affected significantly enough to rank them at 4. Safety concerns are minimal at 1 being a robotic mission.

#### **4.4.7 Structures and Mechanisms Recommendation**

The structure is to be designed to NASA standards to withstand expected g loads, a given impact, and to have sufficient stiffness and damping to minimize issues with vibrations. Mission trajectories are to be planned to minimize the probability of excessive loads and impact with foreign objects. Material selection is to minimize corrosion and creep issues.

### **4.5 Communications**

#### **4.5.1 Orbiter Mission Analysis**

Communications to and from the rover is via a communications satellite in a highly-eccentric 24-hr equatorial orbit around Venus

For calculating the contact time between the orbiter and the Landsailer, the orbit has a periapsis of 400 km and an altitude of apoapsis of 66,410 km. The apoapsis of the orbit is at the longitude of the lander at the midpoint of the mission. The contact time between the orbiter and the Landsailer was modeled and calculated in the SOAP.



The initial analysis was done on the assumption that the location of the Landsailer on the surface of Venus was:

- Latitude =  $-20^{\circ}$
- Longitude =  $315^{\circ}$

This is in the vicinity of the Venera 14 probe that landed on Venus on March 5, 1982. The landing site of the Landsailer was changed later on during the design to be in the vicinity of the Venera 10 probe, which had landed on Venus on October 25, 1975, due to the higher winds and smoother surface seen at that site. The location of the Venera 10 probe on Venus was:

- Latitude =  $15.42^{\circ}$
- Longitude =  $291.5^{\circ}$

That latitude of the new landing site was roughly the same amount above the equator as the original landing site was below the equator ( $15.42^{\circ}$  compared to  $-20^{\circ}$ ). Also, the difference in longitude of the landing sites was relatively small ( $291.5^{\circ}$  compared to  $315^{\circ}$ ). Since the orbiter was assumed to be in an equatorial orbit, the analysis of contact time between the lander and orbiter using the original landing site was conservative for the new landing site, since the revised site was closer to the equator. The new longitude could be accommodated by changing the longitude of periapsis of the orbit.

For the analysis of the contact time between the Landsailer and the Orbiter, the following horizon masks were assumed and applied on the lander:

- $45^{\circ}$  with respect to the Orbiter
- $10^{\circ}$  with respect to the Sun

With the applied horizon masks, the contact times for Zephyr and the Orbiter are as follows:

- Orbiter to Zephyr
  - Minimum contact time per day is 16 hr
  - Maximum contact time per day is 18.5 hr
  - Average contact time per day is 17.5 hr
- Orbiter to DSN
  - Minimum contact time per day is 21 hr
  - Maximum contact time per day is 22.5 hr
  - Average contact time per day is 22 hr

The time of targets in view of the lander and orbiter can be seen in Figure 4.17. The top yellow line shows the time that the Sun is in view of Zephyr with the  $10^{\circ}$  horizon mask applied as mentioned earlier. The remaining lines in Figure 4.17 show what targets are in view with respect to the Orbiter.

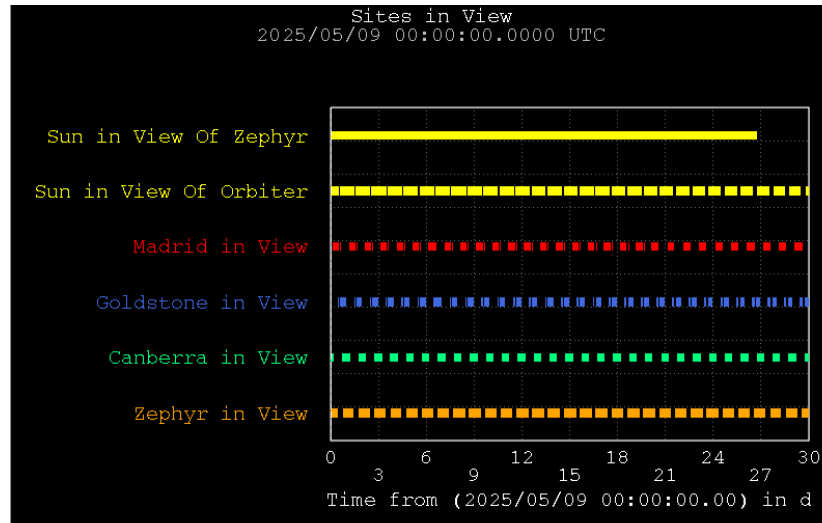


Figure 4.17—Targets in view of Lander and Orbiter.

While Zephyr is in view of the orbiter for the entire duration of the mission, the Sun is in view of Zephyr for just 27 days. This means that with the assumed launch date of December 25, 2024, arrival date of May 9, 2025, and the assumed landing site, the mission would last a maximum of 27 days. Quick analysis in SOAP shows that the Sun can be in view of Zephyr for at least 30 days as long as the longitude of the landing site is greater than  $325^\circ$  but less than  $30^\circ$  such that the Sun is in view when Zephyr arrives as Venus.

#### 4.5.2 Communications Requirements

As mentioned previously the Venus has an extreme environment that excludes all existing space communications hardware. Due to mass constraints to allow the vehicle to be mobile no pressure containment vessels are allowed. As such the communications system will need to be built from SiC components and need to survive the high pressures/temperatures. These same limitations to simple SiC electronics will not allow any coding of the data streams to be done. Communications to an orbiter at 72000 km maximum distance is required with a data rate of 2 kbps, AM modulation, and a 1 month lifetime (on surface). Frequency drift is acceptable and can be handled by the orbiter. Some initial concerns are that the Venus surface may not make a good ground plane and that the electrical components, although individually developed, are at very low integration level

#### 4.5.3 Communications Assumptions

Vehicle power is limited on the Landsailer so only 2 W of RF transmit power are assumed for the vehicle. Such powers should be sufficient when considering an orbiter for relay to Earth. For simplicity a non-tracking system is assumed with a Yagi antenna, with 2 dB of gain. Based upon current SiC technology, no processing or memory is allowed for the system. A frequency of 250 MHz was chosen as were electrically short antennas. No radiation shielding is needed on the Venus surface due to the mass shielding of the thick atmosphere. The notional relay satellite is assumed to have a 4.5 m diameter dish antenna, a G/T of  $-18.2$  dB/K. This is similar to requirements for existing communications satellites.

#### 4.5.4 Communications Design and MEL

The SiC-based receiver and transmitter were laid out, each to use 3 W of DC power. Along with an RF power amplifier the communications system uses a total of 12 W of DC power and maximum of 2 W of RF power. The communications system components are shown in green in Figure 4.18. A small omni antenna completes the system. Table 4.5 contains the communications MEL.



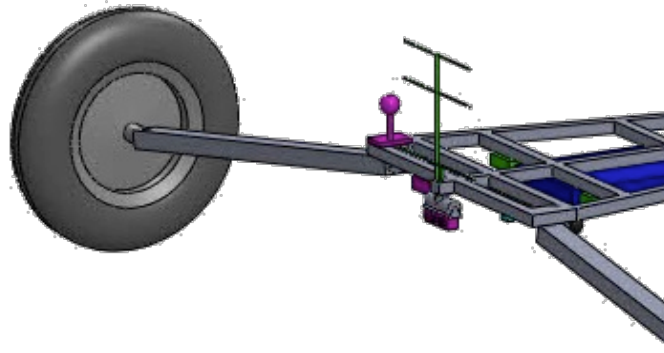


Figure 4.18—Communication components.

Table 4.5—Communications Master Equipment List

WBS	Description	QTY	Unit Mass	Basic Mass	Growth	Growth	Total Mass
Number	Case #1 Venus Landsailer CD-2013-86		(kg)	(kg)	(%)	(kg)	(kg)
06	Venus Landsailer System			1581.03	18.7%	295.74	1876.77
06.1	Landsailer Rover			220.08	20.4%	44.86	264.94
06.1.4	Communications and Tracking			4.00	32.5%	1.30	5.30
06.1.4.a	UHF Band System			4.00	32.5%	1.30	5.30
06.1.4.a.a	Transmitter	1	1.50	1.50	30.0%	0.45	1.95
06.1.4.a.b	Receiver	1	1.50	1.50	30.0%	0.45	1.95
06.1.4.a.c	Cable	1	0.50	0.50	50.0%	0.25	0.75
06.1.4.a.d	Antenna	1	0.50	0.50	30.0%	0.15	0.65

#### 4.6 Command and Data Handling (C&DH)

The C&DH or Avionics subsystem generally provides all telemetry acquisition and processing, before forwarding it to the communication subsystem for transmission to Earth.

##### Design Requirements

- Operate and survive on the surface of Venus at 462 °C, 92 MPa (92 bar)
- Accept primitive bit-level commands relayed from orbiter via comm
- Gather science data and scanning photodiode imager data
- Transmit data to orbiter via addressable bit-level register dumps

##### Assumptions

- Single string
- Devoid of software
- Registered data transferred with multiplexed 1970s style universal asynchronous receiver/transmitter (UART) data streaming to/from comm
- Cyclically service all the needed instrumentation (see below)
- Use SiC 1970s RTL-gate integrated circuit design and packaging (TRL 3)
- Desire lowest possible power per gate/transistor
- Level of integration several hundred transistors per package
- ADC, MPU-level integrations, Motor Drivers—all in flat-packs
- Transistor density comparable to first 4-bit microprocessors of 1971 (2300 transistors)
- Assume 1970s UART-style instrumentation data flows
- Figure 4.19 to Figure 4.23 for block diagrams

### *Design Description*

- Avionics components based on high temperature SiC transistors
- Assume early 1970s packaging density (e.g., DEC PDP-8 and Data General NOVA minicomputers)
- Possible ROM/RAM implementations per HP 9100A calculator of 1969.
- Imaging uses scanning photodiode (similar to Slow Scan TV on Apollo)
- UART data flows at very low baud rate allow several channels of data in 3 kHz bandwidth if analog

### *Concerns, Comments, Recommendations*

- Obvious concern for survivability of transistors, connectors, insulation, integrated circuit packages
- Development of suitable capacitors and resistors

#### **4.6.1 C&DH Requirements**

The design requirements for the C&DH system are as follows:

- Weather Station—comprised the following instruments:
  - Two anemometers
  - Three temperature sensors
  - Two pressure sensors
- Motors needed
  - Sail orientation motor
  - Steering motor
  - Brake motor
  - Camera pan
  - Camera tilt
  - Two robotic arm (azimuth, placement)
  - Robotic arm tool selection
  - Grinder motor

#### **4.6.2 C&DH Assumptions**

The following design assumptions are based on the mission requirements:

- On/off controls are 1-bit
- Some science data is 12-bit (e.g., images)
- Drive and housekeeping
  - Wheel rotation counter
  - Sail position sensor
  - Steering Wheel position sensor
  - Two tilt sensors
  - Battery voltage sensor
  - Two electronics temperature
- Navigation Support

- Two navigation cameras (stereo)
- Science Support
  - Panorama Camera
  - Robotic arm instruments
  - Robotic arm (2 degrees of freedom)
  - Rock Abrasion Grinder
  - APXS
  - X-ray diffraction
- Deployment motors/springs/actuators
  - Three sail segments (one per segment)
  - Three wheel struts
  - Two wheel orientation
  - Latches and separation
  - Three parachute separation

### 4.6.3 C&DH Design and MEL

#### 4.6.3.1 High Temperature Electronics

Silicon carbide electronics while simple can withstand the high temperatures of the Venus environment. Basic SiC logic gates, microcontrollers, analog to digital controllers, scanning cameras and motor drivers are under development. Attributes and schematics of each follow:

##### *The Basic Silicon Carbide Logic Gate*

- All logic functions synthesized from NAND and NOR gates (Figure 4.19)
- NAND/NOR functions can be combined into a single
- Power dissipation of 1.5 mW per gate at temperature

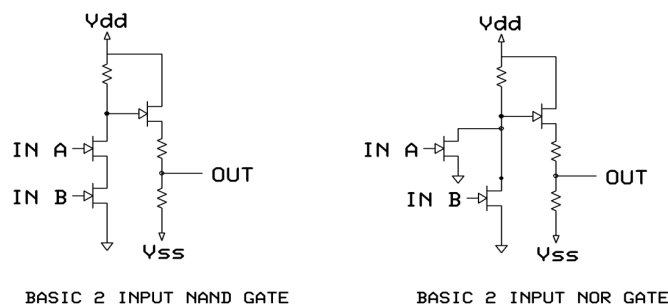


Figure 4.19—SiC logic gate basics.

##### *Processor Core*

- State machine in 64 pin QFP (Figure 4.20)
- RAM 32 pin QFP (X 2)
- ROM 32 pin QFP
- Total power consumption estimated at 3 W

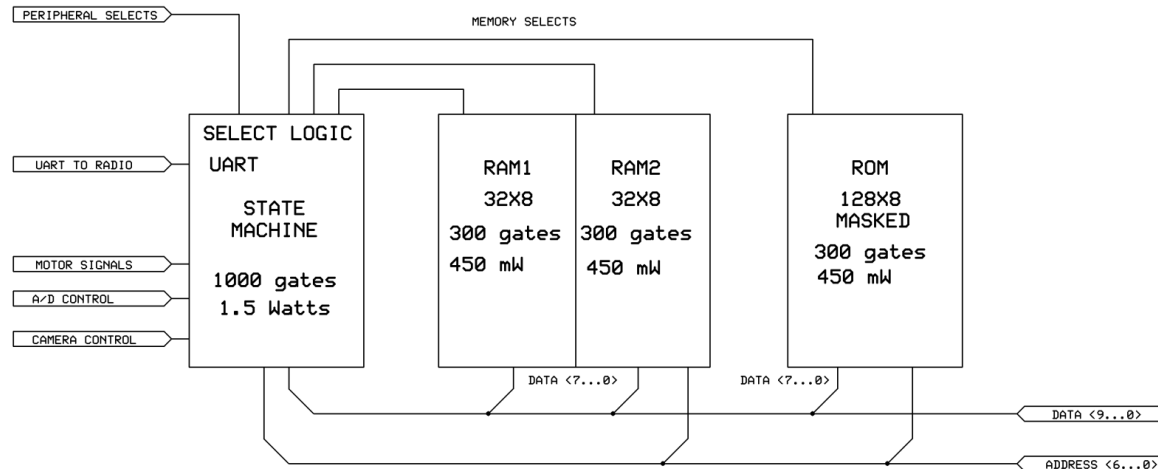


Figure 4.20—SiC microcontroller core, multichip topography, 3 W.

### A to D Converter

- 10 bit successive approximation: 10 clocks per conversion (Figure 4.21)
- Analog multiplexer shown as 10 channels
- 64 pin QFP
- 650 mW estimated power consumption

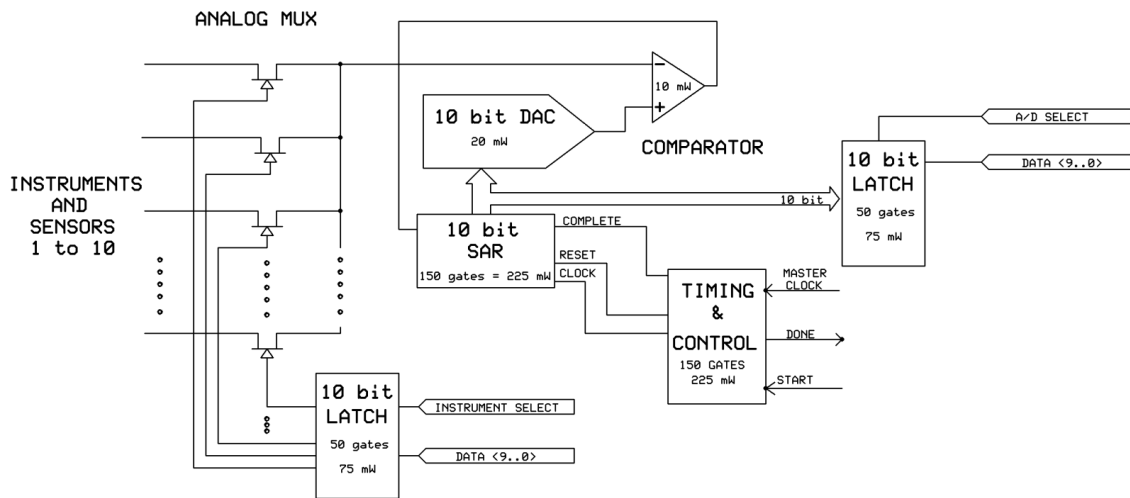


Figure 4.21—The 10 bit analog to digital converter, ~650 mW dissipation.

### Motor Drive Circuit

- Three phase, Pseudo Sinusoidal Drive (Figure 4.22)
- One per motor
- 32 pin QFP
- 600 mW power consumption (not including winding currents)

With these SiC components a simple control system can be created to operate the Landsailer by signals to/from the orbiter (see Figure 4.23). This places the intelligence for the system on the orbiter, away from the harsh environment. No memory storage using SiC is currently available so the orbiter will need to operate the science instruments directly and upload the raw data signals in real time.

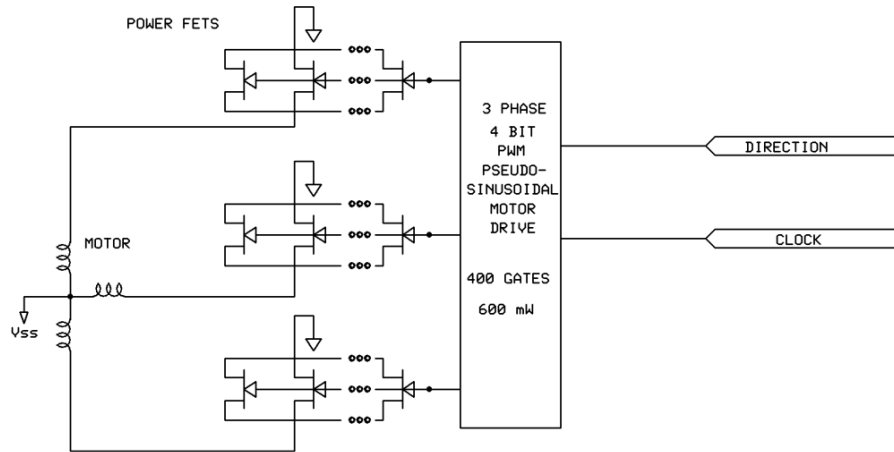


Figure 4.22—SiC motor drive circuit, 600 mW dissipation.

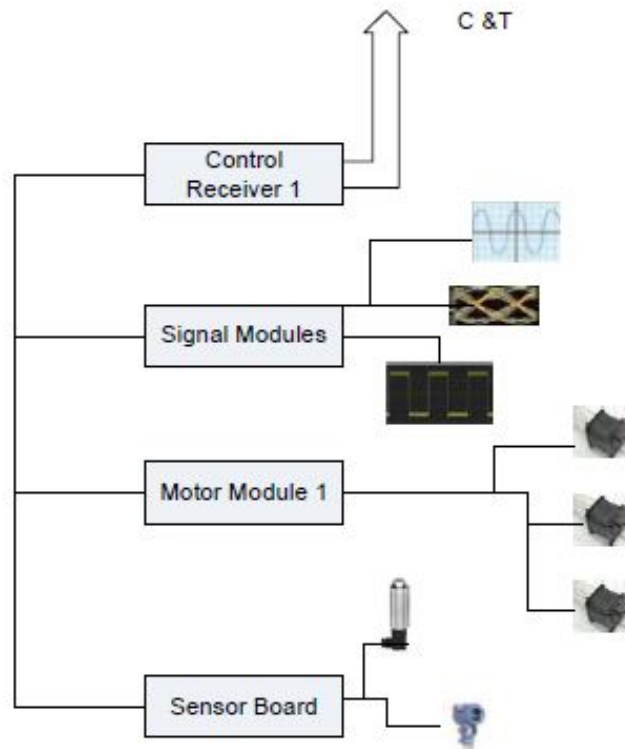


Figure 4.23—Motor control system schematic.

Figure 4.24 shows a notional avionics enclosure notionally shown with front and back removed and boards in loaded configuration. This box is assumed to be gel-filled to prevent corrosion from the Venus atmosphere.

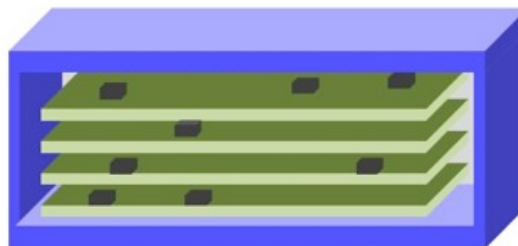


Figure 4.24—Avionics enclosure.

Table 4.6—C&DH Master Equipment List

WBS	Description	QTY	Unit Mass	Basic Mass	Growth	Growth	Total Mass
Number	Case #1 Venus Landsailer CD-2013-86		(kg)	(kg)	(%)	(kg)	(kg)
06	Venus Landsailer System			1581.03	18.7%	295.74	1876.77
06.1	Landsailer Rover			220.08	20.4%	44.86	264.94
06.1.1	Science Instruments			17.90	39.3%	7.03	24.93
06.1.2	Attitude Determination and Control			2.29	30.0%	0.69	2.98
06.1.3	Command & Data Handling			16.30	41.4%	6.75	23.05
06.1.3.a	C&DH Hardware			12.30	38.6%	4.75	17.05
06.1.3.a.a	Control Receiver 1	1	1.30	1.30	50.0%	0.65	1.95
06.1.3.a.b	Signal Module 1	1	1.00	1.00	50.0%	0.50	1.50
06.1.3.a.c	Signal Module 2	1	1.00	1.00	50.0%	0.50	1.50
06.1.3.a.d	Motor Module 1	1	1.00	1.00	50.0%	0.50	1.50
06.1.3.a.e	Sensor Board	1	1.00	1.00	50.0%	0.50	1.50
06.1.3.a.f	Enclosure	1	7.00	7.00	30.0%	2.10	9.10
06.1.3.b	Instrumentation & Wiring			4.00	50.0%	2.00	6.00
06.1.3.b.b	Data Cabling	1	4.00	4.00	50.0%	2.00	6.00

## 4.7 Guidance, Navigation and Control (GN&C)

### 4.7.1 GN&C Requirements

The requirements for the GN&C subsystem were as follows:

- Zero fault tolerant
- Provide acceleration measurements during descent
- Provide tilt sensing
- Provide an estimate on the amount of distance traveled during an excursion

### 4.7.2 GN&C Assumptions

While specific components were used in the design of the GN&C subsystem, the components selected would generally not survive the harsh Venus environment for very long. It was assumed however that by the time the rover is built that the components used in the design could either be modified to survive the Venus environment or components with similar functionality could be procured that would survive the Venus environment for the required amount of time to complete the mission.

### 4.7.3 GN&C Design and MEL

The design of the GN&C subsystem for the Landsailer consists of a tilt sensor, two separate wheel revolution counters and three accelerometers. The accelerometers are Honeywell Q-Flex QA-3000 accelerometers and are used to make acceleration measurements during the descent of the Landsailer. The tilt sensor is a Crossbow CXTA02 dual axis analog tilt sensor that is used to measure the pitch and roll of the Landsailer during excursions. The wheel revolution counters are mechanical incremental encoders with one counter on each of the back wheels of the Landsailer and are used to measure the distance traveled during an excursion.

Table 4.7—GN&C Case 1 Master Equipment List

WBS	Description	QTY	Unit Mass	Basic Mass	Growth	Growth	Total Mass
Number	Case #1 Venus Landsailer CD-2013-86		(kg)	(kg)	(%)	(kg)	(kg)
06	Venus Landsailer System			1581.03	18.7%	295.74	1876.77
06.1	Landsailer Rover			220.08	20.4%	44.86	264.94
06.1.1	Science Instruments			17.90	39.3%	7.03	24.93
06.1.2	Attitude Determination and Control			2.29	30.0%	0.69	2.98
06.1.2.a	Guidance, Navigation, & Control			2.29	30.0%	0.69	2.98
06.1.2.a.a	Tilt Sensor	1	0.07	0.07	30.0%	0.02	0.08
06.1.2.a.b	IMU	0	0.00	0.00	0.0%	0.00	0.00
06.1.2.a.c	Accelerometers	3	0.08	0.23	30.0%	0.07	0.29
06.1.2.a.d	Wheel revolution counter	2	1.00	2.00	30.0%	0.60	2.60

#### **4.7.4 GN&C Trades**

No trades were performed on the GN&C subsystem for this design study.

#### **4.7.5 GN&C Risk Inputs**

One obvious risk is the components surviving and performing accurately in the harsh Venus environment. However, should the components fail it would not necessarily lead to the end of the mission. The mission could continue with a failed tilt sensor with an increased risk of the Landsailer tipping over. Also, should one or both of the wheel revolution counters fail, the mission could continue with a reduced accuracy in the knowledge of the distance traversed during an excursion. The most serious risk due to a component failure is if one or more of the accelerometers fail since they are used to trigger the release of the parachute upon landing. If the parachute is released too early this could lead to the Landsailer hitting the ground with excessive g-loads causing other components to fail and could result in the loss of the mission. If the parachute is released too late it could become tangled in the Landsailer.

#### **4.7.6 GN&C Recommendation**

It is recommended as future work to iterate with the mission design lead to develop an end-to-end trajectory (interplanetary and EDL) that delivers the Landsailer to the specified landing site and the orbiter to the specified orbit.

### **4.8 Electrical Power System**

Electrical power required for Venus landers has in the past been supplied by energy storage systems (batteries) only required to operate for a few hours on the Venus surface, and which therefore operate at terrestrial temperatures, relying on thermal mass to delay the death of the system due to overheating. Recently, proposals have been made to use radioisotope power system (RPS) to allow for long duration (months to years) of operation on the surface of Venus [Landis and Mellott 2004; Dyson and Bruder 2010], however, this system is ruled out for the present design due to cost. The power system assumed for this mission is use of batteries which are charged by solar arrays (SAs).

An analysis by Landis and Haag (2013) shows that photovoltaic cells should still be operational at Venus surface temperatures and illumination levels. Although the effective efficiency is low, due to the high operating temperature and low light levels, the rover has been designed to minimize the power requirements. Landis and Harrison (2008) show that NaS batteries will function under Venus surface conditions.

#### **4.8.1 Power Requirements**

Venus lander power requirements are shown in Table 4.8. For 1 hr out of every 24 hr, 100 W are required for 100 W-hr. For 8 hr, 90 W are required for 728 W-hr followed by a 10 hr charge period followed by a 91 W data transmission operation for 7 hr.

Table 4.8—Venus Lander Power Requirements

Time (hr)	Power (W)	Energy (W-hr)
1	100	100
8	91	728
8	10	80
7	91	637

### 4.8.2 Power Assumptions

Assumption for the power system is that all of the illumination is diffuse, while the solar arrays are located on the sail surface and are therefore not affected by the orientation of the sail. Light reflected from the surface (albedo illumination) was neglected. Battery charge is at 100% charge state upon landing and because there is no possibility of overcharging the system no shunt regulator is required. Battery charge/discharge efficiency is set to 90%. Mission duration is 30 (Earth) days, or one quarter of the Venus solar day (116.75 Earth days) with the start 15 days before local solar noon. This minimizes the solar intensity variation during the mission.

### 4.8.3 Power Design and MEL

In order to meet the power requirements outlined in Section 5.5.1 it is necessary to include both solar arrays and batteries within the Landsailer. The solar cell area used on the sail is about 12 (or 6 m<sup>2</sup> per side) of the sail. Landsailer is designed to begin operation with first operational day at 70% peak solar output. Peak power output is 65 W using an assumed packing factor of 80% and a 20% reduction in peak output due to the elimination of a peak-power tracker circuitry. Figure 4.3.5 shows the power output from the solar array as a function of mission time. Solar array specific area is 1.7 kg/m<sup>2</sup>. NaS batteries are sized to provide 2200 W-hr of energy storage and a specific energy of 220 W-hr/kg (340 kW-hr/m<sup>3</sup>). Daily energy consumption is 1545 W-hr. Maximum DOD is set to 70% to keep the NaS batteries in their flat voltage output portions of their discharge curve with an average power draw of 64.5 W. During the 8 hr rest period each day the batteries are charged.

The state of charge of the battery as a function of each Earth day of operation is shown in figure 4.26. The batteries start fully charged, discharge slightly early in the mission, then recharge as the sun approaches zenith, and discharge again late in the mission.

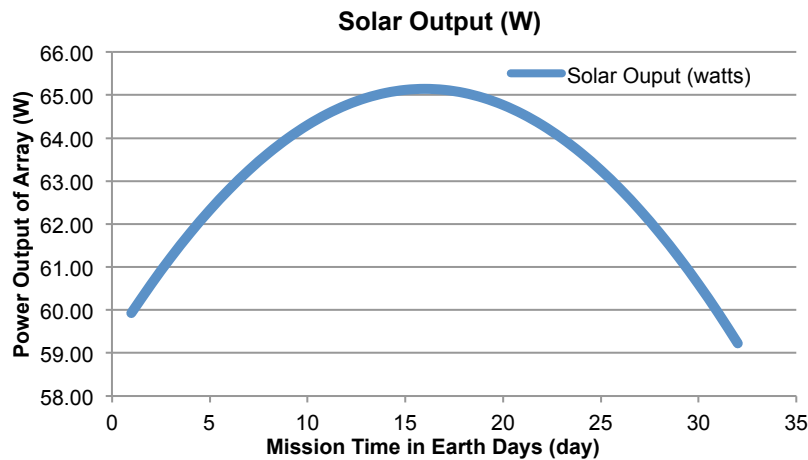


Figure 4.25—Power Output of solar array as function of mission time



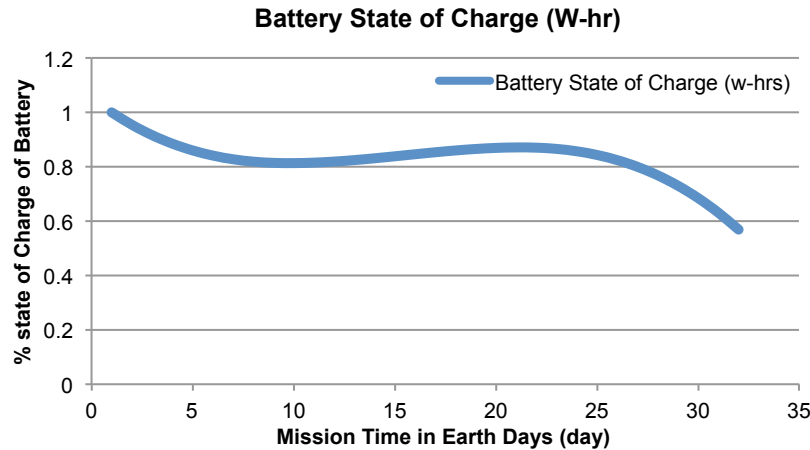


Figure 4.26—battery state of charge during the mission

All of the components of the power subsystem and their masses are shown in Table 4.9.

Table 4.9—Electrical Power System Master Equipment List

WBS	Description	QTY	Unit Mass	Basic Mass	Growth	Growth	Total Mass
Number	Case #1 Venus Landsailer CD-2013-86		(kg)	(kg)	(%)	(kg)	(kg)
06	Venus Landsailer System			1581.03	18.7%	295.74	1876.77
06.1	Landsailer Rover			220.08	20.4%	44.86	264.94
06.1.1	Science Instruments			17.90	39.3%	7.03	24.93
06.1.2	Attitude Determination and Control			2.29	30.0%	0.69	2.98
06.1.3	Command & Data Handling			16.30	41.4%	6.75	23.05
06.1.4	Communications and Tracking			4.00	32.5%	1.30	5.30
06.1.5	Electrical Power Subsystem			32.13	13.8%	4.44	36.57
06.1.5.a	Power Conversion			29.63	15.0%	4.44	34.07
06.1.5.a.a	Solar Arrays	1	19.60	19.60	15.0%	2.94	22.54
06.1.5.a.b	Battery System	1	10.03	10.03	15.0%	1.50	11.53
06.1.5.b	Electrical Power Electronics and Control			2.50	0.0%	0.00	2.50
06.1.5.b.e	Power & Data Cabling	1	2.50	2.50	0.0%	0.00	2.50

#### 4.8.3.1 Technology Maturity

Testing has shown that existing solar cell designs can operate at Venus surface temperatures and illumination levels, however, the technology maturity is extremely low, at approximately TRL 2. Glass encapsulation is required to avoid corrosion in the atmospheric conditions at the surface. Solar cell encapsulants have not been tested at the conditions. Considerable development and testing remains to be done before solar arrays can be qualified for use in the environment.

#### 4.8.4 Power Trades

The solar cells were assumed to be on the sail, and hence oriented on a vertical plane. Placing the solar array on the deck would orient it horizontally, with the array normal aimed at the zenith. This would result in approximately double the power per unit of array area. However, since the cells can be placed on both sides of the sail, an area of sail produces roughly the same power as a horizontal array of the same area.

The constraint for the mission was to design for low cost, and hence the option of radioisotope power was ruled out. An alternate design concept using a wind turbine for power was analyzed [G. Benigno, *et al.* 2013], however, the large size of the sail allows a convenient surface for mounting of solar cells, allowing a simpler design.

An alternate possibility was to design a rover using only primary batteries. This design would be heavier, but could be used as an alternative design if the solar array technology is not sufficiently developed for use.

## 4.9 Thermal Control

The thermal control system is designed to maintain the components of the Landsailer and carrier S/C within their desired temperature operating limits throughout the mission. The mission vehicles are broken down into three segments, the carrier S/C (cruise deck), aeroshell and lander.

### 4.9.1 Cruise Deck Thermal Control

The cruise deck thermal control system has to protect and regulate the temperature of the S/C and lander as it transits from Earth to Venus. The environment in which the thermal control system has to operate to maintain the desired internal operating temperature of the electronics and Landsailer varies from near Earth operation to deep space transit to operation near Venus. The sizing of the components of the thermal system is based on operation within the worst case hot or cold environment during the mission. The heat transfer to and from the S/C is based on a radiative energy balance between the vehicle and its surroundings. Solar radiation is the main source of external heat for the majority of the mission, during transit. Operation near Earth and Venus also involves the albedo (reflected sunlight) from the planet as well as direct radiation (IR) from the planet itself. These environmental conditions are listed in Table 4.10.

Table 4.10—Transit Environment Constants

Constant	Earth	Venus
Solar intensity	1360 W/m <sup>2</sup>	2613 W/m <sup>2</sup>
Albedo	0.3	0.75
Planet IR	240 W/m <sup>2</sup>	141 W/m <sup>2</sup>

To maintain the S/C and Landsailer components at their desired operating temperature the following components were utilized for the cruise deck thermal control.

- Electric heaters, thermocouples and data acquisition for controlling the temperature of the electronics.
- MLI for insulating the electronics and temperature sensitive components.
- Thermal paint for minimal thermal control on exposed structural surfaces.
- Radiator for rejecting heat from the enclosed lander.
- Cold plates with heat pipe connections to the radiator, for channeling the heat from the lander to the radiator.

#### 4.9.1.1 Electric Heaters

The electric heaters were used to provide added thermal control to the cruise deck electronics during transit. Strip heaters, as shown in Figure 4.27, were used to provide heat to the reaction control system propellant lines and other components within the cruise deck. Thermal control is accomplished through the use of a network of thermocouples whose output is used to control the power to the various heaters. A data acquisition and control computer is used to operate the thermal system.



Figure 4.27—DuPont Kapton Strip Heater.

#### 4.9.1.2 Multi-Layer Insulation (MLI) and Thermal Control Paint

MLI was used to insulate the cruise deck electronic components and exposed propellant tanks to minimize their heat loss for deep space operation. MLI is constructed of a number of layers of metalized material with a nonconductive spacer between the layers. The metalized material has a low absorptivity that resists radiative heat transfer between the layers. The insulation can be molded to conform over the exterior of the cruise deck or any individual component, as shown in Figure 4.28.

In exposed areas where MLI cannot be applied, mainly exposed structural components, thermal control paint is applied. Since the S/C will be exposed to direct sunlight for the majority of its operation, this paint is used to minimize the absorption of solar radiation. This helps maintain thermal control of the vehicle by minimizing the temperature of exposed components. The paint utilized is AZ-93. Its characteristics are listed in Table 4.11.

Table 4.11—Specifications for MLI

Variable	Value
MLI emissivity .....	0.07
MLI material .....	Metalized (aluminum) Kapton layers
Layer thickness .....	0.025 mm
Number of MLI layers.....	25
AZ-93 emissivity.....	0.91
AZ-93 absorbtivity .....	0.15

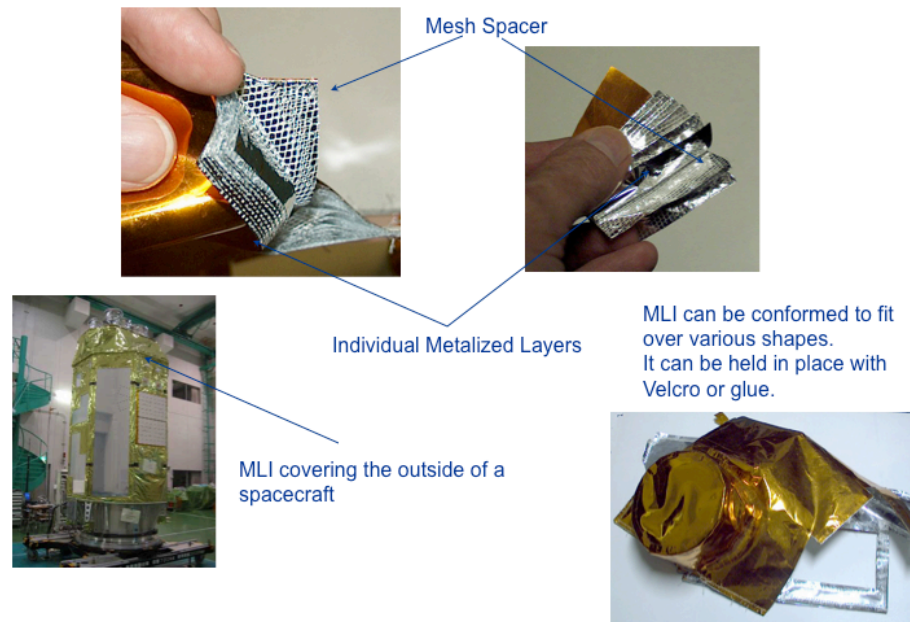


Figure 4.28—Example of MLI Blanket design and application.

### 4.9.1.3 Radiator and Cold Plates

To reject heat from the Landsailer during transit from the Earth to Venus a radiator was utilized. This radiator is coupled to the Landsailer through a cold plate interface. Heat pipes were used to move heat from the cold plates to the radiator panel, which then rejected the heat to space. An example of a cold plate with integral heat pipes is shown in Figure 4.29. The radiator was sized for operation near Venus. This is the worst case operating condition for rejecting heat from the radiator. The radiator was coated to limit its solar radiation absorption characteristics. The details on the radiator sizing are given in Table 4.12.

Table 4.12—Cruise Deck Radiator Sizing

Component	Value
Radiator solar absorptivity .....	0.14
Radiator emissivity .....	0.84
Estimated maximum radiator solar angle .....	70°
Total radiator dissipated thermal power .....	152 W
View factor to Venus.....	0.25
Required radiator area.....	0.24 m <sup>2</sup>
Radiator operating temperature.....	358 K
Cold plate material.....	Aluminum
Cold plate dimensions .....	0.1- by 0.1- by 5-mm

The radiator was surface mounted to the cruise deck and therefore rejected heat from one side. The radiator was sized based on an energy balance approach, utilizing the thermal heat to be rejected and the incoming thermal radiation from Venus and the Sun. An example of an S/C radiator with integral heat pipes is shown in Figure 4.30.

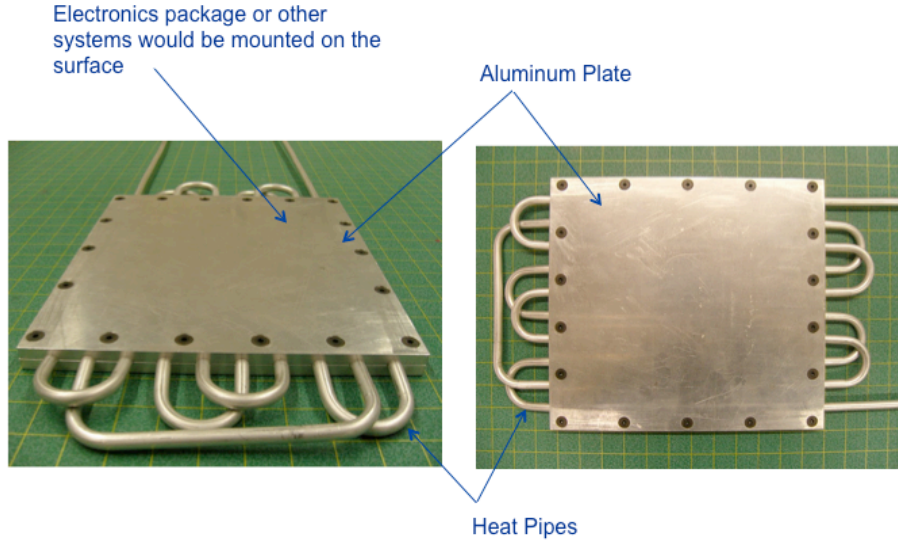


Figure 4.29—Example of a cold plate with integrated heat pipes.

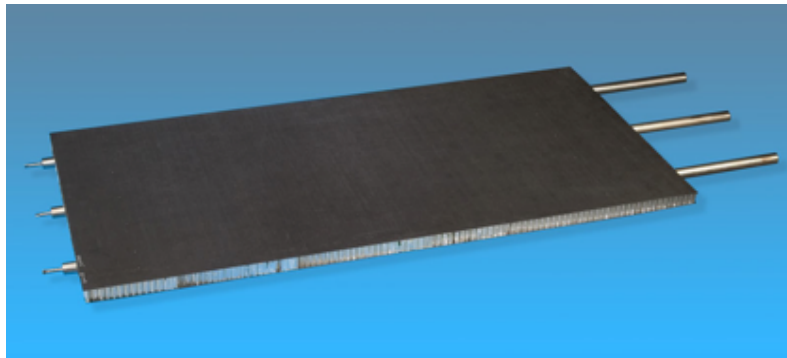


Figure 4.30—Radiator with integral heat pipes (ACT, Inc.).

#### 4.9.2 Aeroshell and Descent Thermal Control

The aeroshell consists of a heat shield and back shell. The heat shield needs to be able to withstand the aerodynamic heating that will be encountered during entry into the Venus atmosphere, as illustrated in Figure 4.31. The heat is generated by friction caused by the drag of the capsule as it enters the atmosphere. The heat load will depend on the entry angle and speed. The heat shield for Venus entry was scaled off of the Stardust and Genesis Earth entry vehicles as well as the proposed Orion entry vehicle. All of these vehicles had similar entry velocities (~ 11 km/s) to what is expected for the Venus Landsailer aeroshell. The heat shield sizing utilized the Orion structural design, shown in Figure 4.32, but substituted AVCOAT for PICA as the ablative material. This was done due to the size of the heat shield. The AVCOAT thickness utilized was 4.3 cm. The materials breakdown for the heatshield is given in Table 4.13.

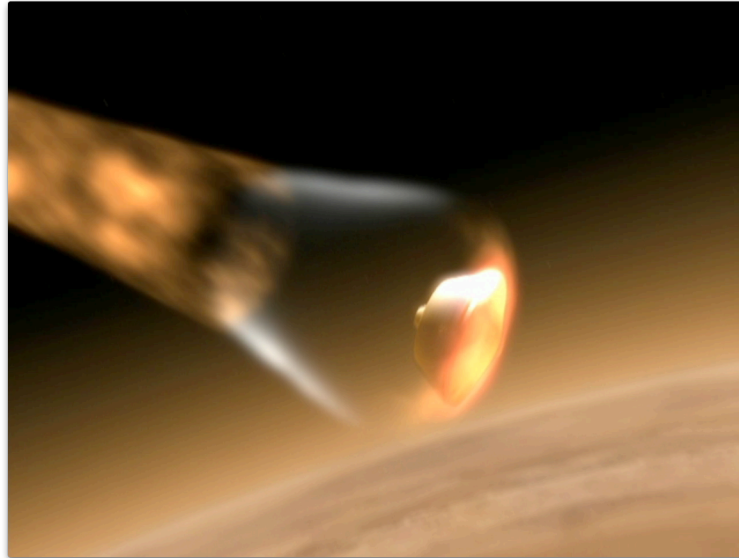


Figure 4.31—Illustration of heated Aeroshell during descent.

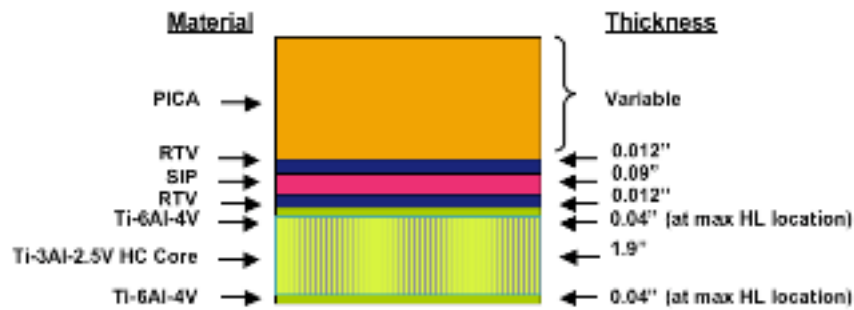


Figure 4.32—Orion Heat Shield structural makeup.

Table 4.13—Heatshield Material Layer Properties

Material	Thickness (cm)	Density (kg/m <sup>3</sup> )
Avcoat	4.3	510
RTV Glue	0.0305	1060
Foam Insulation (SIP)	0.229	70
RTV Glue	0.0305	1060
Ti Alloy (Ti-6Al-4V)	0.102	4430
Ti Alloy (Ti-3Al-2.5V) Honeycomb	4.83	96.3
Ti Alloy (Ti-6Al-4V)	0.102	4430

The heat shield and backshell geometry were scaled up from the Stardust aeroshell design (shown in Figure 4.33). The Stardust aeroshell and entry specifications are:

- Entry velocity was 11.04 km/s
- 60° half angle
- -8.0° entry angle,
- 15 rpm 4 hr before entry
- Backshell thickness 5 cm
- Heatshield/structure thickness 10 cm

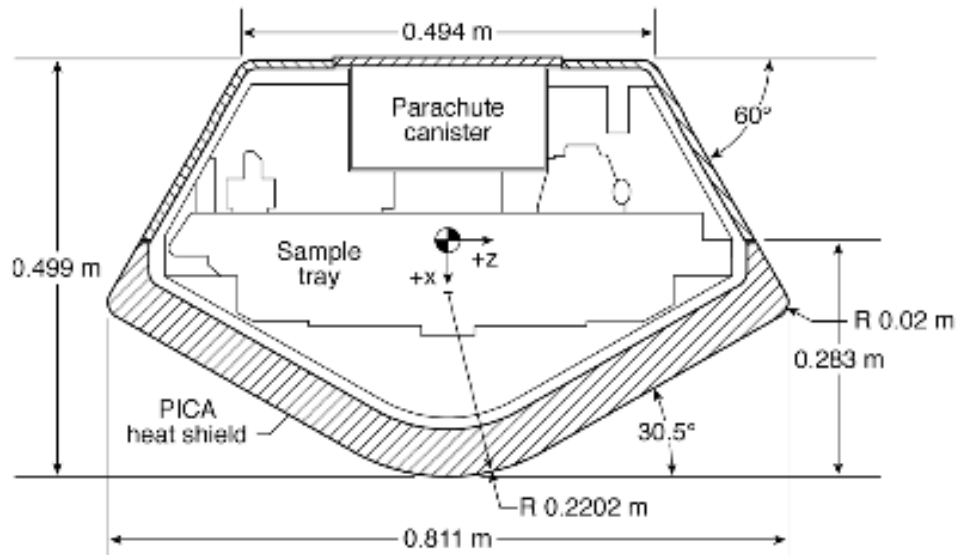


Figure 4.33—Stardust Aeroshell Geometry.

The descent time and velocity for a range of aeroshell masses is plotted as a function of altitude in Figure 4.34. All significant aerodynamic heating will occur above Mach 5, shown on the graph, and the parachute will not be released until after this speed is reached. The graph illustrates the velocity and deceleration time from entry until Mach 5 is reached for different aeroshell masses. As would be expected, the heavier the aeroshell the longer it will take to decelerate and the deeper into the atmosphere it will descend before the parachute can be released.

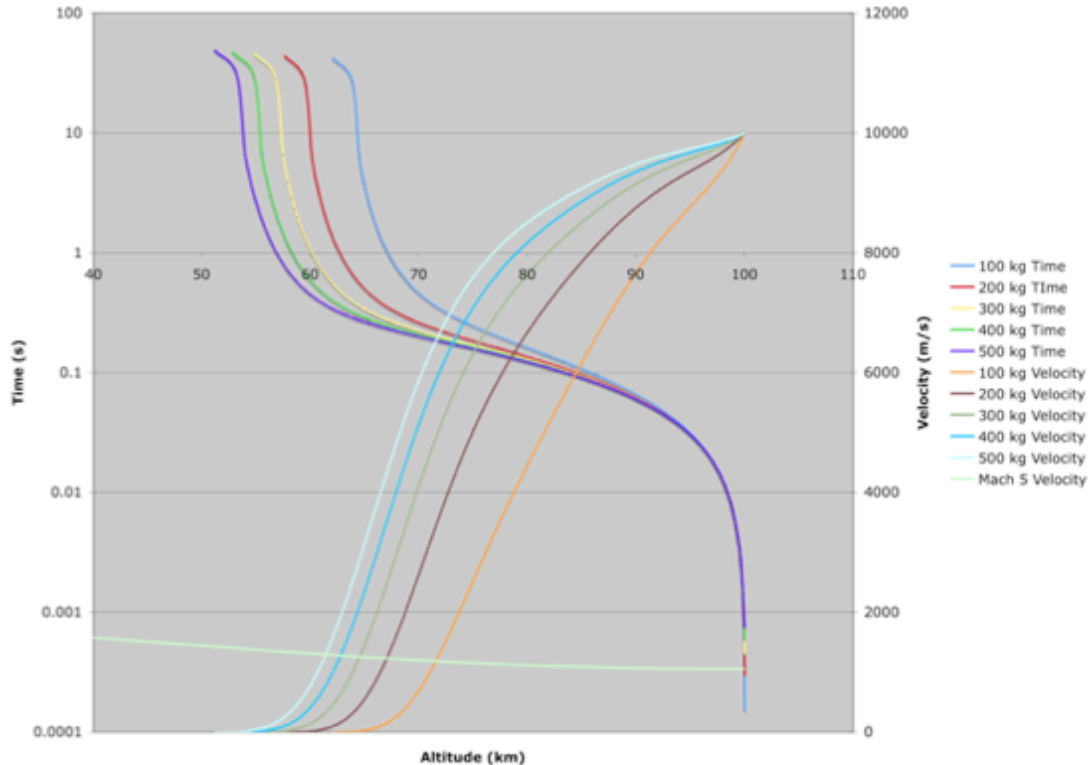


Figure 4.34—Descent velocity and time as a function of altitude

### 4.9.3 Landsailer Thermal Control

The Landsailer thermal control will be completely passive. All the electronics and mechanisms are designed to operate within the ambient surface environment on Venus therefore no active cooling will be utilized. Any excess heat generated will be dissipated to the atmosphere through the use of finned heat sinks. The surface convective heat transfer coefficient is estimated to vary between 17 and 65 W/mK depending on the wind speed range of 0.1 to 0.5 m/s. All electronics boxes and other components will be mounted so that they can be convectively cooled during operation as illustrated in Figure 4.35.

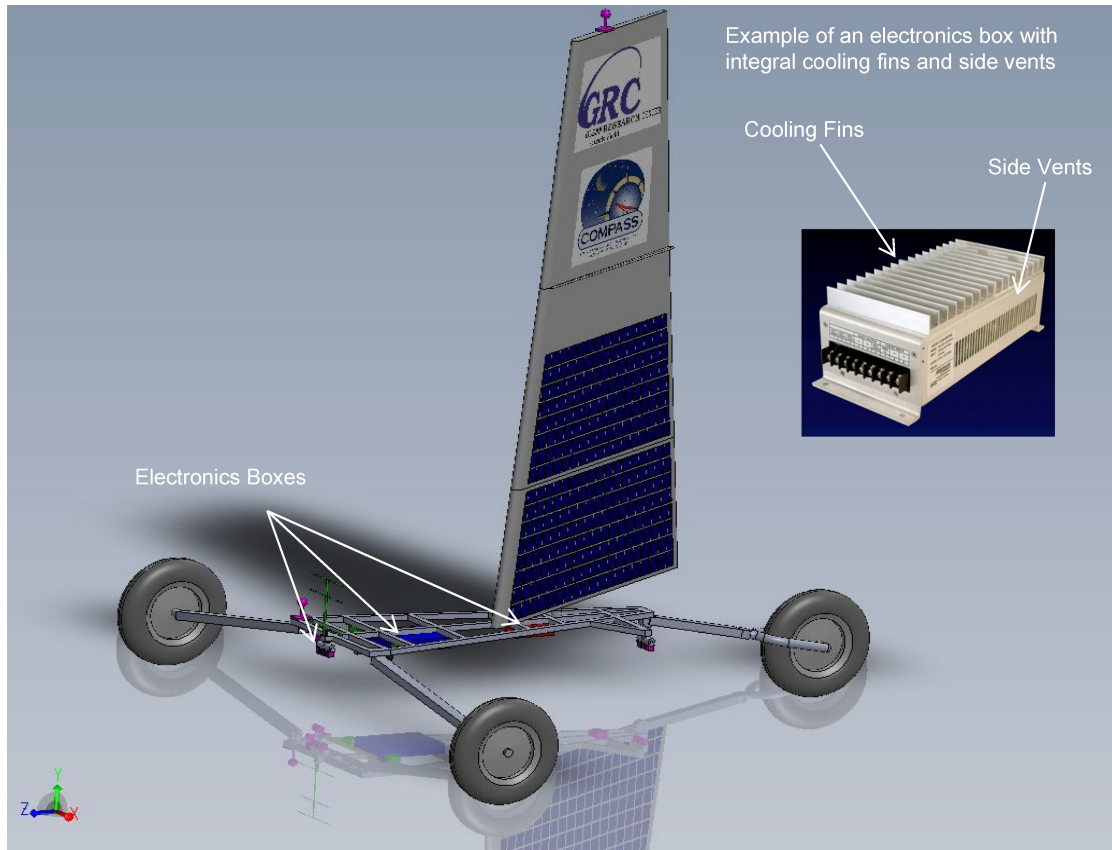


Figure 4.35—Venus Landsailer electronics component locations.

### 4.9.4 Thermal MEL

Table 4.14—Thermal Master Equipment List

WBS Number	Description	QTY	Unit Mass (kg)	Basic Mass (kg)	Growth (%)	Growth (kg)	Total Mass (kg)
06	Case #1 Venus Landsailer CD-2013-86			1581.03	18.7%	295.74	1876.77
06.1	Venus Landsailer System			220.08	20.4%	44.86	264.64
06.1.6	Landsailer Rover			1.02	18.0%	0.18	1.20
06.1.6	Thermal Control (Non-Propellant)			0.21	18.0%	0.04	0.25
06.1.6.a	Heat Sinks			0.81	18.0%	0.15	0.95
06.1.6.b	Heat Sinks	6	0.03	0.21	18.0%	0.04	0.25
06.1.6.b.a	Heat Sinks	6	0.03	0.21	18.0%	0.04	0.25
06.1.6.b.b	Heat Pipes	4	0.15	0.60	18.0%	0.11	0.71





#### 4.9.5 Thermal Recommendation

The thermal system for the carrier S/C utilizes a standard approach for controlling the S/C temperature during deep space transit. The system is mostly passive and therefore does not have a significant risk for failure. To increase reliability redundant components can be utilized for some of the items such as the heat pipes between the interface plates to the radiator.

The thermal components for the descent and operation on the Venus surface are also mostly passive items. However, there have not been many previous vehicles that have successfully operated within this environment to provide design heritage. Therefore to increase the reliability of the thermal system, all components and materials should be extensively tested to verify that they would operate and perform as designed within this environment. This includes passive items such as the cooling fins as well as active items such as the temperature sensors.

### 5.0 COST AND RISK

#### 5.1 Cost

A draft cost estimate was generated based on COMPASS design. Since this is a conceptual design, and not a detailed final design, the costs here should be considered preliminary, or rough order of magnitude (“ROM”) costs and are shown in Table 5.1.

- All costs are in FY13\$M
- Estimates represent prime contractor cost with fee (10% less science payload)
  - Prime contractor design, test & build based on NASA-provided specs
- This estimate assumes the following:
  - Proto-flight development approach
  - Ground spares are not included
  - Considered to be *new development* across the board based on the Venus operating environment
  - Instruments costs based on NASA Instrument Cost Model (NICM) and MER actuals for similar instruments (Cameras, Grinder, and Instrument Deployment Device)
  - Model assumes TRL Level 6
    - This estimate does not include any cost for technology development lower than TRL 6
  - Represents the most likely estimate based on cost-risk simulation results
    - Includes mass growth allowance
  - Parametric estimate based on mostly mass-based CERs using historical cost data
    - Aeroshell is included and is based on MER aeroshell costs
    - Structure, Sail and Chassis estimated at mainly Ti using PRICE estimating tool
  - Planetary systems integration wraps
  - Cost of propellant not included
  - Costs of orbiter, launch vehicle, NASA insight/oversight and reserves not included

Table 5.1—Preliminary Cost ROM (Represents Estimated Prime Contractor Cost Plus Fee)

WBS	Description	DDT&E Total (FY 13\$M)	Flight HW Total (FY 13\$M)	DD&FH Total (FY 13\$M)
06.1.1	Science Instruments	68	27	95
06.1.2	Attitude Determination and Control	1	1	2
06.1.3	Command & Data Handling	10	5	16
06.1.4	Communications and Tracking	24	5	29
06.1.5	Electrical Power Subsystem	12	4	16
06.1.6	Thermal Control (Non-Propellant)	2	1	3
06.1.7	Propulsion (Sail System)	30	9	39
06.1.11	Structures and Mechanisms	12	2	14
06.2	Aeroshell	17	6	23
	<b>Subtotal</b>	<b>176</b>	<b>60</b>	<b>236</b>
	IACO	12	3	14
	STO	10		10
	GSE Hardware	21		21
	SE&I	37	10	47
	PM	18	4	22
	LOOS	19		19
	<b>Spacecraft Total (with Integration)</b>	<b>294</b>	<b>77</b>	<b>371</b>
Prime Contractor Fee (10% less payload)				28
<b>Spacecraft Total with Fee</b>				<b>398</b>

### 5.1.1 Draft Lifecycle Cost ROM

The estimates represent prime contractor cost for the Landsailer only, and not total mission costs. Does this mission fit in a Discovery level cost cap? No. When the orbiter, mission ops, 30% reserves, and NASA insight/oversight costs are added, the full mission cost grows on the order of \$1B (or a small flagship level).

- Costs of required technology development not included:
  - Development cost for technology less than TRL-6 not captured
  - High-temperature electronics costs assumed to be part of the ‘new development’ effort
  - Donated Science Instruments – current estimates are major driver

### 5.1.2 Integration, Assembly and Checkout (IACO)

The IACO element contains all labor and material required to physically integrate (assemble) the various subsystems into a total system. Final assembly, including attachment, and the design and manufacture of installation hardware, final factory acceptance operations, packaging/crating, and shipment are included. IACO charged to DDT&E represents those costs incurred for the integration, assembly, and checkout of major test articles. IACO charged to the flight unit includes those same functions applied to the actual flight unit.

This item excludes the engineering effort required to establish the integration, assembly, and checkout procedures necessary for this effort. These engineering efforts are covered under systems engineering and integration.

### 5.1.3 System Test Operations (STO)

The STO element includes development testing and the test effort and test materials required for qualification and physical integration of all test and qualification units. Also included is the design and fabrication of test fixtures.

Specifically included are tests on all STH to determine operational characteristics and compatibility with the overall system and its intended operational parameters. Such tests include operational tests, design



verification tests, and reliability tests. Also included are the tests on systems and integrated systems to verify acceptability for required mission performance. These tests are conducted on hardware that has been produced, inspected, and assembled by established methods meeting all final design requirements. Further, system compatibility tests are included, as well as, functions associated with test planning and scheduling, data reduction, and report preparation.

#### **5.1.4 Ground Support Equipment (GSE)**

Functional elements associated with GSE include the labor and materials required to design, develop, manufacture, procure, assemble, test, checkout, and deliver the equipment necessary for system level final assembly and checkout. Specifically, the equipment utilized for integrated and/or electrical checkout, handling and protection, transportation, and calibration, and items such as component conversion kits, work stands, equipment racks, trailers, staging cryogenic equipment, and many other miscellaneous types of equipment are included.

Specifically excluded is the equipment designed to support only the mission operational phase.

#### **5.1.5 Systems Engineering and Integration (SE&I)**

The functions included in the SE&I element encompass: (1) the system engineering effort to transform an operational need into a description of system requirements and/or a preferred system configuration; (2) the logistics engineering effort to define, optimize, and integrate logistics support considerations to ensure the development and production of a supportable and cost effective system; and (3) the planning, monitoring, measuring, evaluating, and directing of the overall technical program. Specific functions include those for control and direction of engineering activities, cost/performance trade-offs, engineering change support and planning studies, technology utilization, and the engineering required for safety, reliability, and quality control and assurance. Also included is the effort for system optimization, configuration requirements analyses, and the submittal and maintenance of Interface Control Documents (ICDs).

Excluded from the SE&I element are those functions which are identifiable to subsystem SE&I.

#### **5.1.6 Program Management (PM)**

Elements included in the PM function consist of the effort and material required for the fundamental management direction and decision making to ensure that a product is developed, produced, and delivered.

Specifically included are direct charges for program administration, planning and control, scheduling and budgeting, contracts administration, and the management functions associated with engineering, manufacturing, support, quality assurance, configuration and project control, and documentation.

The PM element sums all of the effort required for planning, organizing, directing, coordinating, and controlling the project to help ensure that overall objectives are accomplished. This element also includes the effort required to coordinate, gather, and disseminate information.

Excluded from the PM element are those functions commonly charged to subsystem level activities.

#### **5.1.7 Launch and Orbital Operations Support (LOOS)**

This category includes the effort associated with pre-launch planning, launch and ascent, and initial on-orbit operations. The pre-launch activities include bus and payload preparation, as well as interface activities with the launch vehicle.

The launch and ascent period includes final assembly, checkout, and fueling, lift-off, telemetry, pre-launch, telemetry, tracking and command, recovery operations, and post-processing of lift-off data. Support during the mission includes drive planning and science operation, attitude and orbit control, support of on-orbit testing, routine monitoring and fault detection of space vehicle subsystem functions,

and support of anomaly investigation and correction. This period ends when the newly deployed satellite is turned over to the operational user, typically after a period of 30 days.

## 6.0 ARCHITECTURAL DETAILS AND MARGIN

Table 6. shows the final spacecraft mass including growth. Detailed analysis of the launch system was outside the scope of this study, however, the mass was sized to fit well within the quoted launch capability of existing expendable launch vehicles. An example calculation, for a Falcon-9 launch vehicle. Strawman launch vehicle calculations, for a launch to Venus with C3 of 7 km<sup>2</sup>/km<sup>2</sup>, are shown in table 6.2, showing a margin of 22%

Table 6.1—Venus Landsailer Summary Mass Calculations

Venus Landsailer Summary Mass Calculations	Basic Mass (kg)	Growth (kg)	Predicted Mass (kg)	Aggregate Growth (%)
Venus Landsailer Total Dry Mass	1581	296	1877	
Venus Landsailer Total Wet Mass	1581	296	1876	16%
Dry Mass Desired System Level Growth	1563	469	2032	30%
Additional Growth (carried at system level)		173		14%
Total Useable Propellant	0		0	
Total Trapped Propellants, Margin, pressurant	0		0	
Total Inert Mass with Growth	1581	469	2049.97	
Venus Landsailer Total Wet Mass with system level growth	1581	469	2050	

Table 6.2—Architecture Details—example Launch system performance

Launch vehicle .....	Falcon V1
Energy, C <sub>3</sub> .....	7.00 km <sup>2</sup> /s <sup>2</sup>
ELV performance (pre-margin).....	2910 kg
ELV margin (%).....	10%
ELV performance (post-margin).....	2619 kg
ELV adaptor (Stays with ELV).....	0 kg
ELV performance (post-adaptor).....	2619 kg
<b>S/C total wet mass with system level growth .....</b>	<b>2050 kg</b>
<b>Available ELV margin .....</b>	<b>569 kg</b>
<b>Available ELV margin (%) .....</b>	<b>22%</b>

## 7.0 BIBLIOGRAPHY

### System

- AIAA S-120-2006, AIAA Standard Mass Properties Control for Space Systems.  
 ANSI/AIAA R-020A-1999, Recommended Practice for Mass Properties Control for Satellites, Missiles, and Launch Vehicles.  
 Larson, W.J. and Wertz, J.R. (eds.), (1999) Space Mission Analysis and Design, Third Edition, Space Technology Library, Microcosm Press.

### Mission

- Anderson, David J., Pencil, Eric J., Liou, Larry C., Dankanich, John W., Munk, Michelle M., and Hahne, David, (2010), “The NASA In-Space Propulsion Technology Project’s Current Products and Future Directions,” AIAA-2010-6648, 46th AIAA/ASME/SAE/ASEE Joint Propulsion Conference & Exhibit, July 25–28, 2010, Nashville, TN.  
 Basilevsky, Alexander T. and Head, James W. (2003) “The Surface of Venus,” *Reports on Progress in Physics*, Vol. 66 (2003) pp. 1699–1734 PII: S0034-4885(03)08878-X  
 “COMPASS Final Report: Mars Earth Return Vehicle (MERV),” CD-2009-31, February–March 2009.  
 Desai, P.N., Braun, R.D., Engelund, W.C., Cheatwood, F.M., Kangas J.A., (1998), “Mars Ascent Vehicle Flight Analysis,” 7th AIAA/ASME Joint Thermophysics and Heat Transfer Conference June 15–18, 1998, Albuquerque, NM, AIAA 98-2850.

- Dillman, Robert and Corliss, James, (2008), "Overview of the Mars Sample Return Earth Entry Vehicle," *Sixth International Planetary Probe Workshop*, June 26, 2008.
- Dux Ian J., Huwaldt, Joseph A., McKamey, R. Steve, Dankanich, John W., (2010) Mars Ascent Vehicle Gross Liftoff Mass Sensitivities for Robotic Mars Sample Return, NASA Deep Space Missions, NASA TM 2010.
- ESA Aurora Program, [http://www.esa.int/esaMI/Aurora/SEM CWB1A6BD\\_0.html](http://www.esa.int/esaMI/Aurora/SEM CWB1A6BD_0.html)
- Garvin, J., Head, J., Zuber M. and Helfenstein, P., "Venus: the Nature of the Surface from Venera Panoramas," *J. Geophys. Res.*, 89, B5, pp 3381-3399, May 10, 1984.
- Holmberg, Neil A., Faust, Robert P., and Holt, H. Milton (1980), "Viking '75 Spacecraft Design and Test Summary Volume III—Engineering Test Summary," NASA Reference Publication 1027, Nov. 1980.
- Johnston, M.D., Esposito, P.B., Alwar, V., Demcak, S.W., Graat, E.J., and Mase, R.A. (1998), "Mars Global Surveyor Aerobraking at Mars," AAS 98-112 <http://Mars.jpl.nasa.gov/mgs/sci/aerobrake/SFMech.html>
- Keldysh, M. V. (1977) "Venus exploration with the Venera 9 and Venera 10 spacecraft." *Icarus* 30, pp. 605-625, 1977.
- Kelley, C., Sinclair, R., and Sengupta, A (2012) "Parachute Development for Venus," 9th International Planetary Probe Workshop (IPPW-9), Toulouse, France, 18-22 June 2012.
- Ksanfomaliti, L. V., Goroshkova, N. V., and Khondyrev, V. K. , "Wind velocity at the Venus surface according to acoustic measurements," *Kosmicheskie Issledovaniia* (ISSN 0023-4206), vol. 21, Mar.-Apr. 1983, p. 218-224 (in Russian; abstract in English at <http://adsabs.harvard.edu/abs/1983Kosls..21..218K>)
- Landis, Geoffrey A. (2004) "Robotic Exploration of the Surface and Atmosphere of Venus," *Acta Astronautica*, Vol. 59, 7, 517-580 (October 2006); originally presented as paper IAC-04-Q.2.A.08, 55th International Astronautical Federation Congress, Vancouver BC, Oct. 4-8 2004.
- Landis, Geoffrey A., Dyson, Rodger, Oleson, Steven J., Warner, Joseph D., Colozza, Anthony J. and Schmitz, Paul C. (2011) "Venus Rover Design Study," paper AA 2011-7268, *AIAA Space 2011 Conference & Exposition*, Long Beach CA, Sept. 26-29, 2011.
- Landis, Geoffrey A. (2012) "A Landsailing Rover for Venus Mobility," *J. British Interplanetary Soc.*, Vol. 65, No. 2, 373-377 (Nov-Dec 2012).
- Landis, Geoffrey A., et al., (2014) "Zephyr: A Landsailing Rover for Venus," to be presented, *65th International Astronautical Congress*, Toronto, Sept. 30-Oct. 2, 2014
- Marov, M. Ya., "Results of Venus Missions," *Ann. Rev. Astron. Astrophys.* 1978, 16, p. 157.
- Matousek, S., Adler, M., Lee, W., Miller, S.L., Weinstein, S., (1998), "A Few Good Rocks: The Mars Sample Return Mission Architecture," *AIAA/AAS Astrodynamic Specialist Conference*, August 10–12, 1998, Boston, MA, AIAA-98-4282."
- Nextel Ceramic Textiles Technical Notebook," Document 98-0400-5870-7, 3M Corporation, St. Paul, MN
- Palaszewski, B. and Frisbee, R., (1988), "Advanced Propulsion for the Mars Rover Sample Return Mission," paper AIAA-88-2900, *AIAA/ASME/SAE/ASEE 24th Joint Propulsion Conference*, July 11–13, 1988, Boston, MA
- Preliminary Planning for an International Mars Sample Return Mission, *Report of the International Mars Architecture for the Return of Samples (iMARS) Working Group*, June 1, 2008.
- Rose, J., (1989), "Conceptual Design of the Mars Rover Sample Return System," *AIAA 27th Aerospace Sciences Meeting*, Jan. 9–12, 1989, Reno, NV, AIAA-89-0418.
- Spencer, D.A., Tolson, R., (2007), "Aerobraking Cost and Design Considerations," *Journal of Spacecraft and Rockets*, Vol. 44, No. 6, Nov/Dec. 2007
- Stephenson, David, (2002), "Mars Ascent Vehicle—Concept Development," 38th Joint Propulsion Conference and Exhibit, July 7–10, 2002, Indianapolis, IN, AIAA 2002-4318.
- Whitehead, John C., (1997), "Mars Ascent Propulsion Options for Small Sample Return Vehicles." 33rd AIAA/ASME/SAE/ASEE Joint Propulsion Conference and Exhibit, July 6–9, 1997, Seattle, WA, AIAA 97-2950.
- Williams, R., Gao, Y., Kluever, C.A., Cupples, M., and Belcher, J., (2005), "Interplanetary Sample Return Missions Using Radioisotope Electric Propulsion," 41st AIAA/ASME/SAE/ASEE Joint Propulsion Conference & Exhibit, July 10–13, 2005, Tucson, AZ, AIAA-2005-4273.
- Zubrin, Robert, (1996), "A comparison of approaches for the Mars Sample Return Mission," AIAA 34th Aerospace Sciences Meeting and Exhibit, Reno, NV, Jan. 15–18, 1996, A9618450, AIAA Paper 96-0489.

### **Electronics: Command and Data Handling**

- Balint, T. S., Kolawa, E. A., Cutts, J. A., and Peterson, C. E., (2008) "Extreme Environment Technologies for NASA's Robotic Planetary Missions," *Acta Astronautica*, Vol. 63, No. 3, July-August 2008, pp. 285-298. See also JPL report D-32832, *Extreme Environments Technologies for Future Space Science Missions - Final Report*, September 19, 2007.
- Neudeck, P. G., Okojie, R. S., and Chen, L.-Y. (2002) "High-Temperature Electronics- A Role for Wide Bandgap Semiconductors?" *Proceedings of the IEEE*, Vol. 90, 2002, pp. 1065-1076.
- Hunter, G. W., Neudeck, P. G., Okojie, R. S., Beheim, G. M., Krasowski, M. J., Ponchak, G. E., and Chen, L.-Y. (2007) "High Temperature Electronics, Communications, and Supporting Technologies for Venus Missions," *5th International Planetary Probe Workshop, IPPW-5*, Bordeaux, France June 23-29 2007.
- Spry, D., Neudeck, P. G., Okojie, R. S., Chen, L.-Y., Beheim, G. M., Meredith, R., Mueller, W. and Ferrier, T. L. (2004) "Electrical Operation of 6H-SiC MESFET at 500 °C for 500 Hours in Air Ambient," *Proceedings 2004 IMAPS International Conference and Exhibition on High Temperature Electronics*, Santa Fe NM, 2004.

- Spry, D., Neudeck, P. G., Chen, L.-Y., Beheim, G. M., Okojie, R. S., Chang, C. W., Meredith, R. D., Ferrier, T. L., and Evans, L. J. (2007) "Fabrication and Testing of 6H-SiC JFETs for Prolonged 500 °C Operation in Air Ambient," in *Silicon Carbide and Related Materials 2007*, Materials Science Forum, T. Kimoto, ed., Trans Tech Publications, Switzerland, 2008.
- Neudeck, P. G., Spry, D., Chen, L.-Y., Chang, C. W., Beheim, G. M., Okojie, R. S., Evans, L. J., Meredith, R. D., Ferrier, T. L., Krasowski, M. J., and Prokop, N. F. (2008) "Long-Term Characterization of 6H-SiC Transistor Integrated Circuit Technology Operating at 500 °C," in *Silicon Carbide 2008, Materials, Processing and Devices, Vol. 1069*, Materials Research Society Symposium Proceedings, Materials Research Society, Warrendale, PA, 2008.
- Son, K.-A., et al. (2010) "GaN-based high-temperature and radiation-hard electronics for harsh environments", *Proc. SPIE 7679, Micro- and Nanotechnology Sensors, Systems, and Applications II*, 76790U, May 05, 2010.
- Herfurth, P., Maier, P., Men, P., Rösch, R., Lugani, L. Carlin, J-F, , Grandjean, N., and Kohn, E. (2013) "GaN-on-insulator technology for high-temperature electronics beyond 400 °C," *Semiconductor Science and Technology. Vol. 28* No. 7, 2013.

### Guidance Navigation & Control

- Norris, L, Tao, Y.C., Hall, R. Chuang, J. and Whorton, M. (2008) "Analysis of Ares I Ascent Navigation Options", AIAA 2008-6290.

### Propulsion/Mobility

- "A High Temperature Electric Motor, Use of Nickel-Clad Silver Palladium Wire," *Platinum Metals Rev.*, 1971, Volume 15, Issue 3, Pages 100-101.
- Asnani, V., Delap, D., and Greager, C., (2009), "The Development of Wheels for the Lunar Roving Vehicle," NASA/TM--2009-215798.
- Benson, Thomas J., (1996), "Interactive Educational Tool for Classical Airfoil Theory," AIAA 97-0849, AIAA Aerospace Sciences Meeting & Exhibit, January 6-9, 1997, Reno, NV.
- Ji, Jerri, (2008), "High Temperature Mechanisms, A Breakthrough Development," 6th International Planetary Probe Workshop, Short Course on Extreme Environment Technologies, Atlanta, Ga.
- Lingard, S., (2005), "Parachutes for Space Use," 3rd International Planetary Probe Workshop, July 2005, Anavyssos, Attica, Greece.
- Sheldahl, Robert E. and Klimes, Paul C.,(1981), "Aerodynamic Characteristics of Seven Symmetrical Airfoil Sections Through 180 Degree Angle of Attack for Use in Aerodynamic Analysis of Vertical Axis Wind Turbines," SAND80-2114, Sandia National Laboratories.

### Science Payload

- Hölling, M., Schulte, Barth S. and Peinke, J. (2007) "Sphere anemometer - a faster alternative solution to cup anemometry," *J. Phys. Conf. Ser.* 75, 012064, 2007
- Honeybee Robotics, "High Temperature Motors and Gearheads," <http://www.honeybeerobotics.com/portfolio/high-temperature-motors-gearheads/>
- Ji, Jerri, Narine, Roop, Kumar, Nishant, Singh, Sase, and Gorevan, Steven (2008) "High Temperature Mechanisms for Venus Exploration", *37th COSPAR Scientific Assembly*, 13-20 July 2008, Montréal, Canada., p.1370.
- Lei J-F., and Will, H. A. (1998) "Thin-film thermocouples and strain-gauge technologies for engine applications," *Sensors and Actuators A: Physical, Volume 65*, Issues 2-3, 15 March 1998, pp. 187-193.
- Okojie, R.S., Beheim, G.M., Saad, G.J., and Savrun, E. (2001) "Characteristics of Hermetic 6H-SiC Pressure Sensor at 600 °C," *AIAA Space 2001 Conference and Exposition*, AIAA Paper No. 2001-4652, Albuquerque, NM, August 28-30, 2001.
- Stenzel, C., Schroer, C., Lengeler, B., Rasulbaev, M., and Vi, R. (2009) "Radioisotope Rh-101 as X-Ray Source for Instruments on Space Missions," *JCPDS-International Centre for Diffraction Data 2009* ISSN 1097-0002, p. 167-174. [http://www.icdd.com/resources/axa/vol52/V52\\_22.pdf](http://www.icdd.com/resources/axa/vol52/V52_22.pdf)

### Structures

- Persons, D., Mosher, L., and Hartka, T. (2000), "The NEAR and MESSENGER Spacecraft: Two Approaches to Structure and Propulsion Design," AIAA-00-I406, A00-24531.
- Zibdeh, Hazim S., and Heller, Robert A., (1989), "Rocket motor Service Life Calculations Based on the First-Passage Method," Virginia Polytechnic Institute and State University, Blacksburg, VA, *Journal of Spacecraft and Rockets*, 0022-4650, Vol. 26, No. 4, pp. 279-284.

### Power

- Benigno, G., Hoza, K., Motiwala, S., Landis G., and Colozza, A. (2013) "A Wind-powered Rover for a Low-Cost Venus Mission," paper AIAA-2013-0586, *51st AIAA Aerospace Sciences Meeting*, Grapevine TX, Jan. 7-10 2013.
- Dyson, R. W. and Bruder, G. A. (2010) Progress Towards the Development of a Long-Lived Venus Lander Duplex System, paper AIAA-2010-6917, 8th International Energy Conversion Engineering Conference (IECEC) , Nashville, Tennessee, July 25-28, 2010; NASA/TM—2011-217018 .



- Landis, Geoffrey A. and Mellott, Ken (2004) "Venus Surface Power and Cooling System Design," *Acta Astronautica*, Vol 61, No. 11-12, 995-1001 (Dec. 2007); originally presented as paper IAC-04-R.2.06, 55th International Astronautical Federation Congress, Vancouver BC, Oct. 4-8 2004.
- Landis G., and Vo, T. (2009) "Photovoltaic Performance in the Venus Environment," *34th IEEE Photovoltaic Specialists Conference*, Philadelphia PA, June 7-12, 2009.
- Landis, G. A. and Harrison, R. (2008) "Batteries for Venus Surface Operation," *Journal of Propulsion and Power*, Vol. 26, Number 4, 649-654, July/Aug 2010; originally presented as paper AIAA-2008-5796, 6th AIAA International Energy Conversion Engineering Conf., Cleveland OH, July 28-30, 2008.
- Landis, G. A., and Haag, E. (2013) "Analysis of Solar Cell Efficiency for Venus Atmosphere and Surface Missions" paper AIAA-2013-4028, *AIAA 11th International Energy Conversion Engineering Conference*, San Jose CA, July 15-17 2013.

### Thermal

- Aerodynamic Heating Wikipedia entry. [http://en.wikipedia.org/wiki/Aerodynamic\\_heating](http://en.wikipedia.org/wiki/Aerodynamic_heating)
- Alexander, M. (ed.) (2001), "Mars Transportation Environment Definition Document," NASA/TM—2001-210935.
- Bejan, A. and Kraus, A.D., (2003), *Heat Transfer Handbook*, John Wiley & Sons.
- Chapman, A.J., (1974), *Heat Transfer, Third Edition*, Macmillan Publishing Company.
- Gilmore, D. G. (ed.), (2002), *Spacecraft Thermal Control Handbook: Volume 1 Fundamental Technologies*, AIAA.
- Hyder, A.J., Wiley, R.L., Halpert, G., Flood, D.J. and Sabripour, S., (2000), *Spacecraft Power Technologies*, Imperial College Press.
- Incopera, F.P. and DeWitt, D.P., (1990), *Fundamentals of Heat and Mass Transfer*, John Wiley and Sons.
- Larson, W.J. and Wertz, J.R. (eds.), (1999), *Space Mission Analysis and Design*, Third Edition, Space Technology Library, Microcosm Press.
- Olds, J. and Walberg, G., (1993), "Multidisciplinary Design of Rocket-Based Combined Cycle SSTO Launch Vehicle using Taguchi Methods," AIAA 93-1096, AIAA/AHS/ASSEE Aerospace Design Conference, February 16-19, 1993, Irvine, CA.
- Penuela, David, Simon, Mathew, Bemis, Eammon, Hough, Steven, Zaleski, Kristina, Jefferies, Sharon and Winski, Rick, "Investigation of Possible Heliocentric Orbiter Applications for Crewed Mars Missions," NIA/Georgia Institute of Technology, Project 1004. [http://www.nianet.org/rascal/forum2006/presentations/1004\\_nia\\_paper.pdf](http://www.nianet.org/rascal/forum2006/presentations/1004_nia_paper.pdf)
- RP-07-100\_05-019-I; *Volume I: Ice Mitigation Approaches for Space Shuttle External Tank Final Report*.
- Sutton, Kenneth and Graves, Randolph A. Jr., (1971), "A General Stagnation Point Convective-Heating Equation for Arbitrary Gas Mixtures," NASA TR R-376.

## 8.0 — ACRONYMS AND ABBREVIATIONS

$\Delta V$	delta velocity	Ge	Germanium
AD&C	Attitude Determination and Control	GEER	NASA Glenn Extreme Environments Rig
AIAA	American Institute for Aeronautics and Astronautics	GLIDE	GLobal Integrated Design Environment
Al	aluminum	GN&C	Guidance, Navigation and Control
Am	Americium	GPHS	general purpose heat source
ANSI	American National Standards Institute	GRC	NASA Glenn Research Center
APXS	Alpha Particle X-ray Spectrometer	GSE	Ground Support Equipment
APXS	Alpha Particle X-ray Spectrometer	IACO	Integration, Assembly and Checkout
C&DH	Command and Data Handling	ICDs	Interface Control Documents
C&T	Communications and Tracking	IPP	GRC Innovative Partnerships Program
CAD	computer aided design	LOOS	Launch and Orbital Operations Support
CBE	current best estimate	LRV	lunar rover vehicle
CER	cost estimating relationships	LRV	lunar roving vehicle
Comm	communications	LSP	Launch Service Program
COMPASS	COlaborative Modeling and Parametric Assessment of Space Systems	LSTO	Launch Service Task Order
CONOPS	Concept of Operations	MALTO	Mission Analysis Low-Thrust Optimization
COTS	commercial off the shelf	MECO	main engine cutoff
DDT&E	design, development, test, and evaluation	MEL	Master Equipment List
DOD	depth of discharge	MER	Mars Exploration Rover
DOF	degree(s) of freedom	MGA	mass growth allowance
DSN	Deep Space Network	MLI	multilayer insulation
EDAX	Energy-Dispersive Analysis by X-rays	MMPDS	Metallic Materials Properties Development and Standardization
EDL	entry, descent, and landing	MPU	makeup power unit
ELV	expendable launch vehicle	MPU	mobile power unit
EP	electric propulsion	N/A	not applicable
EP	electrical power	N <sub>2</sub>	nitrogen
Fe	Iron	NACA	National Advisory Committee for Aeronautics
FOM	figure(s) of merit	NaS	sodium-sulfur
FY	fiscal year	NASA	National Aeronautics and Space Administration
G/T	antenna gain-to-noise-temperature	NIAC	NASA Innovative Advanced Concepts Program
GaAs	gallium arsenide	NICM	NASA Instrument Cost Model
GaInP <sub>2</sub>	gallium-indium phosphide		
GE	General Electric		





NIST	National Institute of Standards and Technology	RPS	Radioisotope Power System
NLS	NASA Launch Services	S/C	spacecraft
OS	operating system	SA	solar array
OSS	Office of Space Science	SEP	solar electric propulsion
OTS	off-the-shelf	SiC	silicon carbide
PEL	Power Equipment List	SMA	semimajor axis
PM	Program Management	SOAP	Satellite Orbit Analysis Program
PMAD	power management and distribution	SOFI	spray-on foam insulation
Pu	plutonium	SPU	solar power unit
QFP	Quad Flat Package	STO	System Test Operations
RAD	radiation dosimetry	TCS	Thermal Control System
RAM	random access memory	Ti	titanium
RASC	NASA Revolutionary Aerospace Systems Concepts	TRL	technology readiness level
RAT	Rock Abrasion Tool	TVI	trans-Venus injection
RCS	Reaction Control System	TVI	trans-Venus insertion
REP	radioisotope electric propulsion	UART	universal asynchronous receiver/transmitter
RF	radio frequency	UHF	ultra high frequency
Rh	Rhodium	VOI	Venus orbit insertion
ROM	read only memory	WBS	work breakdown structure
ROM	rough order of magnitude	WGA	weight growth allowance
		WGS	weight growth schedule
		WSB	weak stability boundary

## Appendix: “A Landsailing Rover For Venus Mobility”

from *Journal of the British Interplanetary Society*, Vol. 65, No. 2, pp. 373-377 (Nov-Dec 2012).

### A Landsailing Rover for Venus Mobility

Geoffrey A. Landis,  
NASA Glenn Research Center  
21000 Brookpark Road, mailstop 302-1  
Cleveland, OH 44135

#### Summary

The surface of Venus is a location that is of great interest for future scientific exploration, but designing a rover that can move and conduct science operations on Venus is a difficult task. Electronic and materials technologies are available that could survive the furnace of Venus, but such a rover represents a challenging design problem. One approach to the problem is to make use of the features of the Venus environment, such as the thick atmosphere. A new approach for rover mobility is proposed, in which the rover motive force is produced by a sail. Such a Venus landsailing rover could be small and low powered, since the main power required for motion is generated by the wind, rather than by motors. Although the wind velocities on Venus are low, estimated at  $0.6 \pm 0.3$  m/sec at the Venera landing sites, due to the high density of the atmosphere, sufficient force would be generated on a sail to allow good mobility for a lightweight rover.

Key Words: Venus, rover, wind, landsailing, sail.

#### 1. Introduction

The surface of Venus has the most hostile environment of any planetary surface in the solar system, with an average temperature of 450 °C and a carbon dioxide atmosphere with corrosive trace gasses at a pressure of 90 bars. Although humans have sent rovers to Mars with operating lifetimes of over nine years, the most long-lived mission to the surface of Venus has been a stationary lander that survived for only 2 hours [1]. Nevertheless, it is a scientifically fascinating planet, and one that, due to its similarity and differences from Earth, for which a mobile exploration rover would produce great public interest.

Exploring the surface of Venus with a rover would be a mission that will push the limits of technology in high-temperature electronics, robotics, and robust systems. Yet it would be an exciting goal, since Venus is an unknown planet, a planet with significant scientific mysteries, and a planet larger than Mars with equally interesting (although less well known) geology and geophysics. A mission to the surface of Venus would expand our knowledge of the surfaces of terrestrial planets.

#### 2. Technology Background and Concept

In work to develop sensors to work inside of jet engines, NASA Glenn Research Center has developed electronics that will continue to function even at the Venus temperature of 450 °C [2-4]. These electronic

components represent a breakthrough in technological capability for high temperatures. Technology has also been developed for a high-temperature electric motors and actuators which operate at up to 500 °C.[5] Thus, the key technologies for operating a rover at Venus temperature have been developed and demonstrated..

Solar cells have been tested at temperatures up to the temperature of the higher elevations of the Venus surface [6], and it has been shown that, although the power density produced is low (because of the high cloud levels and thick atmosphere), it is possible to produce electrical power on the surface [7,8]. So the fundamental elements of a rover for Venus are not beyond the bounds of physics: technologies are available that could survive the furnace of Venus, if we can come up with an innovative concept for a rover that can move on extremely low power levels.

To do this, we need to take advantage of the in-situ resources of Venus for mobility.

The atmospheric pressure at the surface is more than 50 times greater than that of Earth. Even though the winds at the surface of Venus are under 1 m/s, at Venus pressure even low wind speeds develop significant force. We thus propose an innovative concept for a planetary rover: a sail-propelled rover to explore the surface of Venus. Such a rover could open a new frontier: converting the surface of a new planet into a location that can be explored by robotic exploration.

A landsail operates on the same principle as a sailboat with wheels. The basic idea of landsailing is not new: landsailing vehicles on Earth, dating back to the “windwagons” of the 19th century to sail across the American plains (see Fig. 1). Modern landsailing vehicles, such as the one shown in Fig. 2, are much more sophisticated; with good design they can move at speeds of up to ten times the speed of the wind. And yet the basic concept is extremely simple; using the lift force on a sail. While the detailed aerodynamic design of the sail for Venus will be somewhat different, due to the slow wind speeds but high density atmosphere, the basic design principles are well known. Most notably, a landsail can be done with only two moving parts; the sail, and the steering.

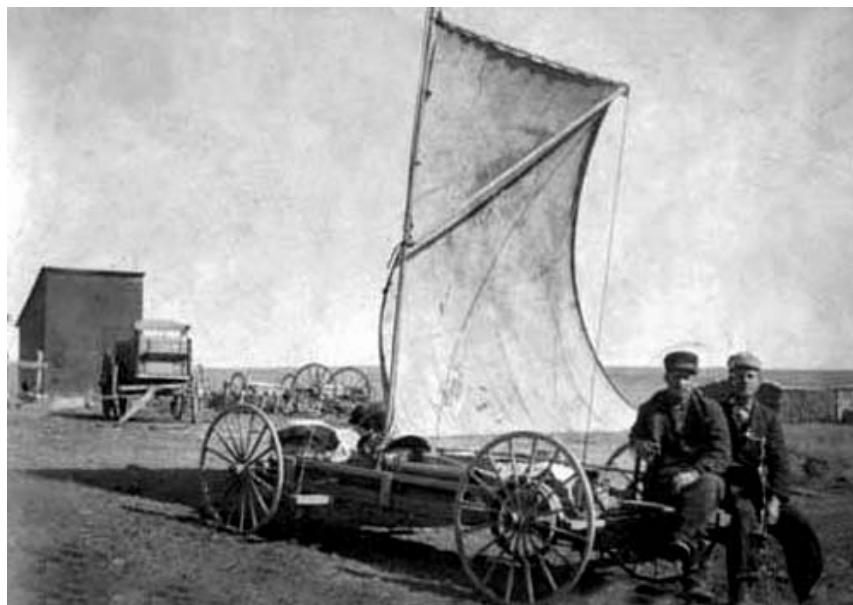


Figure 1: Landsailing vehicles on Earth: a Kansas “Windwagon” from the 1860s



Figure 2: Landsailing vehicles on Earth: A modern landsailing vehicle

## 2.1 Previous Studies

In 2003, a NASA Revolutionary Aerospace Systems Concepts (RASC) study “Robotic Exploration of Venus,” looked at the technologies needed for a future (2048) mission to Venus incorporating rovers, aircraft, and orbiters [9]. This mission baselined use of a future radioisotope power system that would be used to both refrigerate the inside of a rover against the Venus environment, and also provide power.[10]

In 2008 and 2009, NASA’s Venus Flagship Mission Science and Technology Definition Team (STDT) studied possible future missions to the surface. This team came up with science mission objectives and technologies for a more near-term mission, intended as a new-start for a flagship-class mission [11]. Although it was a flagship mission, the surface lander element of this mission conceptual design was baselined for only a 5-hour lifetime on the surface.

In 2010, the NASA Glenn Innovative Partnerships Program (IPP) studied a combination of human and robotic mission to Venus, HERRO-Venus, in which a crew vehicle in Venus orbit operates a rover on the surface via teleoperation, allowing virtual presence on the surface. For this mission, a conceptual design was done of a highly-capable rover design with the ability to operate for extended periods in the Venus environment [12]. While the rover vehicle designed (Fig. 3) was highly capable [13], the design was for a total rover mass of 1059 kg (including anticipated mass growth allowance), intended for a 2039 launch date. Like the earlier RASC study [10], the design study assumed the availability of Radioisotope Stirling power system designed for the Venus environment to operate a cooling system [14], and required 16 plutonium GPHS bricks to provide the thermal input. This amount of plutonium exceeds the amount of plutonium currently available for planetary science missions.

As a result of these and other studies, we can appreciate just how difficult the mission is, and the urgent need for new concepts that would allow the idea of a long-lived Venus mission to be done at a level that could be done on a budget closer to a New Frontiers or even Discovery mission funding levels, rather than as an expensive flagship—and higher—class mission.

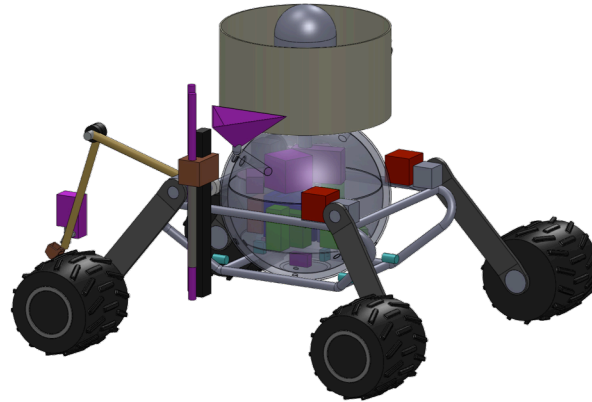


Figure 3: Conceptual design for a Venus rover for the “HERRO-Venus” design study.

### 3. Landsail Design for Venus

Venus is a planet with exceptional high-altitude winds, but the wind speed decreases with altitude. Nevertheless, the wind speeds at the surface are not zero [1], and the high density of the atmosphere means that, although the speeds are low, a significant amount of force is produced.

Fig. 4 shows an artist's concept for landsailing rover on Venus. The vehicle is intended to be small, allowing it to be folded for storage into a small-diameter aeroshell, and will incorporate only high-temperature electronics and components, allowing it to operate without cooling at the ambient temperature of Venus.

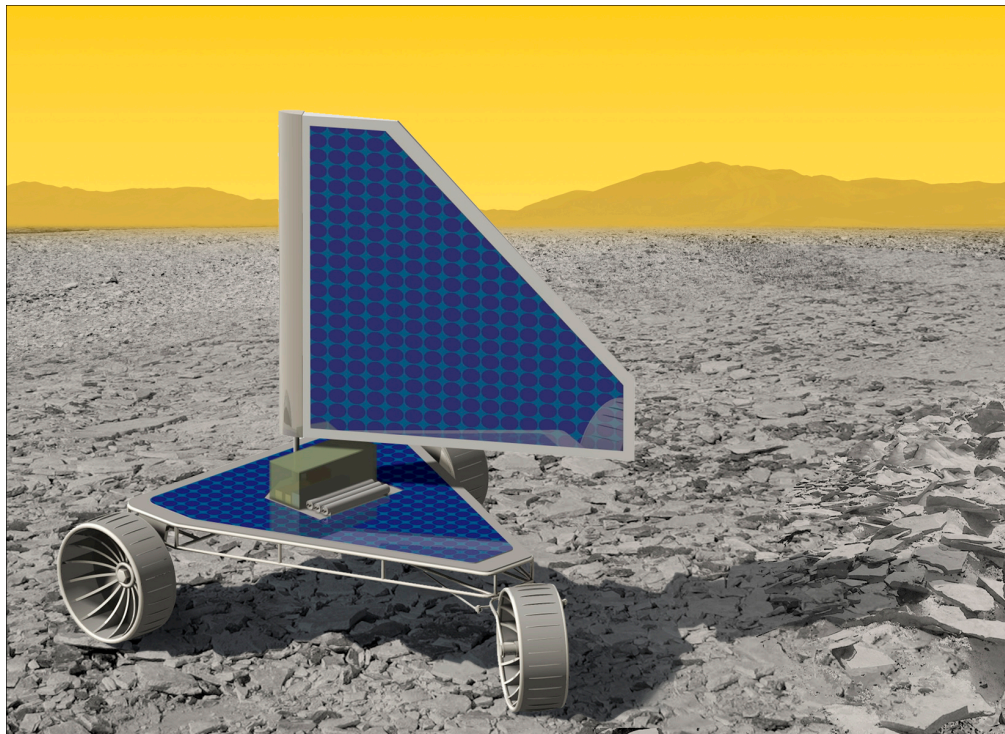


Figure 4: Artist's concept of a landsailing rover on the surface of Venus

### 3.1 Wind on Venus

The four Venera landers that measured surface wind speeds [1, 15, 16] found average wind speed of 0.4 to 0.7 m/sec (Venera 9), 0.8 to 1.3 m/sec (Venera 10), 0.3 to 0.6 m/sec (Venera 13), and 0.3 to 0.6 m/sec (Venera 14). This is a remarkably consistent surface wind of 0.6 m/sec plus or minus 0.3, (with the Venera 10 value slightly less than two standard deviations high). Wind streaks associated with craters and other landforms also indicate nonzero winds at the surface.

The Venus atmospheric density at the surface is 64.8 kg/m<sup>3</sup>, over fifty times higher than the 1.225 kg/m<sup>3</sup> density at Earth's surface. From the density, the momentum density in the wind can be estimated, and using this the force that can be produced on a sail estimated.

### 3.2 Sail Calculation for Venus Landsail

The Reynolds number for the sail increases with the high atmospheric density, but decreases due to the low wind velocity compared to typical terrestrial sails as well as the assumed small size of the vehicle; the net result is that the Venus rover sail will operate at a Reynolds number remarkably similar to that of sailing vehicles on Earth [17], typically on the order of 10<sup>6</sup>.

The force per unit area of the sail can thus be calculated from the lift equation,

$$F = 1/2 C_L A V^2 \quad (1)$$

where  $F$  is the aerodynamic force of the wind on the sail,  $C_L$  the lift coefficient,  $A$  the area, and  $V$  the velocity. Using an assumed lift coefficient of 1.0, the typical force on the sail will be 11.7 N/m<sup>2</sup>,  $\pm 6$ .

The force required to propel a vehicle depends on the rolling resistance, which is a function of both the terrain and the wheel type and diameter:

$$F_r = C_r M g \quad (2)$$

where  $F_r$  is the total force of rolling friction,  $C_r$  is the rolling resistance,  $M$  the vehicle mass, and  $g$  the acceleration of gravity, at the Venus 8.87 m/s<sup>2</sup>. Typical rolling resistance coefficients for off-road vehicles with a wheel diameter of 0.5 m range from 0.1 for medium-hard soil to 0.3 for sand [18]. We will assume that the vehicles will not be designed traversing dunes or soft sand (which in any case is not evident in the Venera photos), and take an intermediate value of 0.2, typical of soil. Thus, setting the two forces equal, the Venus wind will be able to propel a sail vehicle of mass 6.9 kg per square meter of sail. The rover mass will be the result of the detailed design, but picking a typical mass of 20 kg (*i.e.*, twice that Sojourner rover mass of 10.5 kg), a sail of only 2.9 m<sup>2</sup> would be required to propel the vehicle.

Larger wheels would allow lower rolling resistance (and greater tolerance to obstacles), which is a design trade-off that will be done in the study.

On smooth surfaces, landsailing vehicles can easily achieve speeds of up to ten times the wind velocity, so a top speed of 6 m/sec can be envisioned for such a rover. However, because of the time delay in any human input to the vehicle, it is undesirable to operate at high speeds, and hence we will only use a fraction of the speed that the rover would be capable of. In this respect the vehicle will be more similar to the windwagons of the Kansas prairies seen in fig. 1, designed for slow and steady progress over rough terrain, than the high-speed modern landsailers seen in fig. 2.

A landsailing vehicle can move in any direction except straight into the wind; the angle to the wind that is forbidden is a function both of the side force to rolling resistance ratio of the wheels, and the lift to drag ratio of the sail. Typically for a high performance sail [17] we would expect about thirty degrees of azimuth to be unachievable (except by the technique of tacking); for this design, it is more likely that design compromises may be made which will widen the forbidden range, and an unachievable motion vector of plus or minus 45° from the windward will be assumed as a starting point, to be revised on detailed analysis.

Since 75% of the azimuths are directly achievable, is anticipated that this will not be a significant difficulty. In any case, if interesting science targets can only be found in directions directly into the wind, the destinations can be reached by tacking.

Another significant factor in any sail vehicle design is tipping. This is a design trade-off involving the wind speed, wheel base, center of gravity of the vehicle, and the sail height, as well as slope of the land traversed. A larger tolerance to tipping can allow higher speeds of motion at some motion vectors. Unless significant design complexity is added, tipping over would be a non-recoverable maneuver, and hence must be avoided. This can be avoided by slacking the sail if the rover sensors show incipient tilt, and putting in such a failsafe would be relatively straightforward.

Since the side force on the vehicle increases as the motion vector approaches windward [17], the tipping force is a function of the direction of motion, and the trade-off can reduce tipping force by constraining the allowable direction of motion. The moment arm increases as the height of the mast increases, and hence a tall sail will tend to tip more than a short sail. These design trades indicate that a short mast will have advantages over a tall mast.

### 3.3 Effect of Venus Terrain

While landsailing vehicles can climb hills, they require an operating landscape that is not densely packed with obstacles on the scale of meters. In this respect the surface of Venus actually does us a favor: from the views of Venus taken by the Russian Venera probes, the surface of Venus can be seen to have landscapes of flat, even terrain stretching to the horizon, with rocks at only centimeter scale. Two pictures of the Venus surface are shown in Figures 5 and 6, with level terrain covered smooth, platy rock (Venera 14) or by fine sand and low, flat rocks (Venera 13).

In fact, much of the surface seems to comprise such level, obstacle-free plains. Garvin *et al.* commented [16] “A striking aspect of the Venera landing sites is their extreme similarity despite separation distances of thousands of kilometers.” Thus, we know that many locations do exist on Venus (the sites that Venera probes landed) that have terrain similar to the dry lake beds that are used today for landsailing, and perhaps much of the surface is such territory. Venus is ideal terrain for landsailing.

Of the landscapes viewed by the Venera rovers, only the Venera 9 landing site showed any significant amount of rocks on the surface (Fig. 7), with “angular to subangular layered and platy rocks in the 5 to 70 cm range” [16]. Even terrain such as this could be navigated by a landsailing vehicle with sufficient ground clearance and large wheels (notice the large wheels on the Kansas windwagons, Fig. 1); but this would require significant amounts of path-planning. Due to the lightspeed time delay, this would result in very slow traverse, and hence it would be most desirable to choose a landing site that is free of large loose rocks. The surface roughness can be estimated from radar scattering; this technique was used successfully for selecting the Pathfinder and MER landing sites, and the surface roughness validated from ground-truth measurements from the landing sites [19]. In the most conservative case, a flat and obstacle free landing site can be selected simply by choosing one of the Venera landing sites other than Venera-9.

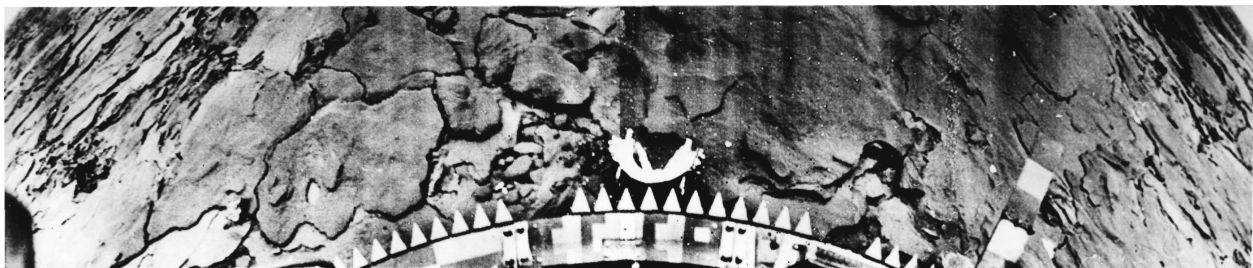


Figure 5: A view of the surface of Venus as seen from the Russian Venera 14 probe during its 2-hr lifetime on the surface. The surface is smooth rock all the way to the horizon, which is visible at the upper left and right of the image.

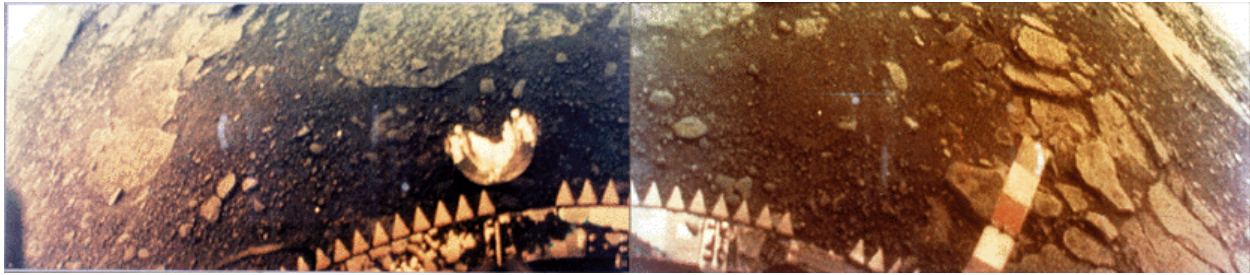


Figure 6: Another view of the surface of Venus, as seen from Venera-13. The surface is smooth, with fine soil and only low flat rocks visible all the way to the horizon; ideal territory for operation of a landsailing vehicle.

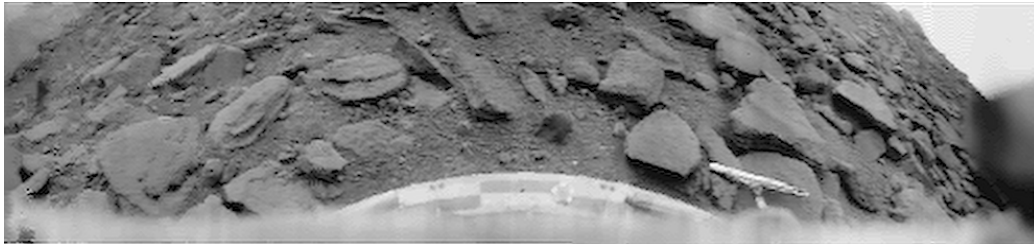


Figure 7: Surface of Venus from the Venera-9. Although the surface here is rockier than any of the other Venera landing sites, the scale of the rocks seen is on the order of ~tens of centimeters.

#### 4. Conclusions

The concept of a wind-powered rover for Venus appears to be credible. This could be a method of making a small, lightweight mission for the Venus surface that would be capable of implementation using high-temperature electronics. This would represent a significant leap in capabilities for planetary exploration beyond any current capability, allowing exploration of a nearly unexplored planetary surface.

The Venus landsailing rover project will have an unexcelled public engagement factor, representing a great leap in capabilities for planetary exploration, allowing us mobility on an unexplored planet. Although the technology is not yet at a stage of development ready to launch a mission, the concept has a sound scientific and engineering basis, and a reasonable implementation path could take us from technical dream to engineering reality within a reasonable period of time.

#### 5. Acknowledgement

The Venus Landsailing rover has been selected by the NASA Office of Chief Technologist for detailed study in their 2012 Innovative and Advanced Concepts (NIAC) Phase-1 study selections.

#### 6. References

1. M. Ya. Marov, "Results of Venus Missions," *Ann. Rev. Astron. Astrophys.* 1978, 16, p. 157.
2. G. W. Hunter, P. G. Neudeck, R. S. Okojie, G. M. Beheim, M. J. Krasowski, G. E. Ponchak, and L.-Y. Chen, "High Temperature Electronics, Communications, and Supporting Technologies for Venus Missions," *5th International Planetary Probe Workshop, IPPW-5*, Bordeaux, France June 23-29 2007.
3. D. Spry, P. G. Neudeck, L.-Y. Chen, G. M. Beheim, R. S. Okojie, C. W. Chang, R. D. Meredith, T. L. Ferrier, and L. J. Evans, "Fabrication and Testing of 6H-SiC JFETs for Prolonged 500 °C Operation



- in Air Ambient,” in *Silicon Carbide and Related Materials 2007*, Materials Science Forum, T. Kimoto, ed., Trans Tech Publications, Switzerland, 2008.
4. P. G. Neudeck, D. Spry, L.-Y. Chen, C. W. Chang, G. M. Beheim, R. S. Okojie, L. J. Evans, R. D. Meredith, T. L. Ferrier, M. J. Krasowski, and N. F. Prokop, “Long-Term Characterization of 6H-SiC Transistor Integrated Circuit Technology Operating at 500 °C,” in *Silicon Carbide 2008, Materials, Processing and Devices, Vol. 1069*, Materials Research Society Symposium Proceedings, Materials Research Society, Warrendale, PA, 2008.
  5. J. Ji, R. Narine, N. Kumar, S. Singh, and S. Gorevan, “High Temperature Mechanisms for Venus Exploration,” paper B06-0021-08, *37th COSPAR Scientific Assembly*, Montréal, Canada, July 13-20 2008, p.1370.
  6. G. A. Landis, D. Belgiovani, and D. Scheiman, “Temperature Coefficient of Multijunction Space Solar Cells as a Function of Concentration,” *37th IEEE Photovoltaic Specialists Conference*, Seattle WA, June 19-24 2011.
  7. G. A. Landis and T. Vo, “Photovoltaic Performance in the Venus Environment,” 34th IEEE Photovoltaic Specialists Conference, Philadelphia PA, June 7-12 2009.
  8. G. A. Landis and E. Haag, “Solar Cell Performance on Venus,” presented at the *22nd Space Photovoltaic Research and Technology Conference*, Brook Park OH, September 20-22, 2011.
  9. G. A. Landis, “Robotic Exploration of the Surface and Atmosphere of Venus,” *Acta Astronautica*, Vol. 59, 7, 517-580 (October 2006).
  10. G. A. Landis and K. Mellott, “Venus Surface Power and Cooling System Design,” *Acta Astronautica*, Vol. 61, No. 11-12, 995-1001 (Dec. 2007).
  11. J. L. Hall, et al., *Venus Flagship Mission Study: Report of the Venus Science and Technology Definition Team*, NASA Jet Propulsion Laboratory, April 17 2009.
  12. G. A. Landis, et al., “Human Telerobotic Exploration of Venus: A New Flexible Path Goal,” paper AIAA-2011-335, *49th AIAA Aerospace Sciences Conference*, Orlando FL, January 4-7, 2011.
  13. G. A. Landis, et al., “Venus Rover Design Study,” paper AIAA-2011-7268, *AIAA Space 2011 Conference & Exposition*, Long Beach CA, Sept. 26-29, 2011.
  14. R. Dyson and G. Bruder, “Progress Towards the Development of a Long-Lived Venus Lander Duplex System,” paper AIAA-2010-6917, *8th Annual International Energy Conversion Engineering Conference*, Nashville, TN, July 25-28 2010.
  15. L. V. Ksanfomaliti, N. V. Goroshkova, and V. K. Khondyrev, “Wind Velocity at the Venus Surface According to Acoustic Measurements,” *Ko smicheskie Issledovaniia* (ISSN 0023-4206), vol. 21, Mar.-Apr. 1983, p. 218-224 (in Russian; abstract in English at <http://adsabs.harvard.edu/abs/1983KosIs..21..218K>)
  16. J. Garvin, J. Head, M. Zuber and P. Helfenstein, “Venus: the Nature of the Surface from Venera Panoramas,” *J. Geophys. Res.*, 89, B5, pp. 3381-3399, May 10 1984.
  17. B. D. Anderson, *The Physics of Sailing Explained*, Sheridan House (2003); also *Physics Today*, Feb. 2008, pp. 38-41.
  18. J. Y. Wong, *Theory of Ground Vehicles*, 2nd ed., John Wiley and Sons (1993), pp. 9-15.
  19. M. P. Golombek, et al., “Assessment of Mars Exploration Rover Landing Site Predictions,” *Nature*, 436, pp. 44-48, 7 July 2005; doi:10.1038/nature03600